PhD degree in Systems Medicine (curriculum in Molecular Oncology)
European School of Molecular Medicine (SEMM),
University of Milan and University of Naples "Federico II"
Settore disciplinare: MED04

Dissecting the role of LSD1 in the response of Acute Myeloid Leukemia cells to retinoic acid treatment

Roberto Ravasio
European Institute of Oncology (IEO), Milan
Matricola n. R11478

Supervisor: Prof. Saverio Minucci
European Institute of Oncology (IEO), Milan

Anno accademico 2018-2019

Table of Contents

Table of Figures

Abstract

The histone demethylase LSD1 is deregulated in several tumors, including leukemias, providing the rationale for the clinical use of LSD1 inhibitors. Treatment of AML cells with LSD1 inhibitors shows a highly variable pattern of response and only a minority of AML cells are sensitive to LSD1 inhibition as single treatment. However, a strong cooperation of LSD1 inhbition and the differentiation agent retinoic acid (RA) can be observed in most of the AML subtypes, even in those resistant to either drug alone.

In acute promyelocytic leukemia (APL), pharmacological doses of RA induce differentiation of APL cells through degradation of the PML-RAR oncogene. APL cells are resistant to LSD1 inhibition or knock-out, but LSD1 inhibition sensitizes them to physiological doses of RA without altering the stability of PML-RAR, and extends survival of leukemic mice upon RA treatment. Non-enzymatic activities of LSD1 are essential to block differentiation of leukemic cells, while the combination of LSD1 inhibitors (or LSD1 knock-out) with low doses of RA releases a differentiation-associated gene expression program, not strictly dependent on changes in histone H3K4 methylation (known substrate of LSD1). An integrated proteomic/epigenomic/mutational analysis showed that LSD1 inhibitors alter the recruitment of LSD1-containing complexes to chromatin through inhibition of the interaction between LSD1 and GFI1, a relevant transcription factor in hematopoiesis.

Same experiments performed in non-APL AML cells confirmed the critical role of LSD1-GFI1 interaction in RA sensitization, beside the APL context.

Introduction

1. Epigenetics

Epigenetics is defined as "the study of mitotically and/or meiotically heritable changes in gene function that cannot be explained by changes in DNA sequence" (Riggs AD et al., 1996; Riggs AD and TN, 1996). This definition reflects the fact that although all somatic cells of an organism carry the same DNA, the gene expression pattern differs and defines the various cell types of the organism, and this diversity can be inherited. The scientific community arrived at the actual definition after more than fifty years from the establishment of the term epigenetics by Conrad H. Waddington in 1947 as "the branch of biology that studies the causal interaction between genes and their products which bring the phenotype into being" (Jablonka and Lamb, 2002). Waddington coined this term to indicate and categorize the developmental events that lead from zygote to mature organism, events that imply a change in the phenotype without a change in the genotype.

The first definition of epigenetics comes from the study of evolution and development, but the definition of epigenetics itself undergone evolution and development during the years, reflecting our increasing knowledge about the molecular mechanisms controlling gene expression and gene regulation (Felsenfeld, 2014). After three-quarter of century, we now know that epigenetic mechanisms govern the inheritance of gene expression patterns not by modifying the sequence of the DNA, but altering the chromatin conformation, which represents the physiological condition in which eukaryotic DNA is stored into cells (Allis and Jenuwein, 2016). Chromatin conformation can be altered by covalent and non-covalent modification of both DNA (without altering its sequence) and histone proteins, the two components of chromatin.

The simplest example to understand epigenetics is given by the huge cellular heterogeneity found in the human body: all the somatic cells have the same genetic information but is the chromatin structure that determines how and when this information has to be read. Thus, it's perceivable that also the cellular differentiation process is ruled by epigenetic mechanisms. Even in a multicellular organism with many cell types with very different phenotypes, all the cells derive from a single totipotent cell and adult tissues are maintained by somatic multipotent stem cells. As Conrad H. Waddington wisely illustrated in its famous "epigenetic landscape" (Figure 1), the cell undergoes different epigenetic changes during differentiation (Goldberg et al., 2007) and every intermediate stage of this process is characterized by a specific chromatin status. Figure 1 represents the process of cellular decision-making during development, with a cell (depicted as a ball) rolling down a hill into one of several valleys (permitted trajectories) and reaching the valley floor, reflecting a terminally differentiated state.

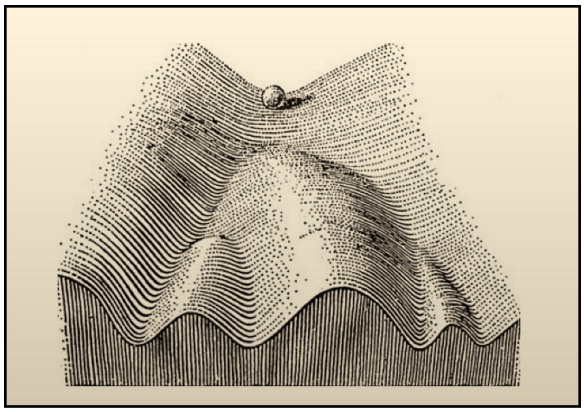

Figure 1. Waddington's epigenetic landscape.
Adapted from Goldberg 2007

Since epigenetic mechanisms govern physiological processes like cellular differentiation, the deregulation of these mechanisms is involved in pathological processes, such as cancer, in

which epigenetics plays a central role. Indeed, tumor cells not only carry genetic mutations, but also have an altered chromatin conformation compared their normal counterpart.

Histone modifications and DNA methylation were the firsts and very fundamental epigenetic mechanisms described, but it became clear that these were only the top of the iceberg. The presence of histone variants and the displacement and reposition of histones are additional epigenetic mechanisms. Long- and short-non coding RNAs, with different mechanisms, take also part in the epigenetic control of gene expression (Murr, 2010).

The combination of all of these processes defines the chromatin conformation of a particular locus and, consequently, determines the transcriptional status of the associated gene. A countless list of epigenetic players has been identified, some of which will be presented in the following sections.

2. DNA methylation

DNA methylation was detected as early as the 1948 (HOTCHKISS, 1948), but only in the mid-1970s a role for DNA methylation in gene regulation was proposed (Holliday and Pugh, 1975). DNA methylation is the covalent addiction of the methyl group to the cytosine at the 5' position of a cytosine located near to a guanine (5'-CpG-3'). In vertebrates, approximately 70%-80% of CpG dinucleotides are methylated (Ndlovu et al., 2011). CpG islands (CGIs), that are clusters of at least 200bp highly enriched in GC, represent an exception. CGIs are usually unmethylated, are characterized by permissive chromatin and are found in about 70% of gene promoters (Illingworth and Bird, 2009).

The enzymes that catalyze DNA methylation are called DNA methyltransferases (DNMTs) (Liyanage et al., 2014) and generally use S-adenosylmethionine (SAM) as a donor for the methyl group. In humans, the DNMT family is composed by three members, DNMT1,

DNMT3a and DNMT3b. The first contributes to the maintenance of DNA methylation by coping, during DNA replication, the methylation pattern from the parental to the newly synthetized strand (Auclair and Weber, 2012). DNMT3a and DNMT3b are instead responsible for the *de novo* methylation.

DNA methylation represents a reversible but heritable modification that can regulate gene expression and is implicated in several biological processes as embryonic development, genomic imprinting, X-chromosome inactivation, reprogramming and cellular differentiation (Liyanage et al., 2014). Overall, DNA methylation is a repressive mark and CGIs promoter methylation is associated with gene silencing. Gene repression can be achieved by creating a direct steric hindrance to transcriptional activators that cannot bind to DNA when it's methylated, or by the recruitment of chromatin repressive complexes with a methyl-binding domain containing protein (MBDs) that can recognize methylated DNA (Klose and Bird, 2006).

Playing a role in so many biological processes, DNA methylation is implicated also in different diseases, especially in cancer. In general, cancer is characterized by local (Feinberg and Vogelstein, 1983) and global DNA hypomethylation, that affects mainly repetitive sequences, coding regions and introns, but also by local DNA hypermethylation at CGIs of promoters of tumor suppressor genes (Kulis and Esteller, 2010).

3. Chromatin organization

A diploid human genome contains approximately 6 billion base pairs. Because each base pair is around 0.34 nanometers, it makes the DNA contained in each cell 2 meters long (Annunziato, 2008). In order to confine this long DNA fiber into the tiny space of the cellular nucleus, a group of proteins called histones folds, condenses and compacts it into a highly

organized structure, known as chromatin. Histones are a small family of positively charged proteins called H1, H2A, H2B, H3 and H4, which can bind DNA, since it is negatively charged due to the phosphate group in its phosphate-sugar backbone. The basic organization unit of chromatin is called nucleosome and it's composed by 146-147 bp of DNA wrapped around an octamer structure formed by couples of the core histones H2A, H2B, H3 and H4 (Kornberg, 1974; Kornberg and Lorch, 1999; Luger et al., 1997; Olins and Olins, 1974; Oudet et al., 1975). Histone H1 further wraps 20 bp of DNA around the basic nucleosome forming a structure called chromatosome.

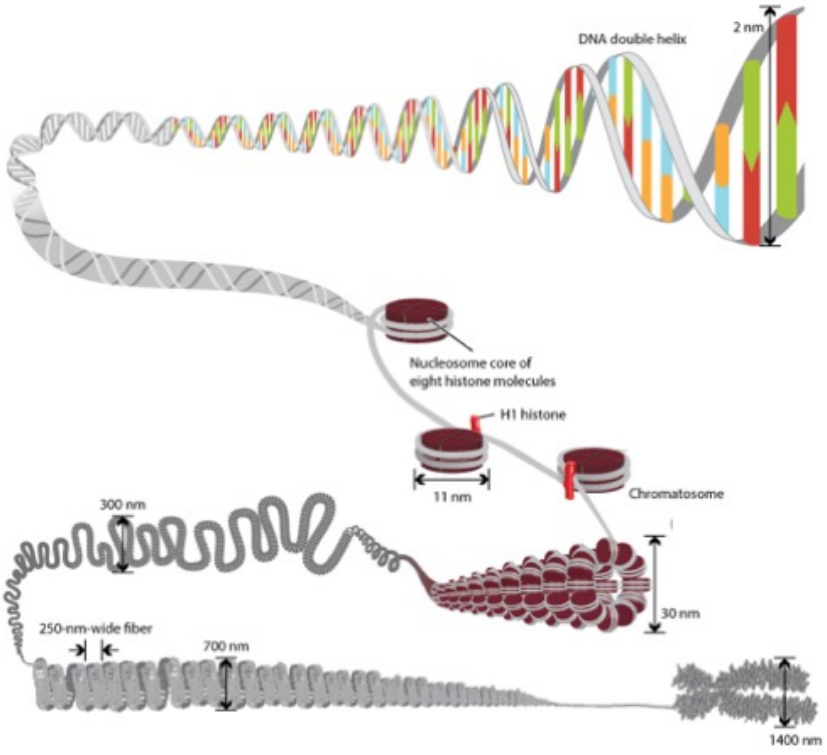

Figure 2. DNA is packed into chromatin.

DNA is wrapped around an octamer of histone proteins to form a nucleosome. Nucleosomes are then condensed into 30nm fiber, which in turn is packed into chromosomes during mitosis. Adapted from Annunziato 2008

Chromatin has a repetitive structure formed by chromatosomes, separated from each other by approximately 140 – 220 bp of linker DNA, thus forming a "beads-on-a-string" structure resembling a pearl necklace. This packaging causes a sevenfold shortening of the DNA fiber, that means a reduction from 1 meter to 14 centimeters long. Nonetheless, this is still not enough to compact the diploid genome into the nucleus. The pearl necklace-like fiber is therefore further condensed into a "30-nanometer fiber" that forms loops averaging 300 nm in length (Figure 2). Finally, in order to partition DNA into daughter cells, during mitosis DNA is highly condensed into the classic chromosomes that can be observed with a light microscope.

Depending on its level of compaction, chromatin is classified either as euchromatin or heterochromatin. Euchromatin is a lightly packed chromatin ("beads-on-a-string") enriched for genes that are actively transcribed or "poised" for transcription and represents the 93% of the human genome (Consortium, 2004). On the contrary, heterochromatin is tightly packed ("30nm fiber") and is therefore refractory to transcription.

The core histones proteins, implicated in the formation of the octamer, are well conserved in eukaryotes. They have a molecular weight ranging from 11 to 15 kDa and have an N-terminal tail particularly rich in lysine and arginine residues, which makes histones positively charged proteins. For this reason, the N-terminal tails can wrap and tightly bind DNA and are implicated in nucleosome-nucleosome interactions. Moreover, many of their residues are subjected to extensive post-translational modification (PTM).

Chromatin plays a fundamental structural role, but it is not only a packaging tool. Chromatin is a dynamic entity that can influence gene expression by allowing DNA accessibility to transcription factors or denying them access to a particular locus compacting the DNA with nucleosomes. Chromatin, indeed, can assume different conformations that reflect the

regulatory cues necessary for the activation or inactivation of appropriate cellular pathways (Margueron and Reinberg, 2010). The normal arrangement and distribution of nucleosome on the "beads-on-a-string" configuration can be altered by *cis*-effects and *trans*-effects of modified histone tails (Figure 3). *Cis*-effects are referred to changes in physical proprieties of modified histone tails that alters the contacts between the histone itself and the DNA or between different nucleosomes (Goldberg et al., 2007). A very well-known example of *cis*-effect is histone, acetylation that neutralize the positive charges of the highly basic histone tails, locally decondensing the chromatin fiber and enabling the access of the transcription machinery to the double helix DNA. Conversely, *trans*-effect is referred to the recruitment of modification-binding proteins to chromatin. In this case, a protein that is able to "read" a particular histone PTM could be part of a much larger enzymatic complex that needs to be recruited on chromatin.

Histone modifications on both the core (Cosgrove et al., 2004) and the tail regions can recruit on the "beads-on-a-string" chromatin also ATP-dependent remodeling complexes. These enzymes use the energy obtained by ATP hydrolyzation to mobilize nucleosome by phasing and spacing, altering the path of DNA wrapped around the nucleosome. Chromatin remodeling complexes can also alter the nucleosome structure by DNA looping or by replacing histone core proteins with histone variants (Clapier et al., 2017). These non-covalent mechanisms are important for gene regulation as much as the covalent modifications of histone proteins (Narlikar et al., 2002). Chromatin-remodeling enzymes can be divided into two families: the SNF2H/ISWI family that mobilizes nucleosomes along the DNA (Tsukiyama et al., 1995; Varga-Weisz et al., 1997) and the SWI/SNF family for which the mechanism of action is still debated.

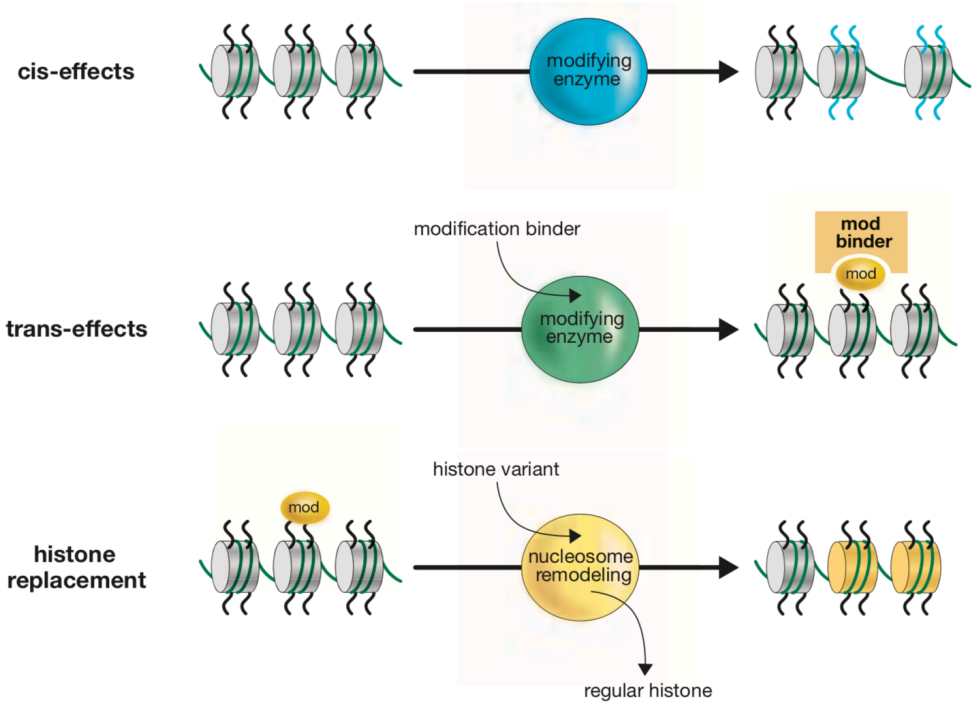

Figure 3. Chromatin transitions (cis/trans).

Covalent modifications of histones that cause an alteration in chromatin structure or charge, resulting in a change in chromatin organization are considered *cis*-effects. The recruitment of a high-affinity mod binder protein that imposes downstream chromatin alterations are considered t*rans*-effects. A histone modification (or another stimulus) could induce also the replacement of a histone protein with a particular histone variant through a nucleosome remodeling complex. Adapted from Allis 2015.

As anticipated, the possibility to incorporate specialized histone variants that differ in the amino-acid sequence from canonical histone proteins contributes to chromatin dynamics. Several histone variants exist (Figure 4) but often represent a minor proportion of the bulk histones present in a cell. Every variant has a particular function and can influence the chromatin landscape of the locus in which it is deposited. H3.3 variant, for example, is found in transcriptionally active genes while CENP-A, another histone H3 variant, is found in centromeric regions and is fundamental for chromosome segregation (Tachiwana et al., 2011). H2A.X is involved in the sensing of DNA damage, indexing the DNA lesion for the

recruitment of DNA repair complexes, while H2A.Z is involved in the regulation of gene transcriptional activity (Buschbeck and Hake, 2017).

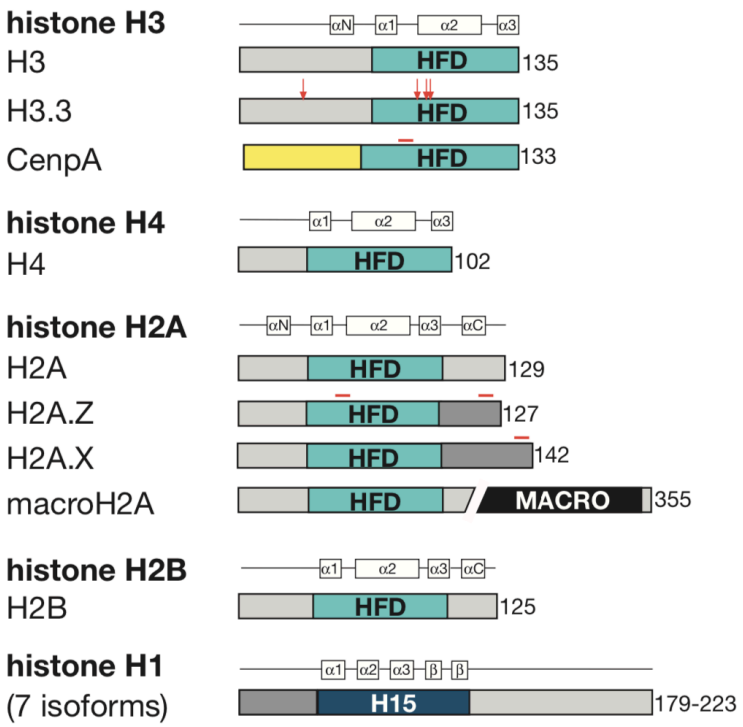

Figure 4. Histone variants.

Protein domain structure of the core histones and of their variants. Regions of the variant protein that differs from the core histone are indicated in red. HFD is histone fold domain. Adapted from Allis 2015.

Histone modifications can have both *cis*- and *trans*-effects on chromatin, and these effects translate into biological outputs. Patterns of histone tail modifications result in "on" or "off" chromatin state, correlating histone modifications with transcriptional regulation. Certain modifications, like acetylation, are associated with chromatin regions permissive to transcription. On the contrary, phosphorylation or methylation of particular residues are generally associate with inactive or heterochromatic regions. Histone PTMs are reversible modifications that can be dynamically established and removed in order to respond to biological stimuli. Proteins that take part in this epigenetic regulation can be generally divided into three families: the enzymes that place the modifications are called "writers",

those that remove them are the "erasers" while proteins that recognize the modifications are the "readers" (Falkenberg and Johnstone, 2014) (Figure 5). Many of these enzymes have a remarkable specificity for only one or few residues but they often reside within large multi-subunits complexes that can catalyze different reactions, altering the epigenetic landscape of the locus in which are recruited. The action of every epigenetic modifier complex is counter-balanced by another one and these antagonistic activities regulate the steady-state balance of each PTM. For example, several histone acetylases (HATs) exist; HATs acetylate specific lysine residue in histone (Roth et al., 2001) and non-histone substrates and their action is reversed by histone deacetylases (HDACs) (Seto and Yoshida, 2014). Similarly, two classes of methyltransferases have been described: the protein arginine methyltransferases (PRMTs) (Bedford and Clarke, 2009) and the histone lysine methyltransferases (KMTs) (Lachner et al., 2003). Even if it's a modification more stable compared to acetylation, also histone methylation can be removed by several demethylases (Pedersen and Helin, 2010; Thinnes et al., 2014).

Altogether, chromatin modifications, their dynamics and their final influence on transcription suggested the existence of a possible "histone code" or even an "epigenetic code" that, however, it's less conserved and less universal compared to the genetic code. Even if the existence of a real histone code is still debated, histone modifications profiling is a useful tool to indirectly infer the transcriptional status of genes but also, and mainly, to pinpoint different regulatory regions along the genome (enhancers, insulators, ecc…).

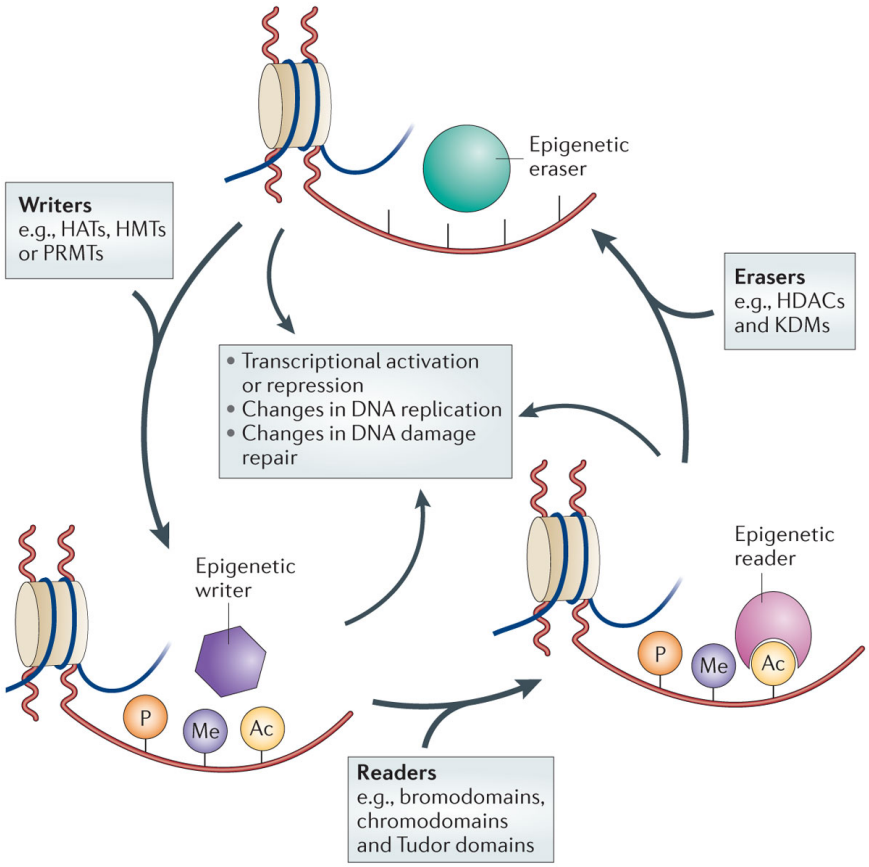

Figure 5. Writers, readers and erasers.

Epigenetic regulation is a dynamic process. Epigenetic writers (e.g. HATs, HMTs and PRMTs) are able to lay down histone and DNA modifications. Proteins containing particular domains as bromodomain, chromodomain or Tudor domain are able to "read" the modifications while proteins like HDACs and KDMs catalyze the removal of these modifications. Adapted from Falkenberg 2014.

4. Histone modifications

The most striking feature of histones is the large number and type of modified residues they possess. Several distinct types of modifications exist, but the most studied are acetylation, methylation, phosphorylation, ubiquitination and sumoylation (Figure 6).

While DNA methylation is usually associated with repression of transcription, histone PTMs can be associated with both transcriptional repression and activation. As already described, histone acetylation by HATs is associated with active transcription because it locally decondenses chromatin, allowing access of transcription factors to regulatory elements of

genes. Most of the acetylated residues are in the N-terminal tails, but few acetylated residues have been found also on the core domain of histones (e.g. H3K56, H3K64 and H3K122) (Di Cerbo et al., 2014; Tropberger et al., 2013; Xu et al., 2005). The action of HATs is counter-balanced by HDACs that, deacetylating histone lysines, induce the compaction of chromatin denying access to DNA and resulting in repression of transcription (Thiagalingam et al., 2003).

Chromatin Modifications	Residues Modified	Functions Regulated
Acetylation	**K**-ac	Transcription, Repair, Replication, Condensation
Methylation (lysines)	**K**-me1 **K**-me2 **K**-me3	Transcription, Repair
Methylation (arginines)	**R**-me1 **R**-me2a **R**-me2s	Transcription
Phosphorylation	**S**-ph **T**-ph	Transcription, Repair, Condensation
Ubiquitylation	**K**-ub	Transcription, Repair
Sumoylation	**K**-su	Transcription
ADP ribosylation	**E**-ar	Transcription
Deimination	**R > Cit**	Transcription
Proline Isomerization	**P-cis > P-trans**	Transcription

Figure 6. Most abundant classes of modifications identified on histones.
Functions associated to each modification is shown. Each modification is discussed in detail in the text. Adapted from Kouzarides 2007.

Differently to acetylation, lysine methylation can be either an active or a repressive mark. Through the most abundant and the most studied residues that can be methylated, 3 are associated with active transcription (H3K4, H3K36 and H3K79) and 3 are associated with repression (H3K9, H3K27 and H3K20). Moreover, methylation can be found in different forms (mono-, di- and tri-methylation) each of which could have a different function. H3K4me1 is widely used as a predictive mark of enhancer (Heintzman et al., 2007), H3K4me3 is enriched at promoters of actively transcribed genes (Liang et al., 2004), while it is still debated whether H3K4me2 is only an intermediate necessary to the final trimethylation or if it has its own

specific role. H3K36 and H3K79 methylation are generally found on the gene body of actively transcribed genes and could have a role in the stabilization of the elongation machinery and in the suppression of inappropriate initiation from cryptic start sites within the coding region (Carrozza et al., 2005). H3K9 methylation is implicated in the formation of silent heterochromatin by recruiting heterochromatin protein 1 (HP1) (Bannister et al., 2001; Jacobs et al., 2001; Lachner et al., 2001). H3K27 methylation is a hallmark of facultative heterochromatin, it's set down by the Polycomb repressive complex 2 (PRC2) (Margueron et al., 2008) and it's implicated in the maintenance of cell identity. In embryonic stem cells, H3K27me3 is often found in gene promoters concurrently with the active mark H3K4me3 (Bernstein et al., 2006). Due to the presence of both an active and a repressive mark these promoters are called "bivalent" and are generally associated with developmentally regulated genes. These genes are not expressed, but removal of H3K27me3 would result in transcriptional activation while removal of H3K4me3 would result in a more stable repression of the gene. Therefore, the bivalent conformation of their promoters keeps the genes poised for fate determination upon the appropriate differentiation stimulus.

Arginine methylation, like lysine methylation, can exists in several forms, namely mono-methylation (R-me1), symmetric di-methylation (R-me2s) and asymmetric di-methylation (R-me2a), and as lysine methylation, also arginine methylation can have both a positive or a negative effect on transcription (Blanc and Richard, 2017). H4R3me2a, deposited by PRMT1, positively influences transcription by recruiting the acetyltransferase p300/CBP-associated factor complex (Bedford and Clarke, 2009). On the contrary, H3R3me2s and H3R8me2s, deposited by PRMT5, and H3R8me2a, by PRMT6, seem to repress transcription antagonizing the neighboring H3K4me3 and preventing the association of the Mixed Lineage Leukemia (MLL) complex (Guccione et al., 2007). The effects of arginine methylation can be obstructed

and by some means antagonized by deimination, the conversion of an arginine into a citrulline mediated by the enzyme PADI4 (Cuthbert et al., 2004).

Histone phosphorylation is a highly dynamic process and can occur on serine, threonine and tyrosine residues. Histone phosphorylation plays a central role in DNA-damage sensing and repair as phosphorylation of the histone H2AX is one of the first events in the DNA-damage response cascade. Although this is its most studied role, histone phosphorylation of certain residues can also positively influence transcription, in particular of proliferation-related genes. Phosphorylation of H2BS32, H3S10 and H3S28 is associated with active transcription of EGF-responsive genes. H2BS32ph and H3S10ph are also linked to the expression of *c-fos* and *c-jun* (Rossetto et al., 2012).

Another component of the histone code is ubiquitylation of C-terminal of histones H2A (K119) and H2B (K120 in human, K123 in yeasts). This modification needs the sequential action of three enzymes (E1, E2 and E3) of which the last one (E3) is the ligase, and it is removed by de-ubiquitin isopeptidases. H2AK119 ubiquitylation is mediated by the Polycomb repressive complex 1 (PRC1), in particular by the proteins Bmi/RING1 (Wang et al., 2004a) and is associated with transcriptional repression and facultative heterochromatin formation. Conversely, ubiquitylation of H2BK120 seems to be an activatory signal for transcription (Zhu et al., 2005).

Sumoylation, like ubiquitylation, is a very large modification. Taking place in some specific lysine residues, this modification antagonizes acetylation of the same residues and consequently has been linked to transcriptional repression (Nathan et al., 2006). The small ubiquitin-related modifier (SUMO) can also indirectly influence chromatin sumoylating other histone modifiers, as HDACs. Sumoylation of HDAC1 for example increases its deacetylase activity and therefore its repressive activity (David et al., 2002).

ADP-ribosylation occurs on histone arginine and glutamine residues and can be mono- or poly-. Mono-ADP-ribosyltransferases (MARTs) and poly-ADP-ribose polymerases (PARPs) are the enzymes responsible for the deposition of the modification, while its removal is carried out by poly-ADP-ribose-glycohydrolases. ADP-ribosylation is generally associated with active transcription (Martinez-Zamudio and Ha, 2012; Messner and Hottiger, 2011).

All these modifications and many more constitute the basal elements of the histone code hypothesis and the several possible combinations and interplay between them result in different downstream effects. There are different ways by which one modification could influence another one. Two modifications can compete for the same residue: H3K27, for example, cannot be acetylated and methylated at the same time on the same histone tail but it's still debated whether they could co-exist in the same nucleosome. Another way is the dependency of one modification from another one: for example, in the canonical interpretation of Polycomb proteins model of action, H2AK119Ub is laid down by PRC1 that is able to read the H3K27me3 modification through its CBXs proteins; in this way, H2AK119Ub is consequential to H3K27me3. A particular modification could also enhance or disturb the binding of a protein to another residue. An example is the aforementioned case of H3R3 and H3R8 methylation that prevents H3K4 methylation by the MLL complex (Guccione et al., 2007).

Extensive analysis of cancer genomes over the last decades revealed that epigenetic players are highly mutated in almost all cancer types and this reflects on the global epigenetic landscape, establishing a causal role for epigenetic dysregulation in tumor initiation and progression (Dawson, 2017). Chromatin can be interpreted as a barrier to cell fate and cell identity plasticity that can be overtaken only with the proper stimulus. Global alteration in

chromatin that occurs in cancer can lead to either restrictive or over permissive chromatin states (Flavahan et al., 2017) (Figure 7).

Cancer epigenome alterations can be due not only by genetic mutations in epigenetic regulators, but also by their aberrant expression. Overexpression of HDACs in many cancer types leads to general histone hypoacetylation and consequently to abnormal transcriptional repression (Li and Seto, 2016). Global histone methylation pattern is also often altered in cancer cells. Increase in H3K9 and H3K27 methylation lead to aberrant repression of key genes, as well as hypomethylation of H3K4 (Cloos et al., 2008). Alterations in the methylation pattern can be mediated by abnormal activity of either histone methyltransferases (HMTs) or the demethylase responsible for the removal of the histone mark. For example, many tumors have an alteration in the global distribution of H3K27me3 due to the overexpression of the methyltransferase EZH2 (Valk-Lingbeek et al., 2004). The H3K4 demethylases LSD1 and the Jumonji C family are frequently overexpressed as well in tumors (Hosseini and Minucci, 2017).

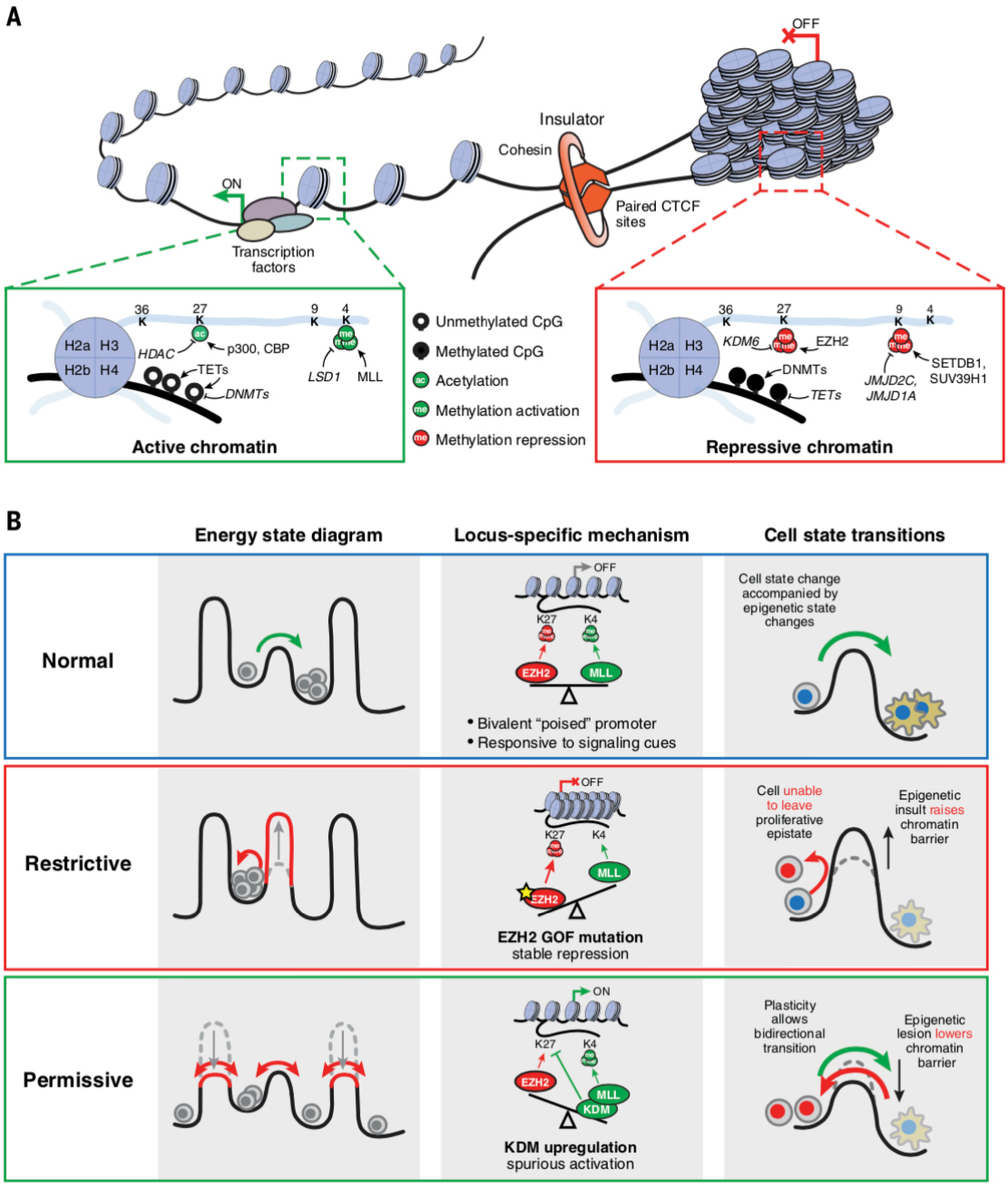

Figure 7. Histone modifications affect cellular identity and state transitions

. **A)** Chromatin can adopt active and repressive states. Active state is mainly characterized by H3K4me3 and H3K27ac, while repressive state by H3K9me3 and H3K27me3. **B)** Chromatin states affect cellular responsiveness to intrinsic or extrinsic cues. Perturbed chromatin due to dysregulation of epigenetic modifiers can lead to either restrictive or overly permissive chromatin states. Adapted from Flavahan 2017.

5. Histone methylation

Although the involvement of histone methylation in transcriptional regulation was first reported more than 50 years ago (ALLFREY et al., 1964), the first histone methyltransferase (SUV39H1) was first discovered in the 2000 (Rea et al., 2000). Unlike other marks, histone methylation was thought to be an irreversible modification until the discovery of LSD1, an H3K4 demethylase (Shi et al., 2004). Now, a multitude of methyltransferases and demethylases has been identified (Figures 8 and 9).

5.1 Histone methyltransferases

Histone methyltransferases can be divided into lysine methyltransferases (KMTs) and arginine methyltransferases (PRMTs). All methyltransferases use the cofactor S-adenosyl-L-methionine (SAM) as a donor of the methyl group and transfer it to either the ε-amino group of lysine or to the arginine guanidino group.

The PRMT family is composed of nine members: PRMT1, PRMT2, PRMT3, CARM1, PRMT5, PRMT6, PRMT7, PRMT8 and PRMT10 (Di Lorenzo and Bedford, 2011). PRMTs can be further divided into two classes: type II enzymes (PRMT5, 7 and 9) catalyze mono- and di-methylation (symmetric) of arginines, while type I enzymes (PRMT1, 2, 3, 6, 8 and CARM1) catalyze mono- and asymmetric di-methylation.

Even KMTs are divided into two families: the SET domain class that contains the 130-aminoacid catalytic domain SET (Su(var)3-9, Enhancer of Zeste, Tritorax), and the DOT1L class that does not contain the SET domain (Allis CD et al., 2015). DOT1L is responsible for the deposition of both mono-, di- and tri-methylation of H3K79 that, differently from other methylations, occurs on the core domain of histone H3 (Nguyen and Zhang, 2011). The SET

domain containing proteins form a large family of more than twenty members responsible of all the other lysine methylations.

Histone and residue	*Homo sapiens*		
	me3	me2	me1
H3R2		CARM1(a); PRMT6(a)*; PRMT5(s); PRMT7(s)‡	CARM1; PRMT6*; PRMT5; PRMT7
H3K4	SETD1A; SETD1B; ASH1L; MLL; MLL2; MLL3; MLL4; SMYD3§; PRMD9	SETD1A; SETD1B; MLL; MLL2; MLL3; MLL4; SMYD3§	SETD1A; SETD1B; ASH1L§; MLL; MLL2; MLL3: MLL4; SETD7
H3R8		PRMT5(s)	PRMT5
H3K9	SUV39H1; SUV39H2; SETDB1; PRDM2§	SUV39H1; SUV39H2; SETDB1; G9a; EHMT1; PRDM2§	SETDB1; G9a; EHMT1; PRDM2§
H3R17		CARM1(a)	CARM1
H3R26		CARM1(a)	CARM1
H3K27	EZH2; EZH1	EZH2; EZH1	
H3K36	SETD2	NSD3; NSD2; NSD1; SMYD2§; SETD2	SETD2; NSD3; NSD2; NSD1;
H3K79	DOT1L	DOT1L	DOT1L
H4R3		PRMT1(a); PRMT6(a)*; PRMT5(s); PRMT7(s)‡	PRMT1; PRMT6*; PRMT5; PRMT7
H4K20	SUV420H1; SUV420H2	SUV420H1; SUV420H2	SETD8

Figure 8. Histones lysine and arginine methyltransferases.

Histone methyltransferases of each residue are indicated, divided in column for their degree of methylation (me3, me2 and me1). Some arginine methyltransferases preferentially establish symmetric (s) or asymmetric (a) methylation. *PRMT6 can also methylate H2AR3 and H2AR29. Adapted from Greer 2012.

Methylated H3K4 is generally associated with active transcription and with open chromatin that allows access to transcription factors. In humans there are at least thirteen H3K4 methyltransferases: MLL (KMT2A), MLL2 (KMT2D, MLL3 (KMT2C), MLL4 (KMT2B), MLL5 (KMT2E), ASH1 (KMT2H), SET7/9 (KMT7), SET1A (KMT2F), SET1B (KMT2G), SMYD1 (KMT3D), SMYD2 (KMT3C), SMYD3 (KMT3E) and PRDM9 (KMT8B) (Copeland et al., 2009; Greer and Shi, 2012; Kouzarides, 2007; Ruthenburg et al., 2007). H3K4 methyltransferases are gene expression activators.

H3K9 methylation is associated with silent chromatin and gene repression and is generally recognized as an heterochromatin hallmark. Seven H3K9 methyltransferases have been identified so far: G9a (KMT1C), GLP (KMT1D), SUV39H1 (KMT1A), SUV39H2 (KMT1B), SETDB1 (KMT1E), SETDB2 (KMT1F) and PRDM2 (KMT8).

The KMTs responsible for the methylation of H3K27 are called EZH1 and EZH2 (Enhancer of Zeste) and are the catalytic members of the Polycomb repressive complex 2 (PRC2). H3K27 methylation is associated with gene repression, but conversely to H3K9me3, it's mainly present on facultative heterochromatin and on genes responsible for cell identity and development (Margueron et al., 2008).

The active mark H3K36 is catalyzed by at least six methyltransferases: NSD1 (KMT3B), NSD2 (KMT3F), NSD3 (KMT3G), SMYD2 (KMT3C), SETD2 (KMT3A) and SETMAR (Li et al., 2009).

As aforementioned, lysine residues can be either mono-, di- or trimethylated but none of them results in an alteration of the electronic charge of the histone tail. This means that histone methylation has primarily *trans*-effects on chromatin by recruiting effector proteins able to recognize the specific methylated lysine. Methylation readers can often discriminate not only the modified residue but also the mono-, di- or trimethylated status of the residue.

The methylation-reader domains are the so called PHD, chromo, tudor, PWWP, WD40, BAH, ADD, ankyrin repeat, MBT and zn-CW domains (Hyun et al., 2017).

5.2 Histone demethylases

To date, arginine demethylases remain elusive. JMJD6, a demethylase containing the Jumonji domain, has been initially described as an arginine demethylase (Chang et al., 2007) but a more recent work indicates the hydroxylation of an RNA-splicing factor as its primary catalytic activity (Webby et al., 2009). However, even if it's not a demethylase, the protein arginine deiminase type 4 (PADI4) can antagonize the effects of arginine methylation by converting mono-methyl-arginine residues into citrulline (Cuthbert et al., 2004; Wang et al., 2004b).

Similar to KMTs, also lysine demethylases (KDMs) can be divided into two different classes: the LSD1 family, composed by the FAD-dependent amino oxidase (Mosammaparast and Shi, 2010) LSD1 and LSD2 (KDM1A and KDM1B), and the Jumonji domain containing family, composed by more than 30 proteins, that are Fe(II) and 2-oxoglutarate-dependent enzymes (Hausinger, 2004; Klose and Zhang, 2007) (Figure 9). KDMs generally have a high substrate specificity and some of them are able to discriminate between the different degree of methylation. LSD1 and LSD2, for example, can only demethylate the di- and monomethyl form of lysine residues, while Jumonji containing proteins can usually demethylate also the trimethylated form.

Since lysine methylation can be associated with both transcriptional activation and repression, KDMs can be either activators or repressors depending on their particular lysine substrate. For this reason, the following KDMs acting on H3K4 are considered transcriptional

repressor: LSD1 (KDM1A), LSD2 (KDM1B), JHMD1B (KDM2B), JARID1A (KDM5A), JARID1B (KDM5B), JARID1C (KDM5C) and JARID1D (KDM5D).

Lysine 9 of histone H3 can be demethylated by seven KDMs: LSD1 (KDM1A), JHDM2A (KDM3A), JHMD2B (KDM3B), JHDM3A (KDM4A), JMJD2B (KDM4B), JMJD2C (KDM4C) and JMJD2D (KDM4D). Methylation of H3K36 is erased by: JHMD1A (KDM2A), JHMD1B (KDM2B), JHMD3A (KDM3A), JMJD2B (KDM4B), JMJD2C (KDM4C) and JMJD5 (KDM8).

Histone and residue	*Homo sapiens*		
	me3	me2	me1
H3R2			
H3K4	KDM2B; KDM5A; KDM5B; KDM5C; KDM5D; NO66	KDM1A; KDM1B; KDM5A; KDM5B; KDM5C; KDM5D; NO66	KDM1A; KDM1B; KDM5B; NO66
H3R8			
H3K9	KDM3B[§]; KDM4A; KDM4B; KDM4C; KDM4D	KDM3A; KDM3B[§]; KDM4A; KDM4B; KDM4C; KDM4D; PHF8; KDM1A; JHDM1D	KDM3A; KDM3B[§]; PHF8; JHDM1D
H3R17			
H3R26			
H3K27	KDM6A; KDM6B;	KDM6A; KDM6B; JHDM1D	JHDM1D
H3K36	NO66; KDM4A; KDM4B; KDM4C	KDM2A; NO66; KDM2B; KDM4A; KDM4B; KDM4C	KDM2A; KDM2B
H3K79			
H4R3			
H4K20			PHF8

Figure 9. Histone lysine and arginine methyltransferases.

Histone demethylases of each residue are indicated, divided in column for their degree of methylation (me3, me2 and me1). Adapted from Greer 2012.

H3K27 methylation is removed by UTX (KDM6A) and JMJD3 (KDM6B) and results in transcriptional activation. UTX and JMJD3 counterbalance the action of EZH1/2, the catalytic components of PRC2, in order to finely regulate H3K27 methylation levels. H3K27 methylation seems to be central in the regulation of several biological processes, *in primis* development, and genetic and non-genetic alterations in proteins that regulate its levels are commonly found in cancer.

6. Lysine Specific Demethylase 1 (LSD1)

The catalytic activity of Lysine Specific Demethylase 1 (LSD1, also KDM1A or AOF2) was discovered in the 2004 (Shi et al., 2004) and LSD1 was the first demethylase reported. From that moment, a plethora of other demethylases have been described. The discovery of LSD1 catalytic activity completely changed the biological interpretation of histone methylation; conversely to the dynamic histone acetylation, histone methylation was thought to be a stable and static modification. From the discovery of LSD1, histone methylation became as dynamic as acetylation.

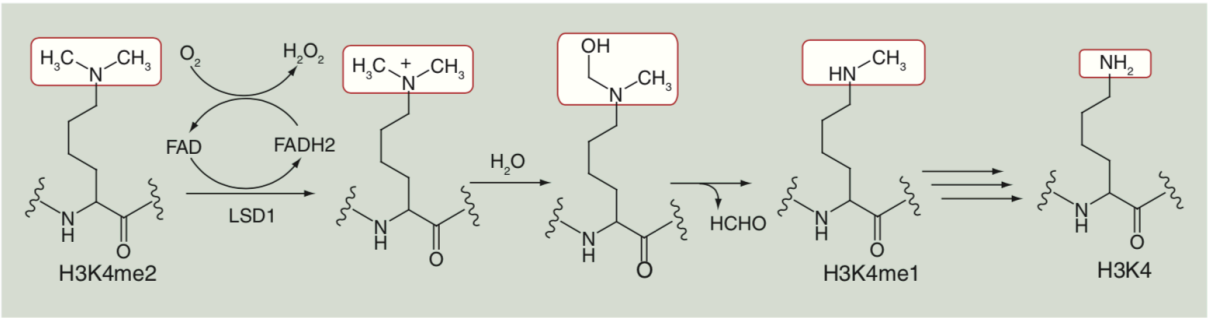

Figure 10. Mechanism of LSD1 catalysis.

Adapted from Zheng 2016.

LSD1 is a flavin containing amino oxidase that catalyzes the cleavage of the α-carbon bond of methylated lysine to generate an imine intermediate by reducing the cofactor FAD. The imine intermediate hydrolyzes and releases a formaldehyde molecule (Edmondson et al., 2007; Forneris et al., 2005) (Figure 10). In this way, LSD1 removes one by one the methyl group from dimethyl- and monomethyl- H3K4, but it's not able to remove the methyl group from the trimethylated form (Zheng et al., 2016).

LSD1 protein is highly conserved throughout different organisms, from yeasts to humans (Mosammaparast and Shi, 2010). It is composed of 833 amino acids and its structure can be divided into three main domains: the SWIRM (SWI3p/Rsc8p/Moira) domain, the C-terminal AOL (Amino-Oxidase Like) domain and the Tower domain (Chen et al., 2006) (Figure 11).

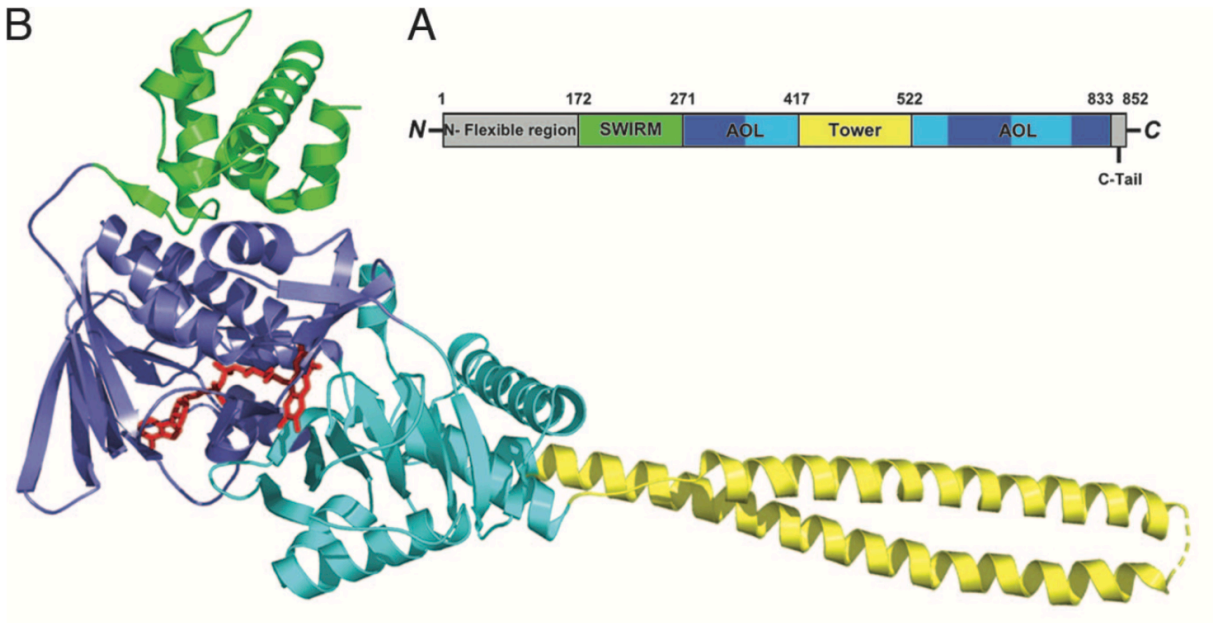

Figure 11. Structure of LSD1.

A) The SWIRM domain is shown in green, the AOL domain in blue (FAD-binding sub-domain dark blue, substrate binding sub-domain light blue) and the Tower domain in yellow. **B)** Ribbon diagram of the structure of LSD1. The protein is colored as in A. Adapted from Chen 2006.

SWIRM and AOL domains closely interact each other and pack together to form a globular structure. The Tower domain, included into the AOL domain, protrudes from the AOL-SWIRM globular structure. The AOL domain can be further divided into two sub-domains: a FAD-binding domain that is similar to other amino oxidases (Rotili and Mai, 2011), and a substrate-binding domain that gives the substrate specificity and that contains the catalytic chamber. Point mutations in the catalytic chamber influence the activity of LSD1 (Chen et al., 2006; Stavropoulos et al., 2006). In particular, K661 is the crucial element of the catalytic center and a point mutation in this residue completely abolishes the demethylation activity of LSD1 (Chen et al., 2006). The Tower domain is critical for LSD1 activity because it mediates the interaction between LSD1 and CoREST, its main interactor. Intriguingly, LSD1 alone is able to demethylate peptides and bulk histones *in vitro*, but it's not able to do it on nucleosomes; only in complex with CoREST (RCOR1), LSD1 efficiently demethylases H3K4 on nucleosomes (Hou and Yu, 2010; Lee et al., 2005; Shi et al., 2005). Finally, the SWIRM domain stabilizes the globular structure and the protein itself since removal of the SWIRM domain renders the protein insoluble when expressed in *E. coli* (Stavropoulos et al., 2006). SWIRM domain of other histone modifier proteins shows DNA binding ability due to a positively charged patch located on the surface of the SWIRM domain. This positive patch is not well conserved in LSD1 and this explains the absence of LSD1 DNA binding ability (Chen et al., 2006; Stavropoulos et al., 2006).

6.1 Context-dependent LSD1 functions

LSD1 plays a central role in several biological processes, from embryonic development, differentiation, control of stemness to epithelial-to-mesenchymal transition (EMT) and metabolism. In order to participate in the regulation of all these processes LSD1 interacts

with other proteins and contributes in the formation of different multi-protein complexes, in a context-dependent manner. In this way, LSD1 can be directed to disparate genomic loci regulating the expression of different genes. Moreover, LSD1, when in complex with androgen and estrogen receptors, can change its substrate specificity to H3K9, becoming a transcriptional activator (Metzger et al., 2005).

Alternative splicing is another mechanism that regulates LSD1 activities. Four LSD1 isoforms have been described so far that result from different splicing and incorporation of exon E2a and E8a. While E2a splicing occurs in all tissues, the E8a isoform displays a neuro-specific expression pattern and contributes to the proper neurite morphogenesis during early phases of cortical development (Toffolo et al., 2014; Zibetti et al., 2010). Moreover, has been reported a change of the neuro-specific LSD1 isoform substrate from H3K4 to H3K9 (Laurent et al., 2015) and to H4K20 (Wang et al., 2015), altering the transcriptional readout of its activity.

Additionally, LSD1 catalytic activity can be influenced by other histone modifications: H3K9 acetylation and H3S10 phosphorylation, for example, negatively affect its H3K4 demethylase activity (Amente et al., 2013; Shi et al., 2005).

6.2 LSD1 as transcriptional repressor

The most common transcriptional repressor complexes of which LSD1 is a member are CoREST and NURD (Hakimi et al., 2003; Wang et al., 2009b) (Figure 12). Both complexes include also HDAC1 and HDAC2 and for this reason are able to change the general conformation and accessibility of chromatin by both demethylating H3K4me2/1 and deacetylating histones.

LSD1, and all the LSD1-containing complexes, are recruited on chromatin by several transcription factors. Indeed, since LSD1 does not have the ability to recognize any particular DNA sequence, the transcription factor gives the locus-specificity for LSD1 action. For example, LSD1 is able to recognize and to bind the SNAG domain of the transcription factors GFI1, GFI1b, SNAI1, SNAI2 and INSM1. By mimicking the N-terminal histone H3 tail, the SNAG domain can interact with LSD1 by entering the catalytic pocket of the enzyme (Lin et al., 2010b).

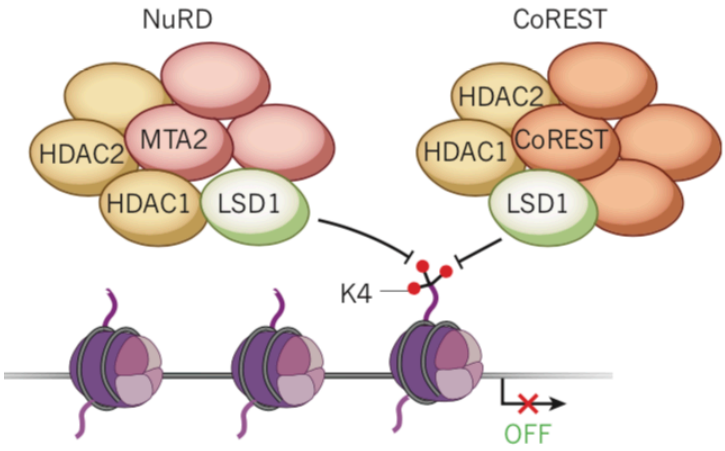

Figure 12. LSD1 as transcriptional repressor.

When part of CoREST complex and NuRD complex, LSD1 catalyzes the demethylation of H3K4me2 and H3K4me1, acting as a transcriptional repressor. Adapted from Helin 2013.

6.2.1 Role of LSD1 in the hematopoietic system

During embryonic hematopoiesis, hematopoietic stem cells (HSCs) develop from endothelium through a trans-differentiation process called Endothelium-to-Hematopoietic transition (EHT). LSD1 promotes the expansion of hematopoietic progenitors by downregulating *Etv2,* an important inducer of EHT (Takeuchi et al., 2015). Later, LSD1

regulates HSCs generation and maturation by interacting with the transcription factors GFI1 and GFI1b that orchestrate these processes (Thambyrajah et al., 2016).

In vivo conditional knock-out of LSD1 in the hematopoietic system of adult mice causes a loss of HSCs self-renewal and an impairment of HSCs differentiation toward granulocytes and erythrocytes (Kerenyi et al., 2013). In HSCs and hematopoietic progenitors, LSD1 interacts with the zinc-finger transcription factor SALL4 and contributes to the regulation of SALL4 targets genes by reducing H3K4 methylation at their promoters (Liu et al., 2013). During hematopoietic differentiation LSD1 interacts with TAL1 and GATA2 to regulate erythroid differentiation (Guo et al., 2016; Hu et al., 2009; Li et al., 2012) and with GFI and GFI1b, which govern granulocytic, erythroid and megakaryocytic differentiation (Saleque et al., 2007).

In addition to CoREST (RCOR1), hematopoietic cells express also its two paralogs RCOR2 and RCOR3. While RCOR2 has the same function of RCOR1, RCOR3 inhibits the demethylating activity of LSD1. By competing for the binding of LSD1, RCOR1/2 and RCOR3 ultimately regulates the differentiation status of hematopoietic cells (Upadhyay et al., 2014).

6.2.2 Role of LSD1 in development

LSD1 is fundamental for the correct development of higher eukaryotes since genetic deletion of LSD1 in mice results in embryonic lethality before embryonic day 7.5 (Wang et al., 2007). LSD1 is highly expressed in embryonic stem cells (ESCs) but its expression diminishes during differentiation. In particular, LSD1 maintains the pluripotency and self-renewal of ESCs by regulating the balance between H3K4 and H3K27 methylation of regulatory regions of key genes such as BMP2 and FOXA2 and knockdown of LSD1 induces differentiation of ESCs (Adamo et al., 2011).

Modulating TLX signaling and demethylating TLX target genes, LSD1 participates in the regulation of neural stem cell proliferation and differentiation; TLX targets demethylated by LSD1 include the suppressor gene PTEN and the cyclin-dependent kinase inhibitor p21 (Ballas et al., 2005; Hakimi et al., 2002). Immoderate repression of PTEN by TLX-LSD1-CoREST complex is at the base of the uncontrolled proliferation of Y79 retinoblastoma cells (Yokoyama et al., 2008).

In addition, LSD1 participates in the maintenance of several other type of adult stem cells and in their proper differentiation (Choi et al., 2010; Kim et al., 2015; Musri et al., 2010; Wang et al., 2007).

6.2.3 Role of LSD1 in Epithelial-to-Mesenchymal Transition (EMT)

The process by which an epithelial cell abandons its phenotype and acquires mesenchymal features is called Epithelial-to-Mesenchymal Transition (EMT) and is a process required for cancer cell invasion and metastasis (Lamouille et al., 2014). One of the key transcription factors that governs the EMT process is SNAI1 that, as aforementioned, possesses an N-terminal SNAG domain through which interacts with LSD1. In this way SNAI1 recruits LSD1 on chromatin and represses the transcription of its target genes (Lin et al., 2010a). Inhibition of SNAI1/LSD1 interaction reactivates SNAI1 target genes expression and blocks cancer cell invasion (Ferrari-Amorotti et al., 2013).

6.3 LSD1 as transcriptional activator

When LSD1 interacts with androgen or estrogen receptors switches its substrate specificity from H3K4 to H3K9 (Garcia-Bassets et al., 2007; Metzger et al., 2005). H3K9 methylation is generally associated with heterochromatin and gene repression: by removing this histone

mark LSD1 becomes a transcriptional co-activator (Figure 13). It has been proposed that interaction with androgen and estrogen receptor could change the structural conformation of the catalytic chamber of SWIRM domain, but the precise mechanism is still to be clarified. In addition, when interacting with androgen receptor, LSD1 can form a complex with other H3K9 specific demethylases. For example, in prostate cancer androgen receptor, LSD1 and JMJD2 colocalize at the same genomic loci and the two enzymes collaborate to demethylase H3K9 residues (Wissmann et al., 2007).

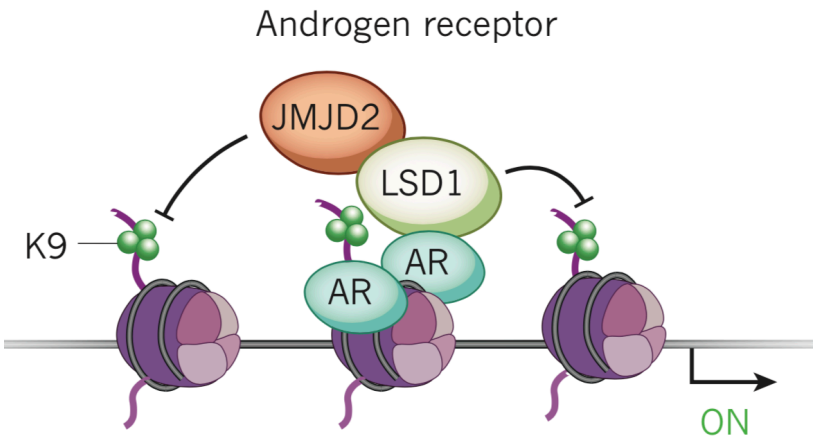

Figure 13. LSD1 as transcriptional activator.

When associated with androgen (or estrogen) receptor, together with JMJD2, LSD1 is responsible for the demethylation of H3K9me2 and H3K9me1. Adapted from Helin 2013.

6.4 Non-histone substrates of LSD1

LSD1 is able to demethylate also non-histone proteins as p53, DNMT1, E2F1, STAT3 and the myosin phosphatase MYPT1, regulating their activities (Cho et al., 2011; Huang et al., 2007; Kontaki and Talianidis, 2010; Wang et al., 2009b; Yang et al., 2010). P53 can be mono- and di-methylated at lysine 370. K370 di-methylation is fundamental for the association of p53 with its coactivator 53BP1. By removing methylation from K370, LSD1 represses p53 pro-apoptotic functions disrupting its interaction with 53BP1 (Huang et al., 2007). Interestingly,

in p53 deficient cells, LSD1 has a completely opposite role in the regulation of apoptosis in response to DNA damage. E2F1 protein levels accumulate in response to DNA-damage and activate its pro-apoptotic target p73. Lysine methylation of E2F1 prevents its ubiquitination and its consequent degradation. LSD1, by demethylating it, induces degradation of E2F1 and ultimately prevents apoptosis (Kontaki and Talianidis, 2010). LSD1 activity affects also global DNA methylation. Since methylation of DNMT1 induces its degradation, LSD1 stabilizes DNMT1 by demethylating it and loss of LSD1 results in a global reduction of DNA methylation (Wang et al., 2009a).

6.5 LSD1 in cancer

High levels of LSD1 protein have been found in several types of cancer such as neuroblastoma, retinoblastoma, prostate, lung, breast cancer and hematological malignancies. Interestingly, the presence of high levels of LSD1 has been proposed as a biomarker of aggressiveness in many of these tumors. Inhibition of LSD1 in breast cancer slows the proliferation rate by inducing expression of p21 (Lim et al., 2010). LSD1 expression directly correlates with cell proliferation also in bladder carcinomas and non-small cell lung cancer (NSCLC), and inhibition or knock-down of LSD1 suppresses cell proliferation (Lan et al., 2013; Mohammad et al., 2015). LSD1 participates in the EMT process in colon and ovarian cancer and its expression is associated with expression of genes that facilitate metastasis. Kock-out of LSD1 in HCT116 colorectal cancer cells stops the cells in G1 phase, reducing their invasiveness and proliferation rate (Huang et al., 2013; Jin et al., 2013).

LSD1 is commonly found overexpressed also in various types of hematological malignancies. Similarly to its role in normal hematopoiesis, LSD1 plays a central role in the regulation of leukemic stem cells (LSCs) by activating LSC associated genes and pathways (Harris et al.,

2012; Somervaille and Cleary, 2006). Knock-down and inhibition of LSD1 result in induction of differentiation, apoptosis and loss of clonogenic activity of leukemic cells, indication of a potential LSC exhaustion. LSD1 depletion and inhibition impair proliferation and induce differentiation also of myelodysplastic syndrome (MDS) cells, acute erythroleukemia and acute megakaryoblastic leukemia cells (Ishikawa et al., 2017; Sugino et al., 2017).

Taken together, these results suggest LSD1 as a potential and intriguing target for novel epigenetic and targeted therapies.

6.6 LSD1 inhibitors

Due to its important role in tumor, LSD1 is an intriguing anti-cancer target. Several inhibitors have been investigated and some of them already entered clinical trials. Since the catalytic domain of LSD1 and monoamine oxidases (MAOs) are very similar, the firsts LSD1 inhibitors were developed starting from the molecular structure of MAO inhibitors. Tranylcypromine, pargyline and phenelzine are the three MAO inhibitors that show also inhibition of LSD1 demethylase activity (Yang et al., 2018). In particular, tranylcypromine (TCP) irreversibly inhibits LSD1 forming a covalent bond to the FAD-binding motif (Yang et al., 2007). To improve its specificity, several tranylcypromine derivates have been synthetized. ORY-1001, an irreversible inhibitor with very low IC_{50} (18nM) and high specificity, entered a phase II clinical trial for AMLs (Maes et al., 2018) while GSK2879552, a selective and orally available inhibitor, showed cell growth inhibition of small cell lung cancer (SCLC) cells and entered a clinical trial for this type of tumor (Mohammad et al., 2015). LSD1 inhibitory activity has been reported also for several natural products. For example, the flavone glycoside Baicalin is a non-covalent inhibitor of LSD1 with an IC_{50} of 3.01μM (Yang et al., 2018). Also resveratrol and geranylgeranoic acid are irreversible inhibitors of LSD1.

Protein-protein interaction (PPI) inhibitors constitute another approach for the generation of novel LSD1 inhibitors. In this direction, inhibitors of LSD1-CoREST and LSD1-SNAIL have been developed and both show enzymatic inhibition and *in vitro* antiproliferative activity against cancer cells (Forneris et al., 2007; Itoh et al., 2016; Kumarasinghe and Woster, 2014).

7. Acute Myeloid Leukemia

Acute myeloid leukemia (AML) is a hematological malignant disorder characterized by the rapid expansion and accumulation of immature myeloid cells in blood and bone marrow. AML represents the 25% of all diagnosed leukemias in adults and is the one with the worst prognosis (Deschler and Lübbert, 2006).

AML is a genetic heterogeneous disorder and, rather than a single disorder, it represents a group of related malignancies characterized by cytological and molecular peculiarities, with different diagnosis, prognosis and treatments. According to the French-American-British (FAB) classification, AML can be divided into 8 different subtypes (from M0 to M7) based on cytological and morphological criteria (Bennett et al., 1976). Although widely used, it is now recognized that a classification based on molecular and cytogenetical criteria could better define prognostic and treatment responsiveness groups (Vardiman et al., 2002). In 2002 the World Health Organization (WHO) published a new AML classification in which 4 molecular/cytogenic-based groups representing the most recurrent abnormalities have been added: AML with t(8:21)(q22;q22) driving the formation of the fusion protein AML1-ETO; AML with chromosome 16 inversion or t(16;16)(p13;q22) which determines the formation of the protein CBFβ-MYH11; AML with abnormalities in the 11q23 region corresponding to the MLL gene; AML with t(15;17) or acute promyelocytic leukemia (APL) with the formation of PML-RARα (Vardiman et al., 2002). All these cytogenetic

rearrangements involve genes encoding transcription factors related to hematopoietic development and lead to the expression of onco-fusion protein with altered features respect to their normal counterpart (Martens and Stunnenberg, 2010). By abnormally interacting with epigenetic modulators, these onco-fusion proteins alter expression of target genes involved in hematopoietic differentiation and create a permissive landscape for leukemic transformation. For example, MLL (KMT2A) is an important epigenetic modulator since directly mediates the methylation of H3K4 and by interacting with other epigenetic regulators acts as a potent transcriptional activator. It is a large multi-domain protein, whose most important are the enzymatic domain SET and the plant homology domain (PHD) through which MLL recruits the acetyltransferase CREB-binding protein (CBP). The MLL gene has been found fused with more than 50 partners which alter the chromatin distribution of the MLL-complex, resulting in an abnormal regulation of MLL target genes (Meyer et al., 2018).

The AML classification has been recently updated in order to integrate novel discoveries in the genomic landscape of the disease (Arber et al., 2016). The panel of recognized recurrent genetic abnormalities has been amplified and the subtypes have been further divided into prognostic risk categories (Döhner et al., 2017) (Table 1). Nevertheless, AML therapeutic approach has not substantially changed in recent years. A single intensive induction cycle of "7+3" regiment (7 days of cytarabine and 3 of anthracycline) is sufficient to induce complete remission (CR) in more than 50% of patients. If CR is not achieved after the first cycle, a second cycle can be administered. Post-remission therapy consists of an intensive myeloablative cycle of cytarabine followed by allogenic hematopoietic-cell-transplant (HCT) and, to date, it represents the only curative option for refractory AML patients.

Acute promyelocytic leukemia (APL) represents an exception and since 1988 prognosis and therapeutic interventions completely differs from all other AMLs.

Risk category*	Genetic abnormality
Favorable	t(8;21)(q22;q22.1); *RUNX1-RUNX1T1*
	inv(16)(p13.1q22) or t(16;16)(p13.1;q22); *CBFB-MYH11*
	Mutated *NPM1* without *FLT3*-ITD or with *FLT3*-ITD^{low}†
	Biallelic mutated *CEBPA*
Intermediate	Mutated *NPM1* and *FLT3*-ITD^{high}†
	Wild-type *NPM1* without *FLT3*-ITD or with *FLT3*-ITD^{low}† (without adverse-risk genetic lesions)
	t(9;11)(p21.3;q23.3); *MLLT3-KMT2A*‡
	Cytogenetic abnormalities not classified as favorable or adverse
Adverse	t(6;9)(p23;q34.1); *DEK-NUP214*
	t(v;11q23.3); *KMT2A* rearranged
	t(9;22)(q34.1;q11.2); *BCR-ABL1*
	inv(3)(q21.3q26.2) or t(3;3)(q21.3;q26.2); *GATA2,MECOM(EVI1)*
	−5 or del(5q); −7; −17/abn(17p)
	Complex karyotype,§ monosomal karyotype‖
	Wild-type *NPM1* and *FLT3*-ITD^{high}†
	Mutated *RUNX1*¶
	Mutated *ASXL1*¶
	Mutated *TP53*#

Table1. 2017 European Leukemia Network (ELN) risk stratification by genetics.
Adapted from Döhner 2017.

8. Acute Promyelocytic Leukemia

In the older FAB classification of AML, acute promyelocytic leukemia (APL) corresponds to the M3 subtype and accounts about 10% of all AMLs.

In more than 95% of cases APL is characterized by the balanced translocation t(15;17)(q22;q12) resulting in the fusion of promyelocytic leukemia (PML) gene and retinoic acid receptor α (RAR) gene. Less frequently RARα has been found fused with other partners,

such as PLZF, NuMA, NPM1, STAT5b and others (Dos Santos et al., 2013; Sanz et al., 2019). APL was first described in 1957 (HILLESTAD, 1957) and is characterized by the accumulation of promyelocytic blasts with azurophilic granules and Auer rods.

8.1 The fusion protein PML/RARα

Fusing PML and RARα genes, the chromosomal translocation t(15;17) generates the fusion protein PML/RARα. Different cleavages can occur in the PML gene, while the breakpoint in RARα is always in the second intron. The longest isoform PML(L)/RARα occurs in more than 70% of APL cases and is characterized by the *bcr1* breakpoint in exon 6. The shorter PML(S)/RARα derives from the *bcr3* breakpoint in exon 3 and represents around 20% of patients, while remaining patients arbor the intermediate isoform PML(V)/RARα with the *bcr2* breakpoint in exon 6. In all isoforms, PML/RARα retains the RBCC domain of PML, that allows its homodimerization, and the DNA binding domain, the ligand binding domain and the dimerization domain of RARα (Alcalay et al., 1991; de Thé et al., 1991; Pandolfi et al., 1992). PML/RARα can still bind DNA at retinoic acid responsive elements (RAREs) but when on chromatin, in contrast to RARα, PML/RARα can homodimerize through the RBCC domain of PML (Melnick and Licht, 1999). Nevertheless, when on RAREs PML/RARα can still dimerize with either RARα and RXR, suggesting that PML/RARα can alter retinoic acid signaling by several mechanisms as RARα and RXR sequestering, competing with RARα for RAREs and binding of new DNA sites (Kamashev et al., 2004).

Normal RARα binds to RAREs located in the regulatory regions of genes involved in hematopoietic development and represses their transcription by recruiting epigenetic modifiers (NCoR/SMRT, SIN3A and HDACs). Retinoic acid binding to RARα provokes a conformational change in RARα that induces the release of the repressor complex and the

recruitment of the basal transcriptional machinery and of co-activators (HATs) that create a favorable environment for transcription (Soprano et al., 2004).

PML/RARα is a more potent transcriptional repressor compared to normal RARα. Indeed, PML/RARα has higher affinity for the co-repressors NCoR and SMRT, which in turn recruit HDACs (Melnick and Licht, 1999). Moreover, PML/RARα homodimers recruit many NCor/SMRT complexes, resulting in an increased concentration of HDACs that create an even more repressed epigenetic environment (Minucci et al., 2000) and is also able to recruit DNA methyltransferases to further repress transcription (Lo-Coco and Ammatuna, 2006). As result, physiological doses (10^{-9} mol/L) of retinoic acid are not sufficient to induce the release of transcriptional co-repressors from PML/RARα, enabling the fusion protein to maintain the repression of myeloid genes expression; higher pharmacological doses (10^{-6}mol/L) are needed to dismantle the repressor complex. Afterwards, it has been reported that high doses of retinoic acid induce also PML/RARα degradation through caspase-mediated cleavage (Nervi et al., 1998).

Partial differentiation of APL cells can be induced also by direct targeting of the repressor complex by overexpressing specific NCoR fragments (Racanicchi et al., 2005), by HDACs silencing (Atsumi et al., 2006) or HDACs pharmacological inhibition (Minucci and Pelicci, 2006). The cell line NB4-R4, derived from the APL cell line NB4, arbors a mutation in the ligand binding domain of PML/RARα that confers resistance to retinoic acid treatment. Interestingly, treatment with the histone deacetylase inhibitor TSA restores retinoic acid sensitivity of NB4-R4 cells (Lin et al., 1998).

In addition to HDACs and DNA methyltransferases, PML/RARα can also interact with histone methyltransferases. In particular, PML/RARα recruitment of PRC2 on its targets results in an increase of H3K27 methylation and inhibition of PRC2 components facilitates APL cells

differentiation (Villa et al., 2007). Altogether, PML/RARα imposes a profound epigenetic silencing of its target genes by histone deacetylation, DNA methylation and Polycomb-mediated H3K27 methylation. Accordingly, retinoic acid treatment reverts both acetylation and methylation status of PML/RARα target genes (Martens et al., 2010; Villa et al., 2007).

8.2 APL treatment: the ATRA revolution

Till 1980s, APL prognosis was one of the worst of all AML subtypes, with a 5-year overall survival of around 25% of patients, and almost the total of patients relapsing within 2 years from the initial complete remission (Fenaux et al., 2007). The clinical history of APL completely changed when in 1988 Huang and collaborators, following the *in-vitro* indication of retinoic acid-induced differentiation of APL cells (Breitman et al., 1981), published the results of a small trial of *all-trans* retinoic acid (ATRA), alone or in combination with chemotherapy, in which all the 24 patients achieved complete hematological remission (Huang et al., 1988). The study has been followed by other clinical trials (Castaigne et al., 1990; Tallman et al., 1997; Warrell et al., 1991) that led to the adoption of the combination of ATRA and anthracyclines as APL standard therapy. ATRA treatment represents the first example of "differentiation therapy" because it reprograms the leukemic cell to normal functions and terminal differentiation (Figure 14) rather than inducing apoptosis and killing it as conventional chemotherapy does. Unfortunately, ATRA monotherapy did not provide a cure for APL since patients treated with ATRA alone inevitably relapsed: retinoic acid-induced differentiation was not sufficient to eradicate all leukemic cells.

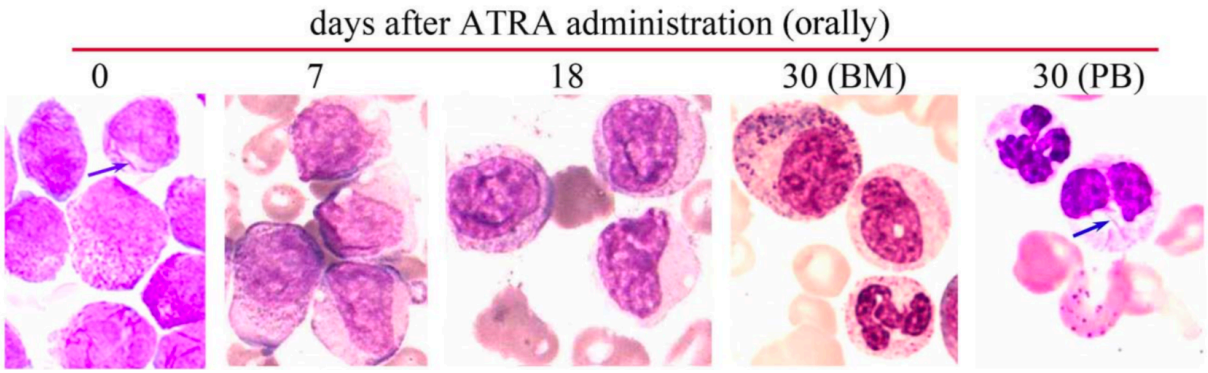

Figure 14. ATRA induces in vivo terminal differentiation.

Arrows indicate Auer rods at the beginning and after 30 days of ATRA treatment, revealing leukemic origin of differentiated cells. Adapted from Wang 2008.

Since 1990s, also arsenic trioxide (ATO, As_2O_3) has been tested as a putative novel APL therapy and in 1997 arrived the first clinical report on the use of ATO on 15 patients relapsed from previous ATRA-induced remission: 14 out of 15 patients achieved a new complete remission (Shen et al., 1997). Several other clinical and pre-clinical studies followed the first one and it is now known that ATO induces both differentiation and apoptosis by two different mechanisms: PML/RARα degradation by favoring the sumoylation of the fusion protein, and apoptosis by interacting with mitochondria that generate ROS (Nasr and de Thé, 2010). Combination of ATRA and ATO showed excellent results both in vitro and in vivo, sharply synergizing to induce long-term survival and leukemia eradication (Jing et al., 2001; Lallemand-Breitenbach et al., 1999; Rego et al., 2000).

Despite the success of ATRA-based therapy, some patients still relapse after ATRA/chemotherapy or ATRA/ATO combined treatment. Relapsed and refractory APLs are frequently resistant to ATRA and can be treated with chemotherapy in combination with ATO, HDAC inhibitors or various experimental drugs in order to achieve remission before to proceed with allo-HSCT. ATRA resistance can also be the result of mutations in either the ligand binding domain (Zhou et al., 2002) or in the DNA binding domain (Ding et al., 1998)

of RARα, as well as the result of cytogenetic rearrangements that do not involve the PML gene (*e.g*. PLZF/RARα and STAT5b/RARα) (Sanz et al., 2019).

9. Transcriptional dysregulation in AML

The blockade of the process of normal cell differentiation is a defining characteristic of acute leukemias. Since cell differentiation and self-renewal are substantially gene expression programs, they are governed by transcriptional regulators; it follows that oncogenic programs are often driven by altered transcriptional regulators.

Oncogenic lesions that involve transcriptional regulators occur indeed in early stages of tumor development and constitute an initiating event. Importantly, targeting and disruption of the altered transcriptional regulator that drives the oncogenic phenotype is not easily bypassed by the cell and often result in the re-activation of a differentiation program. The clearest examples of oncogenic transcriptional regulators in AMLs are the recurrent chromosomal translocations that generate transcription factor fusions, such as AML1-ETO, PML-RARα and the various MLL-rearrangements, but also recurrent point mutations in transcription factors (CEBPα or RUNX1) and in epigenetic modifiers (DNMT3A, TET2, IDH2 and ASXL1). In addition, primary oncogenic drivers can impose a particular gene expression program by altering the expression of secondary factors that are essential transcription regulators. Targeting of these secondary effectors can have the same result of targeting the primary oncogenic drivers themselves, altering proliferation, differentiation status and self-renewal ability of leukemic cells.

Direct targeting of the oncogenic driver leads to leukemic cells exhaustion, and the best example of this approach is represented by the use of ATRA and ATO to induce the degradation of the onco-fusion protein of PML/RARα. Nevertheless, it's not always possible

the direct targeting of the driving oncogene, but there are at least two ideal therapeutic approach to reach the same effect. The first one is to block specific interactions in which the transcriptional regulator participates. This approach has already been evaluated in different contexts and cases: MYC-MAX interaction (Berg et al., 2002; Harvey et al., 2012), NMYC (Müller et al., 2014), MAF (Pellegrino et al., 2014) or MYB interaction with the co-activators CBP and p300 (Fung et al., 2003; Oelgeschläger et al., 1996; Sampurno et al., 2013). The second one is a broaden approach and consists in the use of compounds that inhibits the activity of epigenetic regulators that shut down the oncogenic transcriptional program by re-establishing a normal epigenetic landscape.

10. Epigenetic therapy in AML

Although AML is a heterogeneous disease that can be divided in several subtypes, all AMLs share a severe block in myeloid differentiation and are characterized by a profound alteration of the epigenetic landscape.

Due to their reversible nature, epigenetic modifications are susceptible of pharmacological interventions. The firsts epigenetic drugs approved for cancer treatment were DNA demethylating agents and histone deacetylases inhibitors (Greenblatt and Nimer, 2014). DNA demethylating agents (*i.e.* DNMT1 and DNMT3 inhibitors) azacytidine and decitabine are currently used in the treatment of myelodysplastic syndromes (MDS) and are also approved for the treatment of certain types of AMLs. Despite the extended literature and the promising results in preclinical settings, only few HDAC inhibitors (Vorinostat, Belinostat and Romidepsin) have been approved by FDA for the treatment of T-cell lymphoma, but many others are under clinical investigation also for AMLs and other hematological malignancies (Falkenberg and Johnstone, 2014).

After the discovery of recurrent mutation in AMLs of IDH1 and IDH2, two enzymes involved in the regulation of both DNA and histone demethylation, several inhibitors to target the mutated enzymes have been developed. The IDH2 specific inhibitor R140Q, for example, induces i*n vitro* differentiation of patient-derived acute leukemia cells (Wang et al., 2013). Promising preclinical results have been obtained also with JQ1, a BRD4 inhibitor. BRD4 is an epigenetic "reader" protein that recognizes acetylated lysines through its bromo-domain. Inhibition of BRD4 with JQ1seems to be particularly efficacious in MLL fusion protein-driven leukemias and in MYC-driven malignancies (Dawson et al., 2011; Filippakopoulos et al., 2010; Zuber et al., 2011).

Several lysine demethylases inhibitors have been developed in last years and between these, LSD1 inhibitors show promising results for the treatment of AMLs.

10.1 LSD1 targeting in AML

The anti-depressive agent tranylcypromine (TCP) was one of the firsts discovered molecules that is able to inhibit LSD1 catalytic activity. Interestingly, TCP inhibits cell proliferation and colony forming ability of murine MLL-AF9 leukemic cells. In particular, Harris and colleagues showed that knock-down of LSD1 reduces cell proliferation and induces differentiation of both human and murine MLL-AF9 leukemic cells, and that inhibition of LSD1 with either TCP or two TCP analogs phenocopied the knock-down of the protein (Harris et al., 2012). Recently, another group confirmed these observations also in AML patients by using a novel and more potent LSD1 inhibitor, ORY-1001. The authors profiled gene expression and H3K4 methylation after LSD1 inhibition and found that, despite induction of myeloid-related genes and local increase in the histone modification, alterations in H3K4me2 only partially explain the changes observed in gene expression (Maes et al., 2018).

Not all AMLs are sensitive to LSD1 inhibition. By using both a reversible (GSK90) and an irreversible (RN-1) LSD1 inhibitor on a large panel of AML cell lines, McGrath and colleagues found that erythroleukemia and AML1-ETO-bearing cells are among the most sensitive but many other AML cells do not, or only partially, respond to LSD1 inhibition (McGrath et al., 2016). Moreover, they haven't found global but only local variations of H3K4me2 levels in LSD1i-sensitive cells and they first described a general change in the chromatin localization of LSD1 after its inhibition. In another study, the LSD1 inhibitor NCD38 induces differentiation of erythroleukemia, megakaryocytic leukemia and MDS overt leukemia cells. In this study authors demonstrated that LSD1 inhibition induces cell differentiation by leading the increase of H3K27 acetylation at super-enhancer, and the consequent transcriptional activation, of key hematopoietic regulators (GFI1, CEBPA and ERG). Interestingly, GFI1 knock-out in LSD1i-sensitive cells makes them insensitive, indicating a central role of GFI1 in LSD1 inhibition response (Sugino et al., 2017). Similarly, the LSD1 inhibitor T-3775440 induces differentiation of erythroleukemia and megakaryocytic leukemia cells disrupting the interaction between LSD1 and GFI1b and, consequently, re-activating transcription of GFI1b target genes (Ishikawa et al., 2017).

Acute promyelocytic leukemia (APL) is an AML subtype resistant to LSD1 inhibition but, as previously described, micromolar doses of ATRA can induce differentiation of APL cells. In 2010, Binda and colleagues reported that a TCP-derived they developed acts synergistically with ATRA, reducing from 1μM to 10nM the dose of ATRA necessary to induce growth inhibition and differentiation of NB4 cells, an APL cell line (Binda et al., 2010). Few years later, a report showed that LSD1 inhibition sensitizes also non-APL AML cells to ATRA treatment by increasing H3K4me2 levels and inducing the myeloid differentiation-related genes CD11b and LY96 (Schenk et al., 2012). This study expanded the advantages of differentiation therapy

to a much larger cohort of beneficiaries and paved the way to the various clinical trials in which the combination of LSD1 inhibition and ATRA is tested. Nevertheless, the molecular mechanisms underlying ATRA sensitization by LSD1 inhibition remains unclear.

Aim of the project

LSD1 is the first histone demethylase discovered; its principal substrates are H3K4me2 and H3K4me, markers generally associated with active transcription. The discovery of its enzymatic activity completely revolutionized our interpretation of histone methylation, until that moment considered a stable epigenetic modification. In the last fifteen years, the scientific interest on LSD1 has rapidly grown and its involvement in various physiological and pathological processes became evident. The fact that LSD1 is commonly deregulated, often overexpressed, in cancers makes it an appealing target for cancer therapy. Different LSD1 inhibitors have been developed, some of which already entered clinical trials of several cancers, including Acute Myeloid Leukemia (AML). Nevertheless, AML represents an heterogeneous group of diseases and only a minority of AML cells are sensitive to LSD1 inhibition as single treatment. A synergistic action of LSD1 inhibitors and the differentiation agent retinoic acid (RA) has been however observed also in AML cells resistant to single-agent treatment. Similarly, our group have already shown that LSD1 inhibition sensitizes Acute Promyelocytic Leukemia (APL) cells to low doses of RA, but any understanding of the mechanism of action of LSD1 inhibitors in combination with RA, either in APL or other AML subtypes, has not been reported so far.

The aim of this project is therefore to investigate the molecular mechanisms by which LSD1 inhibition sensitizes AML cells to retinoic acid-induced differentiation. Since the combination of these two drugs is under clinical investigation, any understanding of this phenomenon in cells resistant to LSD1i provides useful insights to optimize the use of LSD1i in a clinical setting.

Materials and methods

Cell lines and growing conditions

All cell lines were grown accordingly to ATCC recommendations. Cultures were maintained in a humidified tissue culture incubator at 37°C in 5% CO_2.

All leukemic cell lines used, their AML FAB subtype, cytogenetic, molecular characterization and their appropriate growth medium are listed in table 2. Of particular interest, NB4 cell line was established by Lanotte and colleagues from an APL patient and has characteristic similar to APL blasts (Lanotte et al., 1991). NB4 cells were maintained in Roswell park memorial institute medium (RPMI) supplemented with 10% fetal bovine serum South America, penicillin (100 U/mL)/streptomycin (1000 mg/mL) and 2 Mm of L-glutamine. In contrast, MOLM13 is an AML cell line carrying the MLL-AF9 fusion transcript due to a chromosomal insertion in MLL gene (Matsuo et al., 1997). MOLM13 cells were maintained in Roswell park memorial institute medium (RPMI) supplemented with 20% fetal bovine serum South America, penicillin (100 U/mL)/streptomycin (1000 mg/mL) and 2 Mm of L-glutamine.

Phoenix-Ampho cells (human embryonic kidney packaging cells) were used for retroviral particles production. These cells were maintained in Dulbecco's modified Eagle medium (DMEM) supplemented with 10% fetal bovine serum South America, penicillin (100 U/mL)/streptomycin (1000 mg/mL) and 2 Mm of L-glutamine.

HEK293T cells (human embryonic kidney cells) were used for lentiviral particles production due to their high transfection efficiency. These cells were maintained in Dulbecco's modified Eagle medium (DMEM) supplemented with 10% fetal bovine serum South America, penicillin (100 U/mL)/streptomycin (1000 mg/mL) and 2 Mm of L-glutamine.

Designation	Source	Subtype and molecular characterization	Medium
NB4	AML (APL)	M3; PML-RARa	90% RPMI 1640+10% FBS (South America) + 2mM L-Glutamine
MONO-MAC-6	AML	M5; MLL-AF9	90% RPMI 1640+10% FBS (South America) + 2mM L-Glutamine +1mM Sodium Pyruvate (NaP)+ 0.1mM Non-Essential Amino Acids (NEAA)+9ug/ml Insulin
GDM-1	AML	transformed from CML	80% RPMI 1640+20% FBS (South America) + 2mM L-Glutamine
KASUMI-1	AML	M2; AML1-ETO, KIT mut	90% RPMI 1640+10% FBS (North America) + 2mM L-Glutamine
HL-60	AML	M2	90% RPMI 1640+10% FBS (South America) + 2mM L-Glutamine
GF-D8	AML	M1	80% RPMI 1640+20% FBS (South America) + 2mM L-Glutamine
THP-1	AML	M5; MLL-AF9	90% RPMI 1640+10% FBS (South America) + 2mM L-Glutamine
KG-1	AML	M6; OP2-FGFR1	90% RPMI 1640+10% FBS (South America) + 2mM L-Glutamine +1mM Sodium Pyruvate (NaP)+10mM HEPES
KG-1A	AML	M6; OP2-FGFR1 ("Undifferntiated" subclone of KG-1)	90% RPMI 1640+10% FBS (South America) + 2mM L-Glutamine +1mM Sodium Pyruvate (NaP)+10mM HEPES
ML-2	AML	M4; MLL-AF6	90% RPMI 1640+10% FBS (South America) + 2mM L-Glutamine
MONO-MAC-1	AML	M5; MLL-AF9 (less diff. Than MONO-MAC-6 sister line)	90% RPMI 1640+10% FBS (South America) + 2mM L-Glutamine +1mM Sodium Pyruvate (NaP)+ 0.1mM Non-Essential Amino Acids (NEAA)
MV4-11	AML	M5; MLL-AF4, FLT3 ITD	90% RPMI 1640+10% FBS (South America) + 2mM L-Glutamine
OCI-AML2	AML	M4; DNMT3A R635W mut	80% alpha-MEM+20% FBS (South America) + 2mM L-Glutamine
OCI-AML5	AML	M4	80% alpha-MEM+20% FBS (South America) + 2mM L-Glutamine +10ng/ml GM-CSF
M-07e	AML	M7	80% RPMI 1640+20% FBS (South America) + 2mM L-Glutamine +10ng/ml GM-CSF
EOL-1	AML	M4eo; MLL-PTD, FIP1L1-PDGFRA	90% RPMI 1640+10% FBS (South America) + 2mM L-Glutamine
PLB-985	AML	M4. subclone of HL-60	90% RPMI 1640+10% FBS (South America) + 2mM L-Glutamine
SKNO-1	AML	M2; AML1-ETO	90% RPMI 1640+10% FBS (South America) + 2mM L-Glutamine +10ng/ml GM-CSF
MOLM-13	AML	M5a; FLT3 ITD, MLL-AF9 occult insertion, 8 trisomy	80% RPMI 1640+20% FBS (South America) + 2mM L-Glutamine
PL-21	AML (APL)	M3; FLT3 ITD. NO PML-RARa	80% RPMI 1640+20% FBS (South America) + 2mM L-Glutamine
MOLM-14	AML	M5a; FLT3 ITD, MLL-AF9 occult insertion	80% RPMI 1640+20% FBS (South America) + 2mM L-Glutamine

Table 2. Leukemic cell lines used in the study.

SILAC labeling of NB4 cells

For standard SILAC labeling, NB4 cells were grown in ''Light'' and ''Heavy'' SILAC RPMI 1640 (Thermo Fisher Scientific 89984) supplemented with either L-arginine and L-lysine, or their heavy isotope-counterparts L-arginine-$^{13}C_6$, $^{15}N_4$ hydrochloride (Arg10, Sigma 608033) and L-lysine-$^{13}C_6$, $^{15}N_2$ hydrochloride (Lys 8, Sigma 608041) (Ong et al., 2002).

All media were supplemented with 10% dialyzed FBS (26400-044 Gibco, Life Technology), 1% glutamine, 100U/mL Penicillin and 100mg/ml Streptomycin.

***In-vivo* studies**

For *in-vivo* studies, lineage negative (lin-) cells were isolated from the bone marrow of 8- to 10-weeks old 129SvEv mice and murine PML-RAR cells were generated using a retroviral transduction and transplantation approach as previously described (Minucci et al., 2002). The animals were checked periodically for clinical signs of disease and for presence of blast cells by May-Grunwald-Giemsa staining of blood smears. ATRA pellets (21-day release, 5 mg) or placebo pellets were implanted s.c. by trocar injection 10 days after cell injection. DDP_38003 was dissolved in a vehicle composed of 40% PEG400 in a 5% glucose solution, and orally administered at the dose of 17 mg/kg two days per week, for three weeks. For the combination, mice were dosed with ATRA pellets (21-day release, 5 mg) and DDP_38003 at the dose of 17 mg/kg following the administration schedule of the single treatment. *In vivo* studies were performed after approval from our fully authorized animal facility and our institutional welfare committee (OPBA) and notification of the experiments to the Ministry of Health (as required by the Italian Law; IACUCs Numbers: 759/2015 in accordance with EU directive 2010/63).

Proliferation assay

200,000 cells/ml were plated at day 0 in duplicate in T25 flasks in a total volume of 10mL in the presence of compound and number of cells were measured by hemocytometer in the indicated days. Two cell suspension were prepared (1:1 with Trypan Blue dye, Sigma) for independent reading and average of two readings represented the cell count. Medium was refreshed every 2/3 days and cell concentration was maintained under 1.5/2 million cells/ml.

Cell viability assay

Cell Titer-Glo viability assay (Promega, Madison, Wisconsin USA) was performed following manufacturer's recommendations. The number of viable cells in culture is determined by quantification of the ATP present, as indicator of metabolically active cells. Briefly, 5000 cells were plated in 100µl of medium containing compounds to be tested in each well of a white 96 well plate. Cells were plated in triplicate. The day of measurement, 100µl of Cell Titer-Glo substrate was added to cells, incubated for 15 minutes at room temperature on an orbital shaker and luminescence was measured with a GloMax® Explorer instrument (Promega, Madison, Wisconsin USA).

Colony forming unit (CFU) assay

1000 cells were plated in a total volume of 1.5ml of methylcellulose medium (MethoCult™ H4444, Stem Cell Technology, Vancouver, BC, Canada) containing 10% fetal bovine serum. Cells were plated in triplicate. Colony forming units were scored 7 to 10 days after plating by direct quantification.

Morphological characterization: May-Grünwald Giemsa staining

Approximately 200,000 cells collected after treatment were spun on a slide by using a cytospin centrifuge (3 minutes, 250 RPM). Cytospins were stained with the May-Grünwald Giemsa method: cells were first stained for 6 minutes with the May-Grünwald stain, washed three times in deionized water and then stained for further 35 minutes with Giemsa stain diluted 1:20 in deionized water. After three more water washes and air dried, cytospins were covered with a slip attached to the slide with Eukitt® mounting medium.

Mature populations were defined based on their morphology: i) increased cytoplasm/nucleus ratio; ii) lighter cytoplasm, often granulated; iii) segmented or multi-lobate nucleus.

FACS analysis and cell sorting

For FACS analysis cells were blocked in PBS 5% bovine serum albumin (BSA) for 30' on ice. Afterward, cells were labeled with fluorochrome-conjugated antibodies directed against CD11b (CD11b-PE clone ICRF44, eBioscience Inc. San Diego, CA). Labeling was performed in PBS 5% BSA with 2µg/mL of antibody for 45' on ice; cells were then washed three times with PBS and resuspended in PBS 2% BSA at a final concentration of $10*10^6$ cells/ml. FACS analyses were performed using a FACScalibur flow cytometer (BD Biosciences, Oxford UK).

For sorting of GFP^+ cells, cells were harvested, wash with PBS and resuspended in PBS 2% BSA at a final concentration of $10*10^6$ cells/ml. Cell sorting experiments were performed using a FACSAria cell sorter (BD Biosciences, Oxford UK).

Immunofluorescence

Approximately 100,000 NB4 cells were transferred by cytospin (3 minutes, 250 RPM) to histological glasses and fixed for 10 minutes with 4% paraformaldehyde. In order to allow entering of blocking and staining agents into cells, a permeabilization step was performed with 0.1% TRITON-X for 10 minutes. Cells were then accurately washed with PBS and soon after subjected to the blocking step with PBS 5% normal goat serum for 30 minutes. Staining was performed for one hour at room temperature with a mouse anti-human PML antibody (PG-M3) (Flenghi et al., 1995) to reveal PML-nuclear bodies or microspeckles. After three PBS washes, a Cy3-conjugated goat anti-mouse secondary antibody (Jackson ImmunoResearch

Laboratories, Inc., West Grove, PA, USA) was added for further 45 minutes in the dark. Following other three washes and a final brief staining step with DAPI to mark nuclei, coverslips are mounted onto microscope slides with moviol reagent for analysis using a wide-field microscope.

Viral production

Both retroviral and lentiviral particles were produced through the calcium-phosphate transfection protocol. The day before transfection, cells (HEK293T for lentivirus, Phoenix-Ampho for retrovirus) were plated at 50% of confluence, so that the day of transfection cells are in exponential growth (approximately 80%-90% of confluence). Two solutions are prepared, mixed through the "bubbling method" and, after 10 minutes, poured on cells. The first solution contains 500µl of 2x Hepes-buffered solution (HBS, composed of 250mM Hepes pH7, 250mM NaCl and 150mM Na_2PO_4). The second solution varies for lentivirus (10µg lentiviral plasmid DNA, 6µg plasmid pΔR8.2, 4µg plasmid pVSVg, 61µl $CaCl_2$ and H_2O to a final volume of 500µl) and retrovirus (10µg plasmid retroviral DNA, 5µg plasmid pKAT, 61µl $CaCl_2$ and H_2O to a final volume of 500µl). Cells were left in incubator at 37°C for 12 hours before replenishing medium (5ml/10cm plate).

48 hours post transfection viral supernatant was collected and 0.45µm filtered to remove floating packaging cells and debris. Viral supernatant was then concentrated through PEG precipitation: 10ml of 5x Polyethylene glycol (PEG) solution (120g PEG 8000, 2.7 NaCl and 200ml H_2O) was added to 40ml of filtered viral supernatant and incubated over-night at 4°C. the day after the solution was centrifuged 1500g for 1 hour at 4°C, the supernatant removed and pellet resuspended in 500µl of PBS to obtain a 100x concentered virus. The viral solution was stored at -80°.

Infection procedure

Cells were cultured in the appropriate medium and plated at a density of 300,000 cells/well (24 wells plate) in a total volume of 500µl/well. Each well was inoculated with 30µl of viral concentrated solution (100X) supplemented with polybrene 8mg/ml. Cells were centrifuged (2500 RPM, 60', RT), and incubated at 37°C for three hours. After incubation, 500µl of fresh culture medium were added to each well to dilute the polybrene; cells were incubated at 37°C over-night. The morning after, the second round of infection was performed under the same conditions. The day after the second cycle of infection cells were washed in PBS and plated in the appropriate medium at a density of 300,000 cells/ml.

After one day of recovery (72 hours from the first cycle of infection), cells infected with PINCO vector were sorted by means of GFP, while cells infected with lentiCRISPRv2 vector were selected with Puromycin (2µg/ml) for three days.

Genome editing

Genetic knock-out of LSD1 was performed using the CRISPR/Cas9 method. CRISPR/Cas is a microbial adaptive immune system based on RNA-guided nucleases. CRISPR (Cluster Regularly Interspaced Short Palindromic Repeat) system consist of a genomic locus of microbial hosts that contains CRISPR associated (Cas) genes, non-coding RNAs and distinctive repetitive elements. These repetitive elements are interspaced with short variable sequences derived from exogenous DNA called protospacers and together constitute the CRISPR RNA (crRNA). Type II CRISPR system is the most characterized and consist of a nuclease (Cas9), the crRNA that contains a 20-nt guide sequence - that recognizes the target DNA via Watson and Crick pairing - with a partial tandem repeat, and a trans-activating crRNA

(tracrRNA) that facilitates the assemble of the DNA-guide RNA-Cas9 complex. In addition, the Cas9 needs that the target DNA sequence - complementary to the guide RNA – is followed by a protospacer adjacent motif (PAM). Orthologs Cas9 of different bacteria could recognize different PAM sequences: for example, the Cas9 derived from *Streptococcus pyogenes* needs that the target sequence is preceded by a 5'-NGG PAM, while the Cas9 derived from *S. thermophilus* needs a 5'-NNAGAA PAM and the Cas9 of *Neisseria meningitis* a 5'-NNNNGATT PAM.

Though the endogenous expression of a human codon-optimized Cas9 flanked with a nuclear localization signal, the RNA-guided nuclease activity of CRISPR/Cas9 can be reconstituted also in mammalian cells. To make the system easier to use, the crRNA and the scaffold tracrRNA can be fused together to form a single guide RNA (sgRNA). In this way, Cas9 can be directed toward almost any target of interest preceded by the appropriate PAM sequence only manipulating the 20-nt sequence of the sgRNA. When recognizes the DNA target sequence, the nuclease Cas9 induces a double strand break (DSB) in the genomic sequence that can be repaired by either the error prone "non homologous end joining" (NHEJ) or, only in the presence of an appropriate DNA template, by the error-free "homologous recombination" (HR). If no DNA template is given, the cell repairs the DSBs with NHEJ which can result in random insertions/deletions (indels) at the site of junction. Indel mutations in the coding region of a gene can result in frameshifts, with the creation of premature stop codon and, consequently, in gene knockout.

Both the human codon optimized Cas9 flanked with a nuclear localization signal and the sgRNA can be delivered with a single expression plasmid, either by transfection or lentiviral infection. Construction of the expression plasmid consists in a single cloning step with a pair

of partially complementary oligonucleotides encoding the 20-nt target sequence annealed and ligated into the backbone plasmid.

Oligonucleotides design

Oligonucleotides for LSD1 knockout were designed with the online CRISPR Design tool provided by the Zhang lab of the Massachusetts Institute of Technology (http:// tools.genome-engineering.org). The following sequence, mapping in the first exon, was selected for LSD1 knockout: CGCGGAGGCTCTTTCTTGCG.

Plasmid and oligonucleotides cloning

The third-generation lentiviral vector lentiCRISPRv2 (Shalem et al., 2014) was used for LSD1 knockout. The plasmid contains two expression cassettes, one encoding a flagged human codon optimized Cas9 derived from *S. pyogenes* and the cDNA conferring Puromycin resistance, and the other one encoding the chimeric guide RNA under the U6 promoter. The vector was digested with *BsmBI* restriction enzyme, the *2kb filler* removed and the annealed oligos ligated into the chimeric guide RNA. Ligated vector was then transformed in Stbl3 bacteria, a recombination deficient RecA$^-$ strain of *E. coli*.

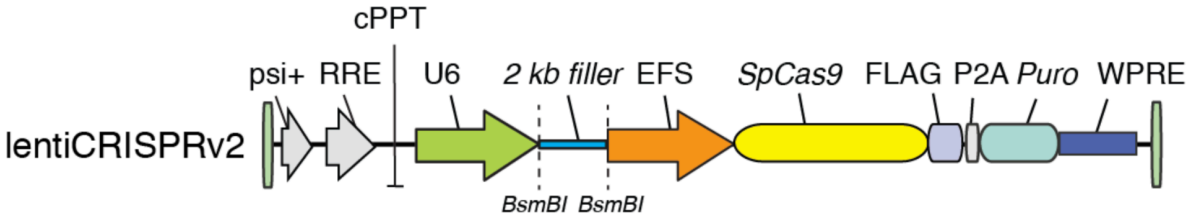

Figure 15. LentiCRISPRv2 vector.

Infection, clonal isolation and knockout validation

Lentiviral particles production and cell infection were performed as described in previous *Materials & Methods* sections. Infected cells were selected with puromycin (2µg/µl) for three days. After selection, 250 cells were plated in a total volume of 1.5ml of methylcellulose medium (MethoCult™ H4444, Stem Cell Technology, Vancouver, BC, Canada) supplemented with 10% fetal bovine serum. Compared to liquid culture, methylcellulose medium results in better clonal growth efficiency. After 5 to 7 days, every single-cell derived colony was transferred in a well of a 96-well plate and expanded in liquid culture. After expansion, single clones were screened by western blot and genetic knockout confirmed by Sanger sequencing.

LSD1 WT and mutant plasmids

LSD1 N-terminal truncated (172-833) wild-type and catalytic mutant (K661A-LSD1) constructs were a kind gift by Prof. Elena Battaglioli (University of Milan). Constructs were PCR-amplified from original vectors and cloned into pCR-TOPO 2.1 (Invitrogen) using the following primers:

LSD1 forward: ATGTCGGGTGTGGAGGGCGCAGCTTTC

LSD1 reverse: TCACATGCTTGGGGACTGCTGTGC

To make the D553,555,556A triple mutant construct described in (Lin et al., 2010b), the following primers were used in three sequential site-directed mutagenesis reactions using the pCR-TOPO-LSD1WT as the template vector:

LSD1_D553A forward: CTTAAGCACTGGGCTCAGGATGATGACTTTGAGTTC

LSD1_D553A reverse: GAACTCAAAGTCATCATCCTGAGCCCAGTGCTTAAG

LSD1_D553,555A forward: CTTAAGCACTGGGCTCAGGCTGATGACTTTGAGTTC

LSD1_D553,555A reverse: GAACTCAAAGTCATCAGCCTGAGCCCAGTGCTTAAG

LSD1_D553,555,556A forward: CTTAAGCACTGGGCTCAGGCTGCTGACTTTGAGTTC

LSD1_D553,555,556A reverse: GAACTCAAAGTCAGCAGCCTGAGCCCAGTGCTTAAG

Products were then sub-cloned from pCR-TOPO 2.1 into the EcoRI site of the retroviral PINCO vector for ectopic expression. retroviral vector expressing the gene of interest under the control of the viral LTR (*long terminal repeats*), and GFP (*green fluorescent protein*), used as a selection marker, under the control of CMV *(cytomegalovirus)* promoter.

Protein extraction and western blot

Cells were lysed in Urea 8M plus protease inhibitors. Cell lysates were then sonicated (30'', 15% amplitude) with a Branson Sonifier 250. After sonication, samples were centrifuged for 10 minutes at 4°C, 13000 rpm. Proteins were quantified by a Bio-rad Bradford assay. 1X volume of Bradford reagent was diluted with 4X volume of MilliQ water to prepare a working Bradford solution. For measuring protein concentration of sample at absorbance 595 nm, Urea 8M was first measured as blank, and 1µl sample in 999µl Bradford (dilution factor 1: 20) was measured. 15 to 100µg of proteins were mixed with 5x Laemmli loading buffer (10% SDS, 50% glycerol, 25% 2-ß-mercaptoethanol, 0.02% bromophenol blue and 0.3125 M Tris HCl) and denaturated for 8 min at 95°C. Cell lysates were loaded into polyacrylamide gel and run in SDS Running Buffer. Transfer to nitrocellulose membranes was performed at 100V for 1 hour and 30 minutes at 4°C or overnight at 30V in Transfer Buffer containing 20% methanol. Correct transfer of proteins to nitrocellulose membrane was evaluated using Ponceau S staining. Membranes were blocked in 5% milk/ TBS-Tween for 1 hour at room temperature or overnight at 4°C and then probed with primary antibodies diluted in TBS-Tween + 5% milk at 4°C for 2h or overnight. After three washes with TBS-Tween (5 minutes each) of 10 minutes

each, membranes were incubated with the appropriate secondary antibody in TBS-Tween+ 5 % milk for 30 min at room temperature. After 3 more washes, signals were revealed using ECL (Enhanced Chemiluminescence) for 5 minutes at room temperature. Images were acquired with image scanning methods for chemi-luminescence and colorimetric detection. Antibodies used for western blot analyses were: Actin (Sigma #A4700, clone AC-40), GFI1 (Santa Cruz sc-376949, clone B9), GSE1 (Proteintech #24947-I-AP), H3 (abcam #1791), H3K4me1 (abcam #8895), H3K4me2 (abcam #32356), H3K4me3 (Activ Motif #39159), HDAC1 (abcam #7028), HMG20B (Proteintech #14582-1-AP), LamininB (abcam #16048), LSD1 (Cell signalling #2139 and abcam #17721), RAR (santa cruz sc-551), Tubulin (Santa Cruz sc-32356), Vinculin (Sigma #V9131, clone hVIN-1) and ZMYM3 (abcam #106626).

RNA extraction and RT-qPCR

Total RNA was extracted from NB4 cells with and purified using the RNeasy kit (QIAGEN). Reverse transcription was performed with the Superscript II Kit (Invitrogen), according to the manufacturer's protocol. qPCRs were performed in triplicates in 20 µL of final reaction volume containing SYBR green buffer (Applied Biosystems), 20 ng of cDNA retrotranscribed from the RNA, and 0.4µM of each primer mix. All the qPCR amplifications were performed in the AB-7500 sequence detection system (Applied Biosystem), 95^{O}C hold for 10 minutes followed by 40 cycles of 95^{O}C for 15 seconds and 60^{O}C for 60 seconds. mRNA levels were normalized against GAPDH mRNA.

For RT-qPCRs the following primers were used:

GAPDH forward: GCCTCAAGATCATCAGCAATGC

GAPDH reverse: CCACGATACCAAAGTTGTCATGG

CD11b forward: AACCCCTGGTTCACCTCCT

CD11b reverse: CATGACATAAGGTCAAGGCTGT

RNA sequencing and data analysis

mRNA-seq libraries were prepared according to the True-seq Low sample protocol (Illumina, San Diego, California USA), starting with 1ug of total RNA per sample. Raw reads were mapped to the human reference genome hg18 using TopHat2 package (Langmead et al., 2009) obtaining comparable number of reads among the samples. Differentially expressed genes were determined using Cufflinks and CuffDiff (Trapnell et al., 2010). Using the normalized RPKM counts for each sample, we first added a pseudo count to the data which was chosen to be the smallest non-zero value. Genes with a fold change greater than absolute $Log_2(1.5)$ respect to DMSO, FDR≤ 0.05 and FPKM ≥ 0.5 were defined as differentially expressed genes. Pathway analysis was performed with QIAGEN's Ingenuity Pathway Analysis (IPA, QIAGEN Redwood City, www.qiagen.com/ingenuity). Gene ontology was performed through DAVID and visualized by a custom script in R.

Chromatin immunoprecipitation (ChIP)

Cells were cross-linked in culture medium with 1% formaldehyde in PBS and the reaction was stopped after 10 min at RT by adding 0.125 M glycine for 5 min at 4°C. The cells were washed twice with ice cold PBS and collected by centrifugation. Pellets were stored at -80° in SDS buffer (50 mM Tris•HCl pH 8.1, 0.33% SDS, 150mM NaCl, 5 mM EDTA, and protease inhibitor cocktail) or directly processed. Fixed cells were resuspended in IP buffer (100mM tris pH 8.6 0.3% SDS 1.7% TRITON x-100 and 5mM EDTA). Chromatin was then fragmented to obtain ~300 bp in average size length by using a Branson Sonifier 250. Chromatin pre-clearing was obtained with protein A-sepharose beads (Amersham) pre-blocked with bovine serum

albumin (BSA). The supernatant was immunoprecipitated overnight in the presence of 30-50µl of protein G magnetic beads. For histone modification 1 ml corresponding to $3x10^6$ cells per each IP and 4ug/ml primary antibody were used; for LSD1 and GFI1 Chip-Seq $40x10^6$ cells per each IP; 10ug/ml. Before IP 2.5% of input was stored prior to the decrosslinking procedure. Decrosslinking was performed for all the IP samples and corresponding inputs, overnight in 0.1% SDS and 0.1% $NaHCO_3$. The day after, enriched DNA was treated with proteinase K at 56°C for 40 min and purified with a DNA purification kit (Qiagen). The obtained DNA was then quantified by picogreen and processed for ChIP-Seq library preparation (as described for the Illumina protocol) or used for quantitative real-time PCR (qPCR). For libraries preparation, 2ng of immunoprecipitated DNA was used.

Ab used for ChIP: H3K4me1 (abcam #8895), H3K4me2 (abcam #32356), H3K4me3 (Activ Motif #39159), H3K27ac (abcam #4729), LSD1 (abcam #17721), GFI1 (abcam #21061), PML (sc-5621, Santacruz) and IgG rabbit (Jackson ImmunoResearch, Lot #134230).

ChIP- Seq analysis

Short reads obtained from Illumina HiSeq 2000 were quality-filtered according to the Illumina pipeline. Analysis of the datasets was automated using the Fish the ChIPs pipeline (Barozzi et al., 2011) and includes alignment to the hg18 reference genome using Bowtie v1.0.1 (Langmead et al., 2009) and MACS version 1.4.1 as peak caller to identify regions of ChIP-seq enrichment over background. Only reads with a unique match to the genome and with two or fewer mismatches (-m 1 –v 2) were retained. MACS was used with a p-value threshold of 10^{-5} for all the data sets except for the LSD1 ChIP where the thresholds were set by qPCR validation. Each sample was compared to input DNA derived from NB4 cells (DMSO). When calling differentially enriched regions among treated and untreated samples, we

filtered the resulting regions keeping only those found enriched against the input as well. All the lists were annotated over RefSeq genes according to GIN (Cesaroni et al., 2008) while intergenic regions were considered as those at a distance higher than 22kb from the nearest gene. The bigwig files for UCSC browser visualization of genome profiles were normalized with the deepTools suite (Ramírez et al., 2016) using RPCG.

ChIP q-PCR

ChIP-qPCRs were performed for the validation of specific regions. Immunoprecipitated DNA was diluted in 9,6µl of H_2O per reaction, plus 400 nM primers in a final volume of 20µl in SYBR Green. Each ChIP experiment was performed at least three times with biological replicates.

For ChIP-qPCRs the following primers were used:

Negative control forward: AGCTATCTGTCGAGCAGCCAAG

Negative control reverse: CATTCCCCTCTGTTAGTGGAAGG

PRAM1 forward: CCACAGAGCCTCCCCTAGA

PRAM1 reverse: TGCAACACCTCCCTGTGA

PI16 forward: AGCCCTCACAGATGAGGAGA

PI16 reverse: GCCACACTTACCATGTGCAG

ITGAM forward: GGAGGAGAAGTGACATGGCT

ITGAM reverse: AGGCAAAGTGGAGATGGTGA

TGM2 forward: CAGATACAGACACACGCAGC

TGM2 reverse: TGGGGAGGTGTTCTTGATCC

CD86 forward: ACAGTCATTGCCGAGGAAGG

CD86 reverse: CTCATCCGTGTGTCTGTGCT

GFI1b forward: CAGGGAGGGGAACAGAAGAG

GFI1b reverse: GAACTGCAAAGCCTCTCTCG

Active enhancers, active promoters and super-enhancer identification and analysis

Active enhancers were defined as regions with overlapping peaks of H3K4me1 and H3K27ac which fall into distal genomic regions (defined as -20/-5kb and +5/+20kb from TSS). Active promoters were defined as regions with overlapping peaks of H3K4me3 and H3K27ac falling within 5kb of Refseq TSS. Coordinates of active enhancers and active promoters overlapping LSD1 peaks were used for histone mark analysis. Reads coverage in those regions was computed with BEDTools suite v2.17.0 (Quinlan and Hall, 2010) and normalized according to sequencing depth of each sample.

MACS peaks of H3K27ac over background were used for super-enhancer identification. Constituent enhancers within 12,500bp were stitched together, and ranked by input-subtracted signal of H3K27ac; enhancers located within a window of +/-2.5kb around TSS of RefSeq genes were excluded from the analysis. Super-enhancers were identified as those above the inflection point of the H3K27ac signal versus enhancer rank (Hnisz et al., 2013).

TFBS enrichment analysis

Motif discovery was performed by using Pscan-ChIP (Zambelli et al., 2013) with LSD1 validated peaks as genomic input regions, NB4 set as background and Jaspar 2018 NR as descriptors.

Subcellular fractionation

For the preparation of cellular sub-fractions, cells were harvested, washed twice with PBS and resuspended in 3 volumes of Hypotonic Buffer (10 mM Tris HCl pH 7.6, 1.5 mM $MgCl_2$, 10

mM KCl, 1X Roche Protease Inhibitors, 0.5 mM PMSF). After 10 minutes on ice, 1/30 of the original volume of Triton 10% was added to the cells resuspended in Hypotonic Buffer. Cells were vortexed for 30 seconds and centrifuged for 1 minute at 11000 rpm. The supernatant (representing the fraction enriched of cytoplasmic protein) was collected and the pellet (corresponding to the fraction enriched of nuclei) was re-suspended in 2 volumes of Nuclear Extraction Buffer (50 mM Tris HCl pH 7.6, 150 mM NaCl, 0.5% NP-40, 20% Glycerol, 2 mM $MgCl_2$, 1:100 Benzonase). The suspension was rocked 1h at 4°C and, then, centrifuged at 13000 rpm for 30 minutes. The supernatant, representing the nucleosol fraction, was collected and used for the subsequent immuno-precipitation analyses.

Protein co-immunoprecipitation (co-IP) analysis

NB4 nuclear fraction was quantified and diluted in IP buffer (10 mM Tris HCl pH 7.6, 150 mM NaCl, 0.2% NP-40) supplemented with 1X Roche Protease Inhibitors and 0.5 mM PMSF, in order to obtain a concentration of 2 mg/ml. Preclearing of the lysate was carried out by 1hr incubation with protein G magnetic beads. The lysate was re-quantified and diluted with the IP buffer supplemented with protease inhibitors up to a concentration of 1.3 mg/ml. An aliquot of the Input was collected before the addition of the antibody. The samples were incubated with the antibody overnight on a rotating wheel at 4°C. The following day, 50-100µl of DynaBeads-protein G pre-equilibrated in PBS and supplemented with 0.5% BSA were added to the extracts and incubated for 3 hours on a rotating wheel at 4°C. Beads were then washed 3 times with IP buffer and once with Washing Buffer IP (10 mM Tris HCl pH 7.6, 250mM NaCl, 0.2% NP-40). Then, bound material was eluted by incubation with LSD Sample Buffer (NuPAGE), supplemented with 100mM DTT, at 95°C for 5 minutes. Eluted samples

were loaded on SDS-PAGE for protein separation and subsequent analysis. Antibodies used for protein co-immunoprecipitation: LSD1 (LSD1 AbCam #17721), GFI-1 (sc-376949).

LSD1 co-IP for mass-spectrometry analysis of protein-protein interactions

The protein content of the nuclear fraction of Light and Heavy samples was quantified by Bradford assay and diluted to a concentration of 2mg/ml in IP buffer (10 mM Tris HCl pH 7.6, 150 mM NaCl, 0.2% NP-40), supplemented with 1X Protease Inhibitors (Roche) and 0.5 mM PMSF. Preclearing of the lysates was achieved by incubation with protein G magnetic beads for 1 hour on a rotating wheel at 4°C. The lysates were then re-quantified and diluted with the IP buffer supplemented with protease inhibitors to a concentration of 1.3mg/ml. A minor fraction (1/20) of input was collected before adding 10µg of anti-LSD1 antibody to each sample. All samples were then incubated on a rotating wheel at 4°C overnight. For the acquisition of the basal LSD1 interactome, 120-fold molar excess of LSD1 blocking peptide was incubated together with the antibody as negative control. This peptide competes with the bait and all its co-associated factors for the antibody binding (Soldi and Bonaldi, 2013). The peptide was added to the light channel in the Forward experiment (Rep1 and Rep2) and to the heavy channel in the Reverse experiment (Rep3). Instead, for the dynamic LSD1 interactome the inhibitor MC_2580 was added to the heavy channel in the Forward experiment and in the light one in the Reverse replicate. The following day, 100µl of Dynabeads-protein G, pre-equilibrated in PBS supplemented with 0.5% BSA, were added to each sample and incubated for 3 hours on a rotating wheel at 4°C. Beads were then washed 3 times with IP buffer and once with the Washing Buffer IP (10mM Tris HCl pH 7.6, 250mM NaCl, 0.2% NP-40). In the last washing step, light and heavy samples of each SILAC replicate were mixed, and the co-immunoprecipitated proteins were eluted by incubation at 95°C for

5 minutes with the LSD Sample Buffer (NuPAGE-Invitrogen) supplemented with 100 mM DTT. Samples were loaded on an SDS-PAGE gradient gel for subsequent protein separation and mass spectrometry analysis.

Antibody used for the preparative LSD1 co-immunoprecipitation: LSD1 AbCam #17721.

The blocking peptide used as mock control was Human KDM1 / LSD1 peptide (ab17763).

In-gel digestion of immunoprecipitated proteins

In gel digestion of gel-separated proteins was carried out with Trypsin, as previously described (Shevchenko et al., 2006). After digestion and extraction from the gel pieces, the digested peptides were desalted and concentrated by reversed-phase chromatography onto C18 Stage Tip micro-columns (Rappsilber et al., 2007). Peptides were then eluted from the stage tips with buffer B (80% ACN, 0.5% acetic acid), lyophilized, re-suspended in 0.1% Formic Acid and subjected to LC-MS/MS analysis.

MS-based histone PTM profiling

Cells were homogenized in lysis buffer (10% sucrose, 0.5mM EGTA, 60 mM KCl, 15mM NaCl, 15mM HEPES, 0.5mM PMSF, 5µg/ml Aprotonin, 5µg/ml Leupeptin, 1mM DTT, 5mM NaButirrate, 5mM NaF, 30µg/ml Spermine, 30µg/ml Spermidine and 0.5% Triton X-100) and nuclei were separated from cytoplasm by centrifugation on sucrose cushions for 30 minutes at 3750 rpm. Then, histones were extracted through 0.4 N hydrochloric acid for 5 hours at 4°C. Extracted histones were lyophilized, resuspended in milliQ water and quantified by Bradford assay. 5µg of histones were in-solution digested prior to LC-MS/MS analysis through the hybrid chemical labelling "Pro-PIC" method. This approach is based on an initial conversion of free lysines to their propionylated forms under mild aqueous conditions

followed by trypsin digestion and labelling of new peptide N-termini with phenyl isocyanate (PIC) (Maile et al., 2015). The digested peptides were desalted and concentrated by reversed-phase chromatography onto micro-column C18 Stage Tips. Peptides were then eluted from the stage tips with Elution Buffer (60% ACN, 0.1% trifluoroacetic acid), lyophilized, re-suspended in 1% trifluoroacetic acid and subjected to LC-MS/MS analysis. The samples were analysed onto a Hybrid Quadrupole-Orbitrap Q Exactive Mass Spectrometer, upon separation with a gradient of 10-40% solvent B over 100 min, followed by a gradient of 40-60% for 10 min and 60-95% over 3 min at a flow rate of 250nL/min. MaxQuant software v.1.6.0.1 is used for the analysis of MS data, for both protein and peptides identification including as variable modifications mono-, di- and tri-methyl lysine, mono- and di- methyl arginine and lysine acetylation. The Uniprot HUMAN histones 1502 database was used for histone peptide identification. Enzyme specificity was set to ArgC, since the propionylation of lysine residues allows the trypsin cutting only at the C-terminal of arginine residues. A maximum of 3 missed cleavages were permitted, and the minimum peptide length was fixed at 6 amino acids. PIC at the N-terminal of each peptide was set as a fixed modification. Histone modifications were quantified by label-free approach, in particular by calculating the area under the curve (AUC) of each modified histone peptide and, then extrapolating the percentage relative abundance (%RA), which corresponds to the ratio of the AUC of each individual modified peptide over the sum of the AUC of all modified isoforms of the same peptide.

Results

1. LSD1 inhibition sensitizes AML cells to physiological doses of retinoic acid

Our lab has previously characterized a TCP-derived LSD1 inhibitor, MC_2580, that shows high specificity to LSD1 (100-fold more than TCP) and that acts at relatively low concentrations (Binda et al., 2010). As already reported, LSD1 inhibition with TCP can sensitize some AML cells to retinoic acid, synergizing with it to induce cell differentiation (Schenk et al., 2012).

Through Cell-Titer Glo assay, we tested the effect of the LSD1 inhibitor MC_2580 (LSD1i), alone or in combination with retinoic acid (RA), on a panel of twenty-one AML cell lines representative of all AML subtypes. After 6 days of treatment, LSD1i alone considerably reduced the growth (>70% inhibition) of only a small subset of cell lines (Kasumi-1, SKNO-1 and EOL-1 cells). It is interesting to note that both Kasumi-1 and SKNO-1 cells are classified as FAB M2 subtype and are the only two tested cell lines that harbor the AML1-ETO translocation, suggesting a potential therapeutic effect of LSD1 inhibition in AML1-ETO positive cells. EOL-1 cell line is classified as FAB M4eo and carries an MLL partial tandem duplication (MLL-PTD). The role of LSD1 in this particular contest should be further investigated.

Similarly to LSD1 inhibition, low doses of RA (RA 0.01 – 0.1μM) had a minor effect on the great majority of the cell lines, and only a few of them responded to treatment (EOL-1, MonoMac1 and MV4-11 cells). In this case, all the three cell lines carry an MLL rearrangment, respectively MLL-PTD, MLL-AF9 and MLL-AF4, but not all the cell lines that carry an MLL rearrangment responded equally to RA, suggesting that other factors could influence the response.

Interestingly, the combination of RA with MC_2580 had a remarkable impact on the viability of almost all tested cell lines, both resistant and sensitive to LSD1 inhibition alone (Figure 16).

Confirming previous findings, APL cells (NB4) were not sensitive to LSD1 inhibition or to physiological doses of RA (0.01μM, RA low), while the combination of LSD1i and RA low affected dramatically cell viability.

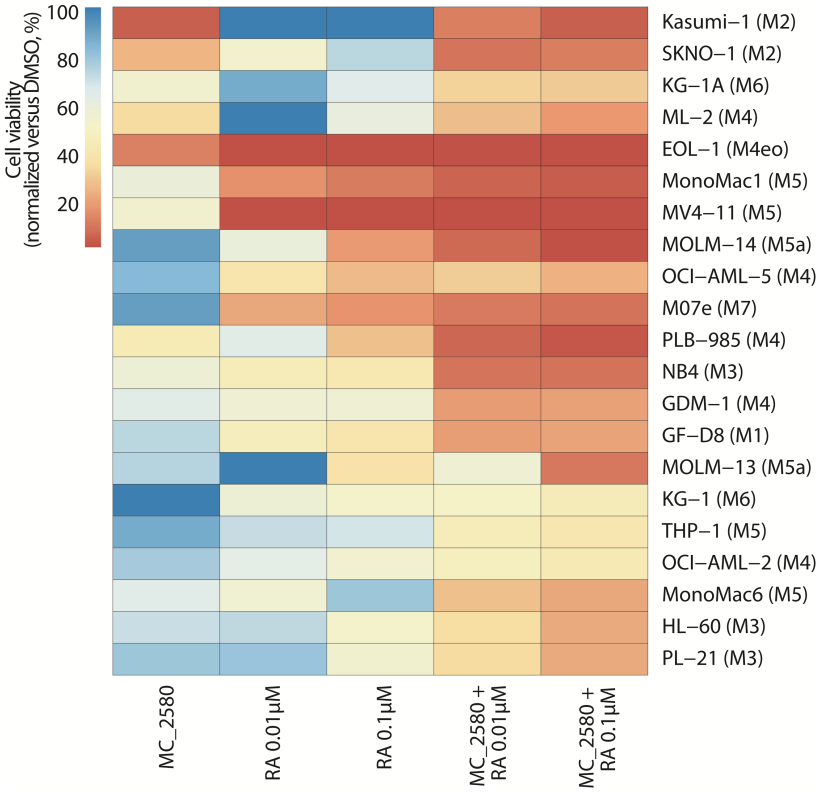

Figure 16. LSD1 inhibition sensitizes AML cells to retinoic acid treatment.

Heatmap representing the result of cell proliferation assay of 21 AML cell lines treated with MC_2580 (2μM) and/or RA as indicated. Values are normalized on DMSO treatment. In brackets, the AML French-American-British classification of each cell line.

We therefore tested the drugs in liquid culture by direct counting cells and we confirmed the findings obtained with Cell-Titer Glo viability assay (Figure 17a). Intringuely, the

combination of LSD1i with RA low reduced also colony forming ability in semi-solid culture, a surrogate read-out for the self renewal ability of leukemic cells (Figure 17b).

Given the results, we decided to use NB4 cells as a model system to investigate the molecular mechanisms beyond sensitization to retinoic acid by LSD1 inhibition.

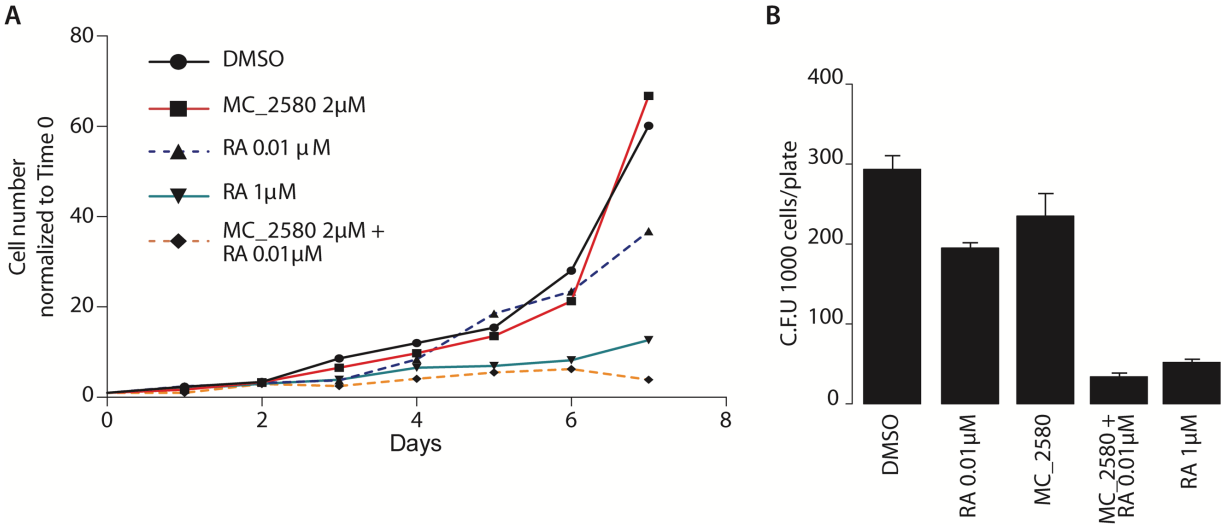

Figure 17. LSD1 inhibition sensitizes NB4 cells to physiological doses of retinoic acid.

A) Growth curve of NB4 cells treated as indicated. **B)** Colony forming ability, scored after 7 days, of 1000 NB4 cells plated in methylcellulose medium and treated with LSD1 inhibitor MC_2580 (2µM) and/or RA 0.01µM and 1µM. Mean and standard deviation of three independent experiments are shown.

Retinoic acid is a well-described differentitation inducing agent. As already described (Breitman et al., 1981), high doses of retinoic acid induce differentiation of APL cells, while low doses fails to do it. Consistently, we observed that inhibition of proliferation of NB4 cells after combination of LSD1i and low doses of retinoic acid is a consequence of cell differentiation, as assessed by the induction of the myeloid differentiation marker CD11b. Morphological changes associated with neutrophilic differentiation, such as the increase of the cytoplasm/nucleus ratio and the more lobated shape of the nucleus, can also be noticed (Figure 18).

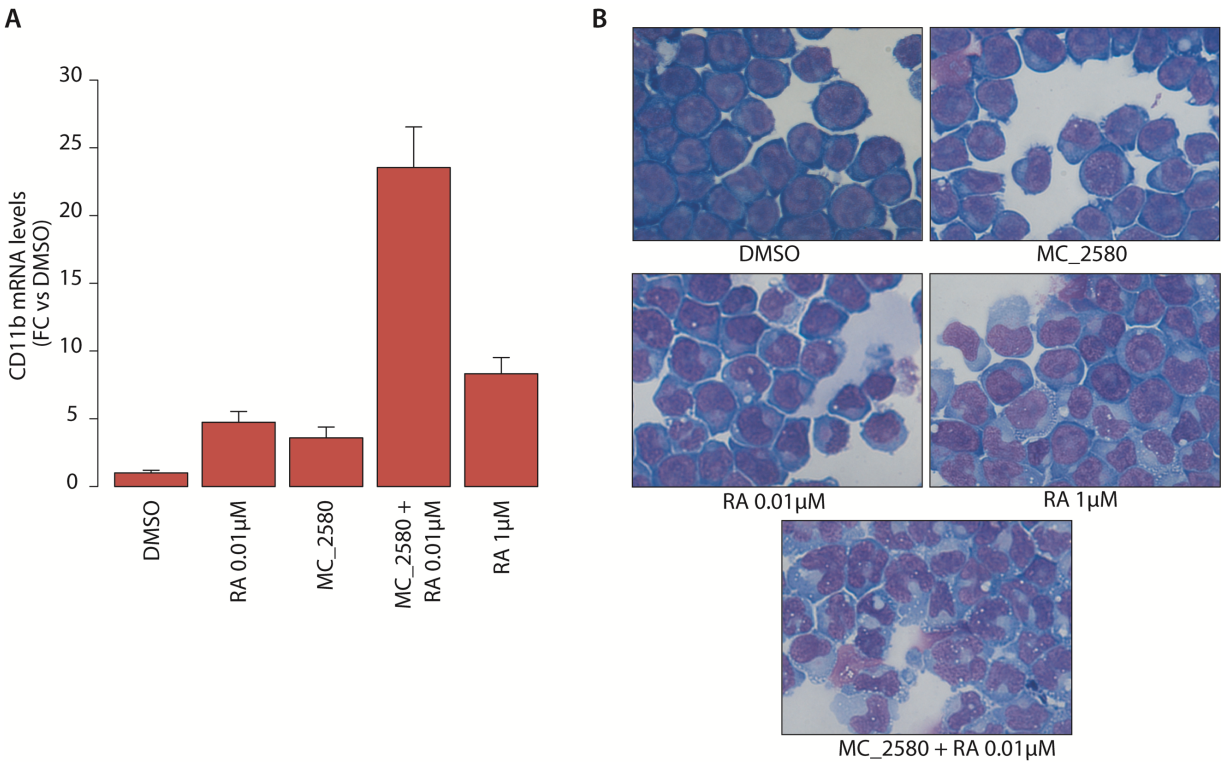

Figure 18. Combination of LSD1 inhibition and low doses of retinoic acid induces differentiation of NB4 cells.

A) Analysis of CD11b mRNA levels in NB4 cells treated as described for 96 hours in liquid culture. Values are normalized against GAPDH and referred to DMSO. Graph represents the mean and standard deviation of three independent experiments. **B)** Morphologic analysis of NB4 cells treated as described for 96 hours in liquid culture; May Grümwald-Giemsa staining.

Finally, in collaboration with the Drug Discovery unit of IEO, we tested the effect of LSD1i and RA combination *in vivo* (Figure 19). We used DDP_38003 as LSD1 inhibitor (Vianello et al., 2016), since MC_2580 is not well-tolerated *in vivo*. One million murine leukemic cells generated by PML-RARα transduction (Minucci et al., 2002) were intravenously injected into non-irradiated 129SvEv mice. Treatments started once blast cells were detected in peripheral blood of recipients mice (10 days after cell injection).

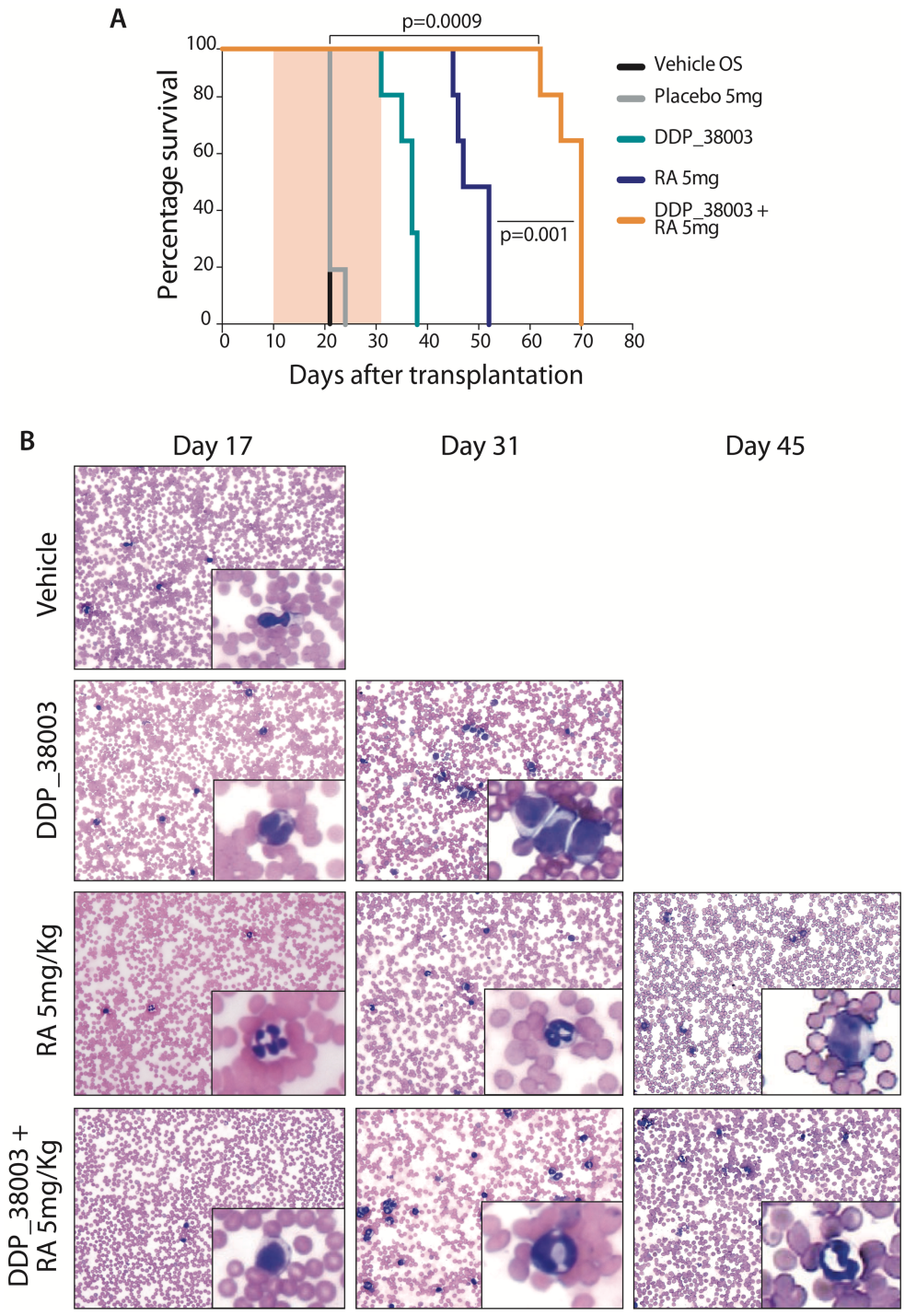

Figure 19. LSD1 inhibition potentiates the RA therapeutic effect in vivo.

A) Kaplan-Meier survival plot for mice transplanted with APL murine cells and treated as indicated (n = 6 for each treatment group). Pink shaded area indicates the duration of RA treatment (21days pellet) while LSD1i (DDP_38003) was administrated twice a week *per os* for the entire duration of RA treatment (tot 6 times). P-values were obtained using ANOVA. **B**) May Grümwald-Giemsa staining of blood smears of mice treated as indicated (referred to figure 4a). Smaller boxes represent an higher magnification of the same image.

All control mice (either treated with placebo or vehicle) died within 3 weeks (median survival 21 days) and RA treatment significantly prolonged survival (median survival 49 days). Treatment with the LSD1 inhibitor alone prolonged survival to a lesser extent than RA (m.s. 37 days), while the combination of RA with LSD1i strongly potentiated the therapeutic effect of RA (m.s. 70 days, p=0.001 over RA treatment, p=0.0009 over placebo). As for *in vitro* results, the prolonged survival observed *in vivo* is a consequence of long-lasting cell differentiation (Figure 19b). No significant body weight differences among the groups were observed during the treatment.

2. LSD1 depletion mimics the effects of LSD1 inhibition in NB4 cells

We next depleted LSD1 in NB4 cells by CRISPR-Cas9 (Figure 20a). LSD1 depletion, as LSD1 inhbition, did not significantly affect viability of NB4 cells in liquid culture neither their colony forming ability (Figure 20b, c). Conversely, LSD1 deplation enhanced NB4 cells sensitivity to low doses of RA, as evidenced by the reduction of cell proliferation and the induction of CD11b (Figure 21). LSD1 depletion thus mimics the effects of LSD1 inhibition, confirming the specificity of the LSD1 inhibitor previously used and furthfer indicating that LSD1 partecipates in the establishment of a differentiation block that cannot be easly overcame. However, the removal of the barrier by both LSD1 depletion or inhibition renders cells more responsive to a differentiation stimuls, such as retinoic acid.

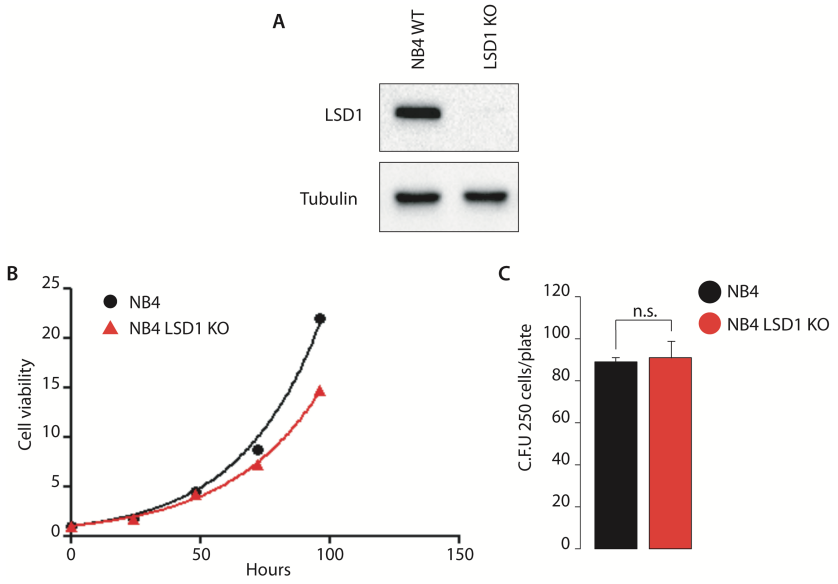

Figure 20. LSD1 knock-out does not affect viability of NB4 cells.

A) Western blot showing depletion of LSD1 in NB4 knockout cells. Tubulin served as loading control. **B)** Cell viability of NB4 and NB4 KO cells in liquid culture at 24, 48, 72, 96 hours. **C)** Colony forming ability, scored after 7 days, of 250 NB4 and NB4 KO cells plated in methylcellulose medium. Mean and standard deviation of three independent experiments are shown. Two-tailed unpaired Student's t-test, n.s. = not significant.

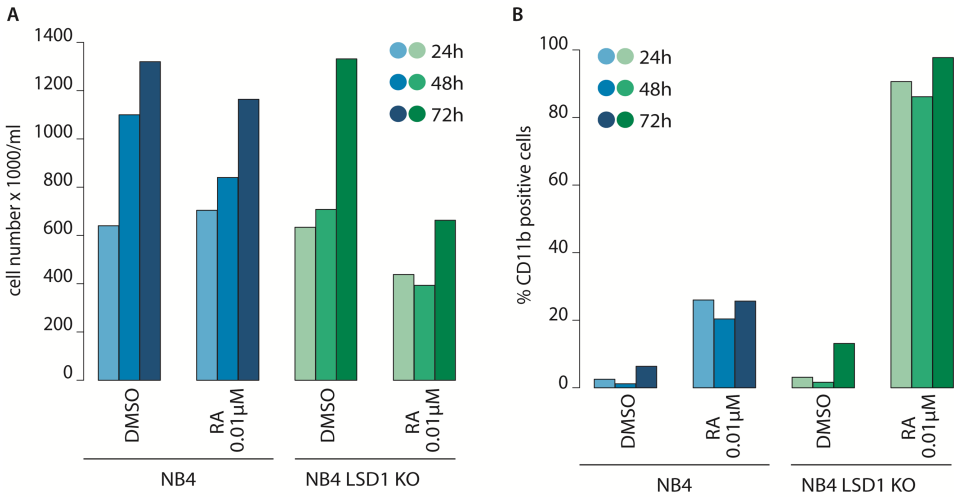

Figure 21. LSD1 knock-out sensitizes NB4 cells to physiological doses of retinoic acid.

A) Proliferation of NB4 and NB4 knockout cells after 24, 48 and 72 hours of the indicated treatments (DMSO as control). **B)** Percentage of CD11b expressing cells measured by fluorescent activated cell sorting (FACS) in NB4 and NB4 LSD1 knockout cells after 24, 48 and 72 hours of indicated treatments (DMSO as control).

Since LSD1 is a histone demethylase and its primary target is H3K4, we measured the effect of LSD1 depletion/inhibition on global levels of histone H3K4 methylation by quantitative mass spectrometry (Figure 22). We observed in all cases an increase in global H3K4me2 and a slight increase in H3K4me3 levels, with the latter likely being a consequence of H3K4me2 accumulation.

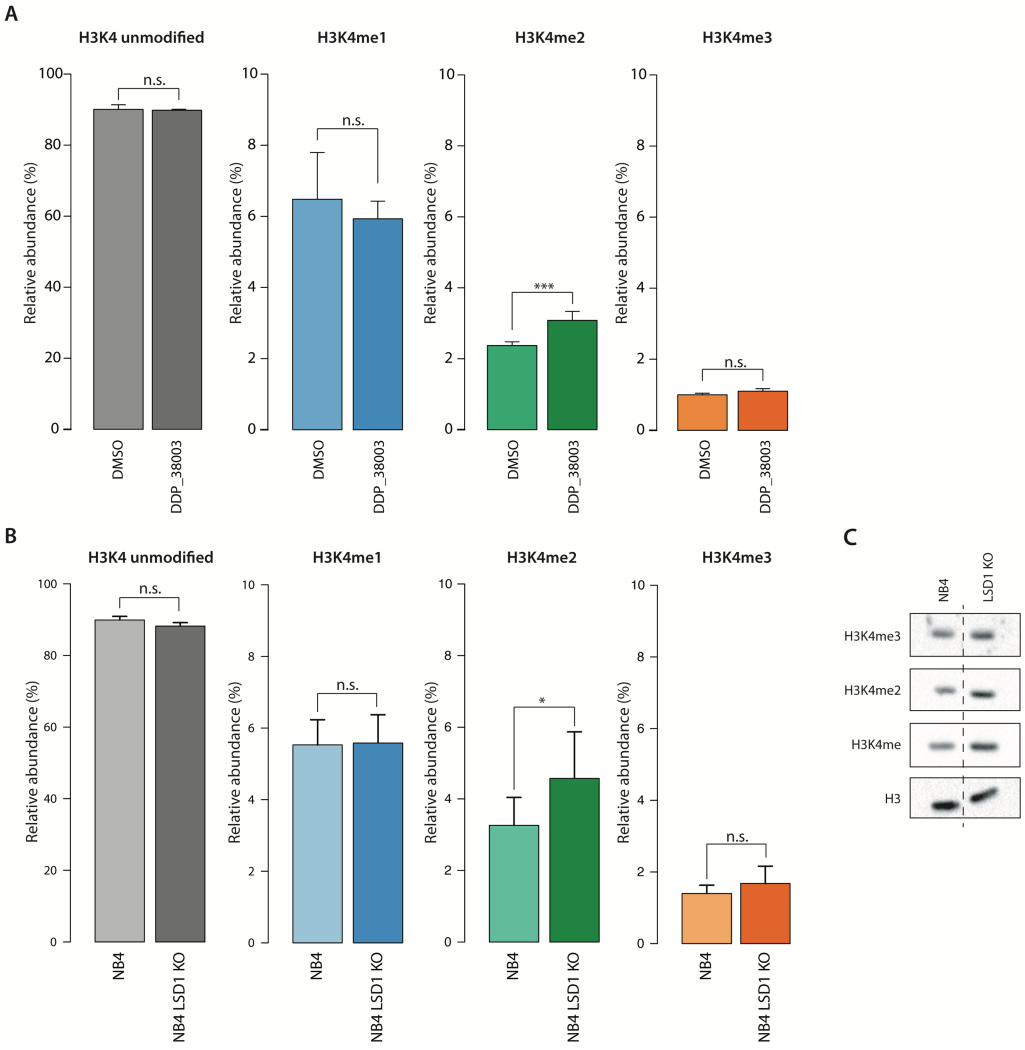

Figure 22. LSD1 inhibition and KO induce H3K4 methylation accumulation.

A) Mass Spectrometry-based quantification of the differently modified isoforms of H3(3-8) peptide, bearing unmodified, H3K4me1, H3K4me2 and H3K4me3. Histones were purified by strong acid extraction of nuclei from NB4 cells treated with DDP_38003 and DMSO as control (measurements were obtained with 3 biological replicates and 3 technical replicates for each biological replicate). P-values were obtained by two-tailed paired Student's t-test (n.s. = not significant; *** $p < 0.001$). **B)** Mass Spectrometry- based

quantification of the differently modified isoforms of H3(3-8) peptide, bearing unmodified, H3K4me1, H3K4me2 and H3K4me3. Histones were fractionated by strong acid extraction of nuclei from wild type and NB4 LSD1 KO cells (n = 3 each). P-values were obtained by two-tailed paired Student's t-test (n.s. = not significant; * $p < 0.05$). **C)** Western blot analysis of H3K4me, H3K4me2 and H3K4me3 of histone extracts NB4 and NB4 KO cells. H3 served as loading control. Dashed line indicates that lanes have been cropped and paired from the same original membrane.

3. LSD1 inhibition allows APL cells differentiation bypassing the oncogenic function of PML-RARα

It has been shown that pharmacological doses of RA trigger PML-RARα degradation and this mechanism has been proposed as crucial for the eradication of APL (Nasr et al., 2008; Nervi et al., 1998).

While pharmacological doses of RA (RA high) trigger PML-RARα degradation, physiological doses of RA (RA low) do not. Interestingly, in NB4 cells we observed that PML-RARα protein levels remained stable upon LSD1 inhibition, whether in the presence or in the absence of RA low (Figure 23). Thus combination of RA low and LSD1i can induce differentiation without altering PML-RARα protein stability.

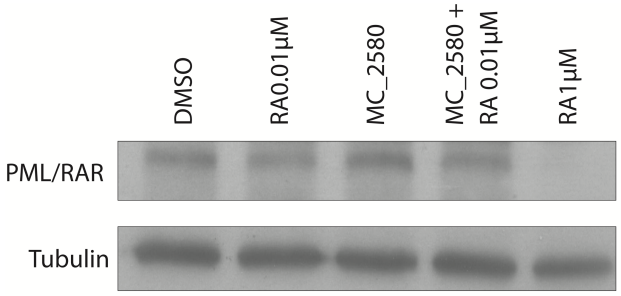

Figure 23. LSD1 inhibition allows APL cells differentiation without altering PML-RARα stability.
Western blot analysis of PML-RAR levels in NB4 cells treated as indicated for 24 hours. Tubulin served as loading control.

PML physiologically is organized in macromolecular assemblies of proteins whithin the nucleus, called PML nuclear bodies (PML-NBs), that are essential for PML functions. PML-RARα interacts with normal PML generated by the allele not involved in the t(15;17) translocations and alters the normal assembly of PML nuclear bodies. In particular, PML-RARα recruits PML on chromatin and induces a micro-speckled pattern of PML (de Thé and Chen, 2010). As expected, RA high, inducing degradation of PML-RARα, caused the restoration of the normal pattern of PML nuclear bodies. Consistently, since MC_2580 does not induce PML-RARα degradation, it did not even altered the micro-speckled pattern of PML both in the presence or in the absence of RA low (Figure 24). This is an indirect indication that only high doses of RA can induce PML-RARα degradation, while in all the other treatments PML-RARα is not degraded and is still on chromatin.

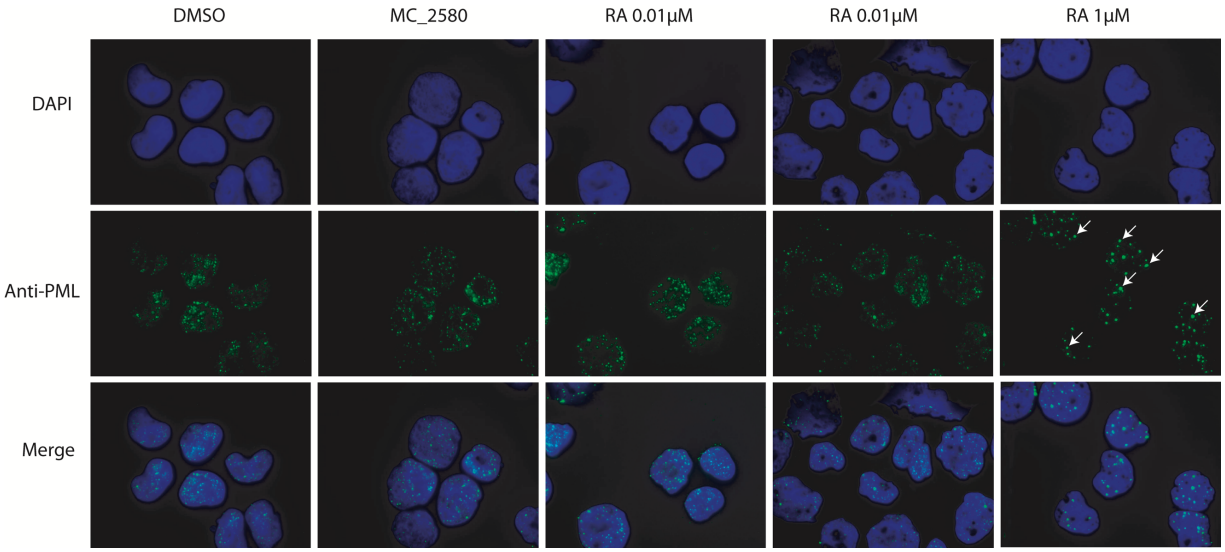

Figure 24. LSD1 inhibition permits APL cells differentiation without restoration of PML-nuclear bodies.

Representative images showing immunostaining for PML in NB4 cells treated as indicated. Nuclei are identified by DAPI staining. White arrows indicate examples of PML nuclear bodies.

In order to further verify whether LSD1 inhibition alters PML-RAR recruitment at its targets, we performed ChIP-qPCR on PRAM1 and PI3KD, two established PML-RARα targets in NB4 cells (Martens et al., 2010). We observed that LSD1 inhibition and RA low did not alter PML-RAR recruitment on those genes, while RA high displaced PML-RARα from chromatin and/or triggered degradation of the fusion protein (Figure 25). Overall, these results demostrate that the combination of LSD1 inhibition and low doses of RA can induce differentiation of APL cells without affecting PML-RARα functions, suggesting a role for LSD1 independent from PML-RARα.

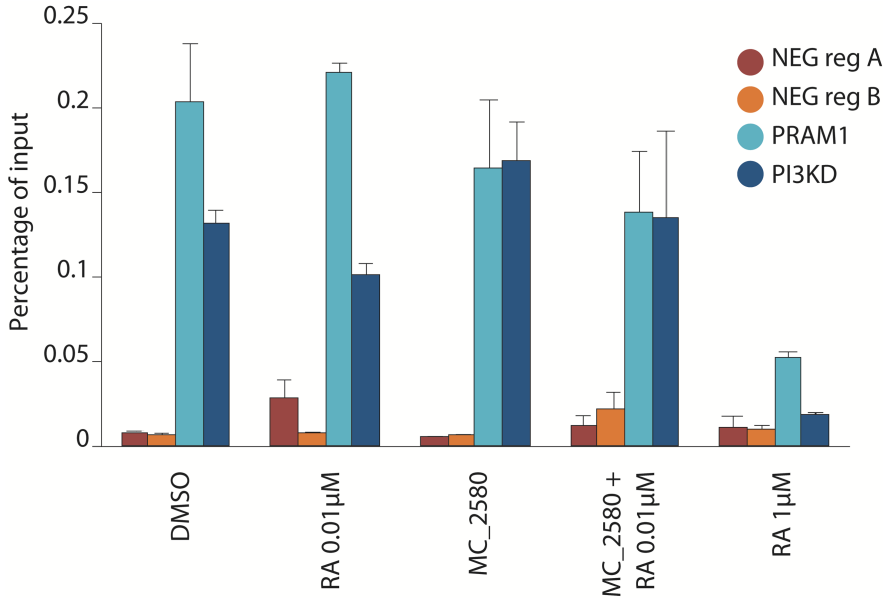

Figure 25. LSD1 inhibition allows APL cells differentiation without altering PML-RARα recruitment. PML-RAR recruitment at target genes assessed by Chromatin Immunoprecipitation (ChIP) of PML in NB4 cells. The results represent percentage of input chromatin and error bars indicate s.d. from triplicate experiments.

4. LSD1 regulates differentiation of APL cells.

In order to dissect the effects of LSD1 inhibition on APL cells and to investigate the mechanisms leading to retinoic acid sensitization, we determined, though RNA-seq, the

gene expression profile of NB4 cells after 24 hours of treatment with MC_2580 and/or RA. LSD1 inihibition had only a modest effect on gene transcription, both in terms of number of modulated genes and in the magnitude of their regulation (Figure 26) and, consistent with the repressive function of LSD1 in this leukemic contest, most of the differentially espressed genes are up-regulated. Also LSD1 knock-out had a little effect on global transcription (Figure 27), confirming LSD1 inhibitors data. Nevertheless, LSD1 inhibition dramatically potentiated the effect of physiological doses of RA, since the combination of RA low with LSD1 inhibition almost dobled the number of genes induced by RA low alone. However, in line with LSD1 inhibition alone and LSD1 knock-out, there were no variations in the down-regulated genes.

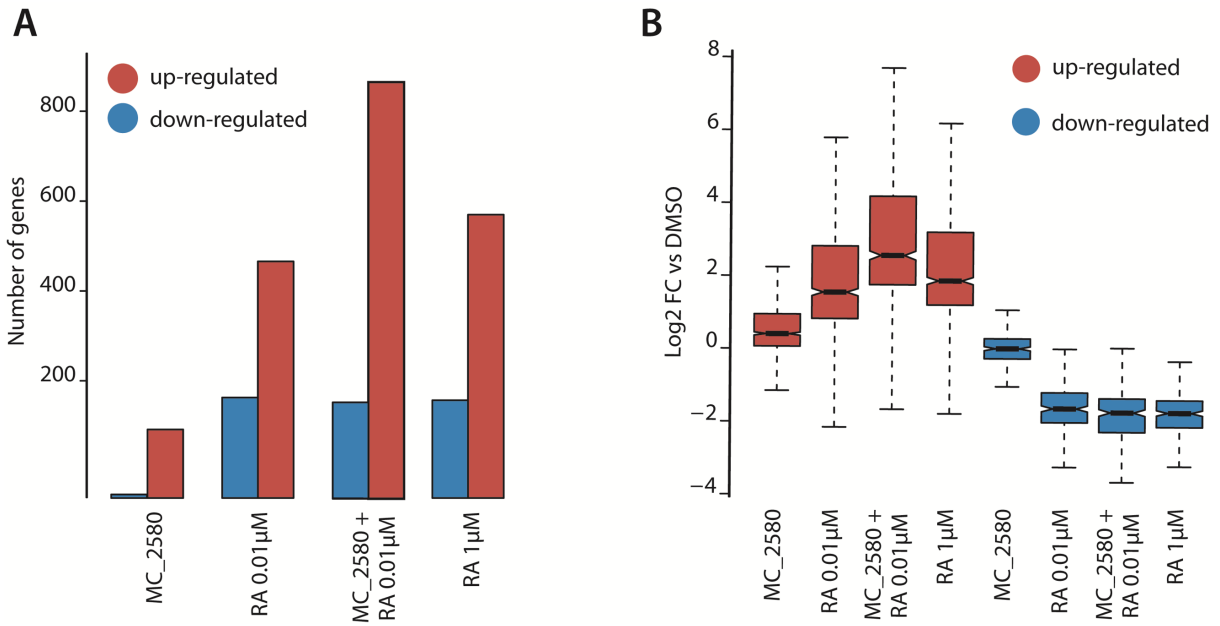

Figure 26. Differentially Expressed Genes in NB4 cells after 24 hours of LSD1i and/or RA treatment. **A)** Barplot represents number of genes regulated (up or down regulated respect to control, RPKM>0.5, log_2(FC)>1.5) upon the indicated treatments. **B)** Boxplot shows magnitude of induction by the indicated treatment vs control (DMSO).

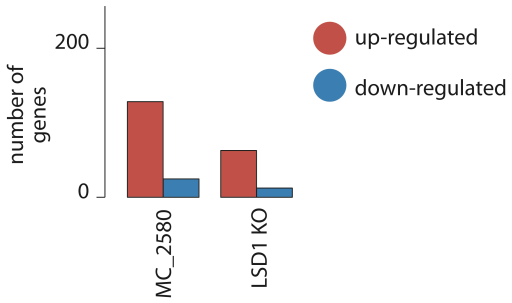

Figure 27. Differentially Expressed Genes in NB4 cells after 24 hours of LSD1i and in NB4 KO cells.
Barplot represents number of genes regulated (up or down regulated respect to control, RPKM>0.5, log_2(FC)>1.5). DEGs of MC_2580 treated NB4 cells are reported also in figure 26.

Since treatment with high doses of retinoic acid (1μM, RA high) is able to induce differentiation of NB4 cells, we compared the effects of the combination of LSD1i and RA low to RA high. Interestingly, the combination induced almost all of the genes regulated by RA high, plus 382 unique genes (Figure 28a). The large majority of regulated genes, either by RA high or by LSD1i and RA low, falls within gene categories associated with hematopoietic development and differentiation (Figure 28b).

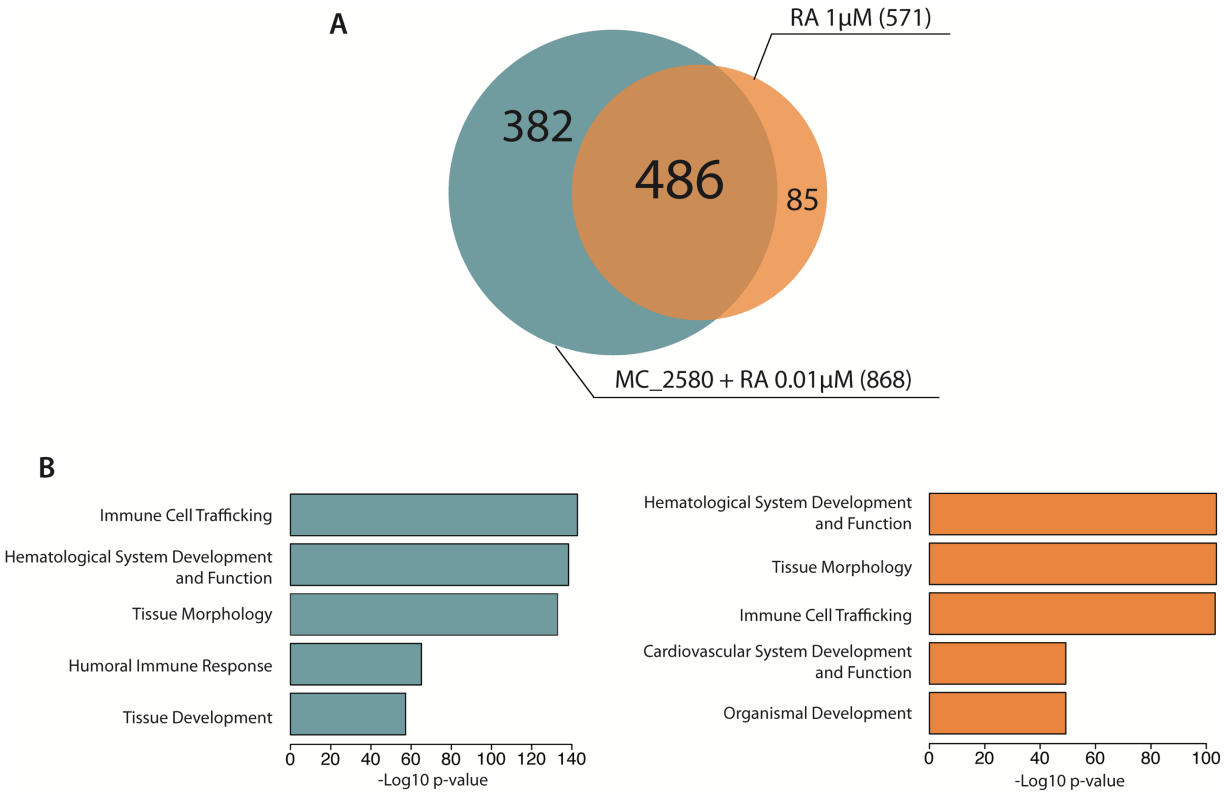

Figure 28. Comparison of Differentially Expressed Genes after LSD1i and Ra low versus RA high.
A) Venn diagrams with numbers of total, individual and overlapping genes regulated in NB4 cells treated with MC_2580 + RA 0.01μM versus RA 1μM. **B)** Ingenuity Pathway Analysis (IPA) of genes up-regulated upon MC_2580 plus RA 0.01μM (n = 868, left panel) or all genes up-regulated by RA 1μM (n = 571, right panel). Adjusted p-value for each class is shown.

These observations suggest that while the combinatorial treatment and RA high induced a similar differentiation program, the combination had a larger impact on transcription than RA high: indeed, the combination had a stronger effect on cell proliferation then observed with RA high alone (Figure 17).

To further investigate the role of LSD1 in APL cells and the mechanism by which its inhibition sensitizes APL cells to retinoic acid, we assayed its genomic distribution by ChIP-Seq. We found that LSD1 binds preferentially gene regulatory regions, with 18% of all peaks occurring in gene promoters (Figure 29). As expected, LSD1 bound regions are enriched for hematopoietic related transcription factors binding sites, suggesting possible functional interactions with some of the main hematopoietic regulators.

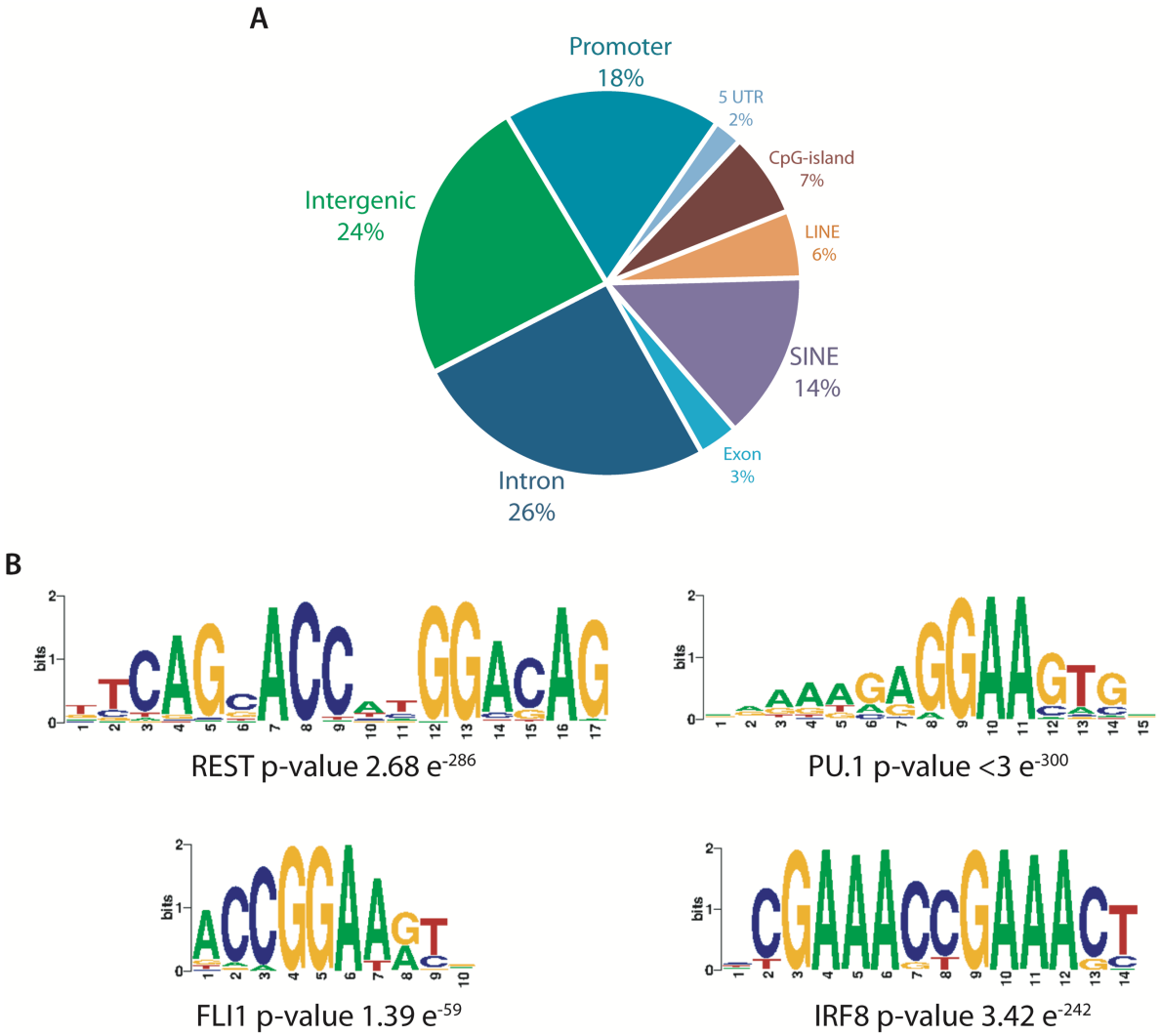

Figure 29. LSD1 binds gene regulatory regions enriched for hematopoietic related TFs binding sites.

A) Pie chart indicates genome annotations for LSD1 binding peaks. **B)** example of some of the most enriched TF binding sites in LSD1 bound regions.

LSD1 peaks mainly occur in the regulatory regions of genes involved in hematopoiesis and cell differentiation, and in genes that are involved in chromatin regulation (Figure 30). This observation highlights the central role of LSD1 in hematopoietic development and differentiation. Intriguingly, LSD1 inhibition/depletion alone does not have a major impact on transcription, suggesting that LSD1 is involved in epigenetic remodeling/mechanism that render cells more prone to a differentiation stimulus (RA).

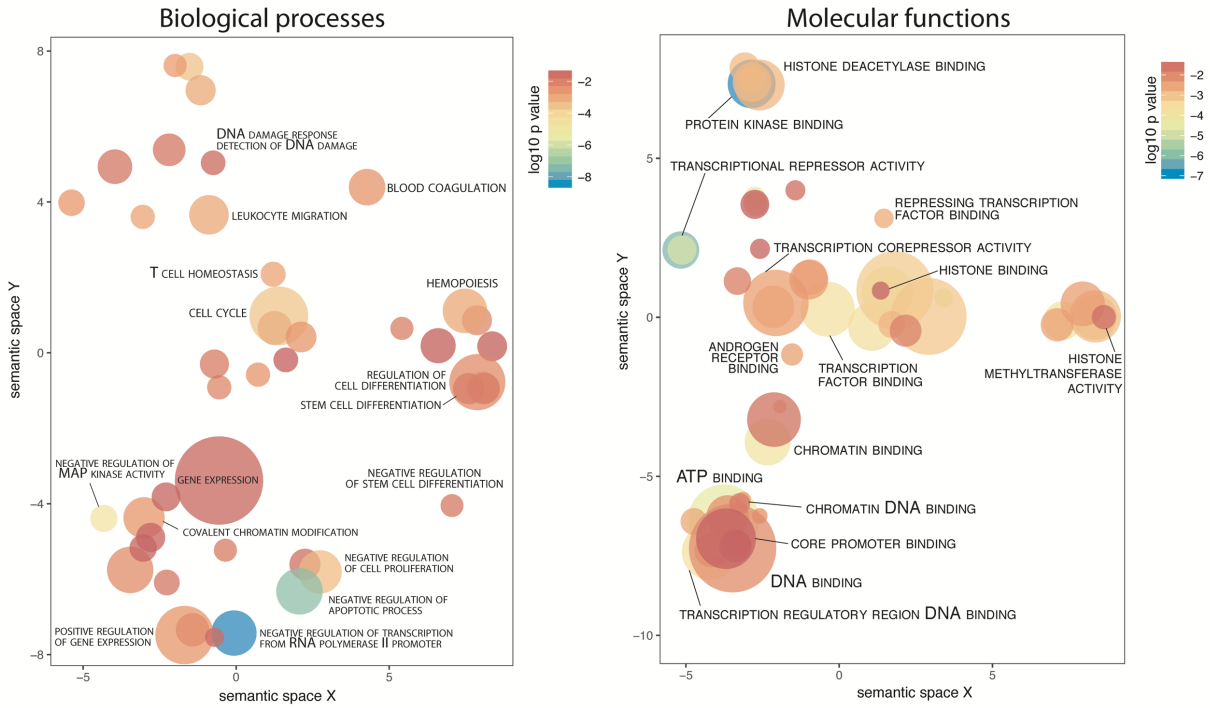

Figure 30. LSD1 binds regulatory regions of genes involved in hematopoiesis and epigenetic regulation.

Gene Ontology analysis of LSD1 target genes in NB4 cells. Biological processes (left panel) and Molecular functions (right panel). Adjusted p-values and relative enrichment (color coded) are shown for each class.

By taking advantage of a PML-RARα ChIP-seq in NB4 cells already present in literature (Martens et al., 2010), we next compared LSD1 and PML-RARα genomic distribution (Figure 31). Interestingly, PML-RARα shares most of its binding sites with LSD1, but more than 85% of LSD1 bound regions in NB4 cells do not show any PML-RARα signal, further suggesting PML-RARα-independent roles for LSD1.

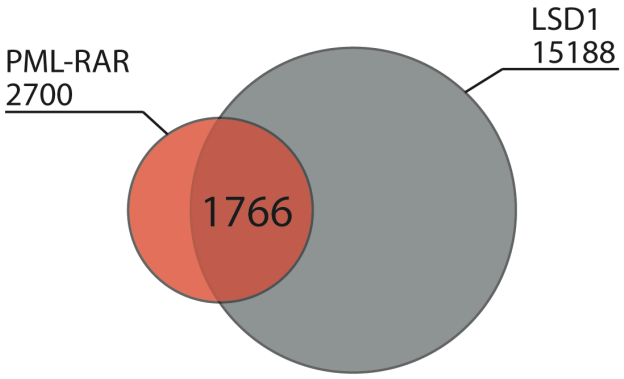

Figure 31. Comparison of LSD1 and PML-RARα genomic distribution in NB4 cells.

Venn diagram with number of total and overlapping ChIP-Seq peaks of LSD1 and PML-RAR in NB4 cells.

5. LSD1 inhibition and RA treatment remodel chromatin landscape of NB4 cells

In order to elucidate the role of LSD1 in epigenetic regulation and the effects of LSD1 inhibition on the epigenetic organization of NB4 cells, we performed ChIP-seq of H3K4me, H3K4me2, H3K4me3 and H3K27ac upon the different treatments and we observed a dramatic reorganization of the chromatin. In particular, analyzing the variations in H3K27 acetylation, we noted an evident rearrangement of active super-enhancers after the combination of LSD1 inhibition and RA low. Out of 362 active super-enhancer identified in LSD1i and RA low treated NB4 cells (Figure 32), 207 were newly activated compared to not treated (DMSO) NB4 cells and 118/207 were uniquely activated in the cotreatment and not after high doses of RA. Confirming RNA-seq and LSD1 ChIP-seq, we found that the combination of LSD1 inhibition and RA low induced the activation of super-enhancers associated to main hematopoietic regulators, some of which specifically induced by the cotreatment and not by RA high (*eg* IRF8).

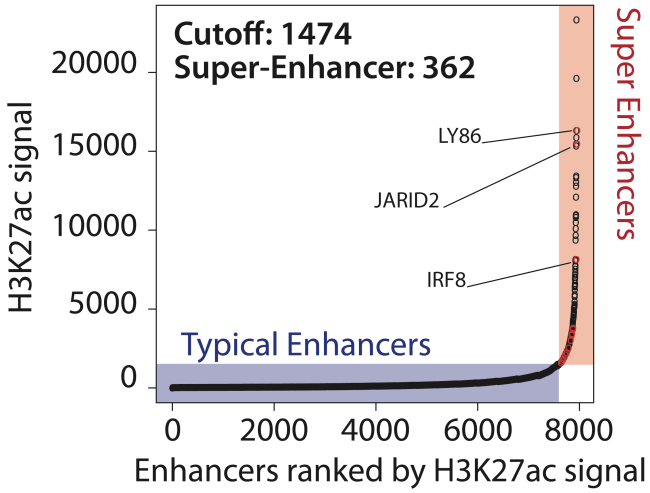

Figure 32. Active super-enhancers in APL cells treated with LSD1 inhibitor and RA low.

Scatter plots of Super-Enhancers in cells treated with MC_2580 + RA 0.01μM. All stitched regions were ranked by H3K27ac signal, Super-Enhancers (SE) and Typical Enhancers (TE) were in different colors as indicated.

We then separately analyzed chromatin changes upon the different treatments occurring in the subset of genes specifically induced by the cotreatment (n = 382), and those similarly induced by both RA high and cotreatment (n = 486). In order to analyze the variations in chromatin marks more related to LSD1 activity, we selected only LSD1-bound genomic regions and we analyzed the signal variations of each chromatin mark occurring in those regions. Every regions was then associated to a gene following standard GREAT parameters (Proximal 5Kb upstream and 1Kb downstream of TSS plus Distal up to 1000Kb from TSS). Only genomic regions that met the gene regulatory domain criteria were considered for analysis. As expected, active transcription positively correlates with the presence of both H3K4me3 and H3K27a and genes specifically transcribed after the combination (n = 382) have low levels of acetylations after RA treatment alone (either low or high doses) (Figure 33).

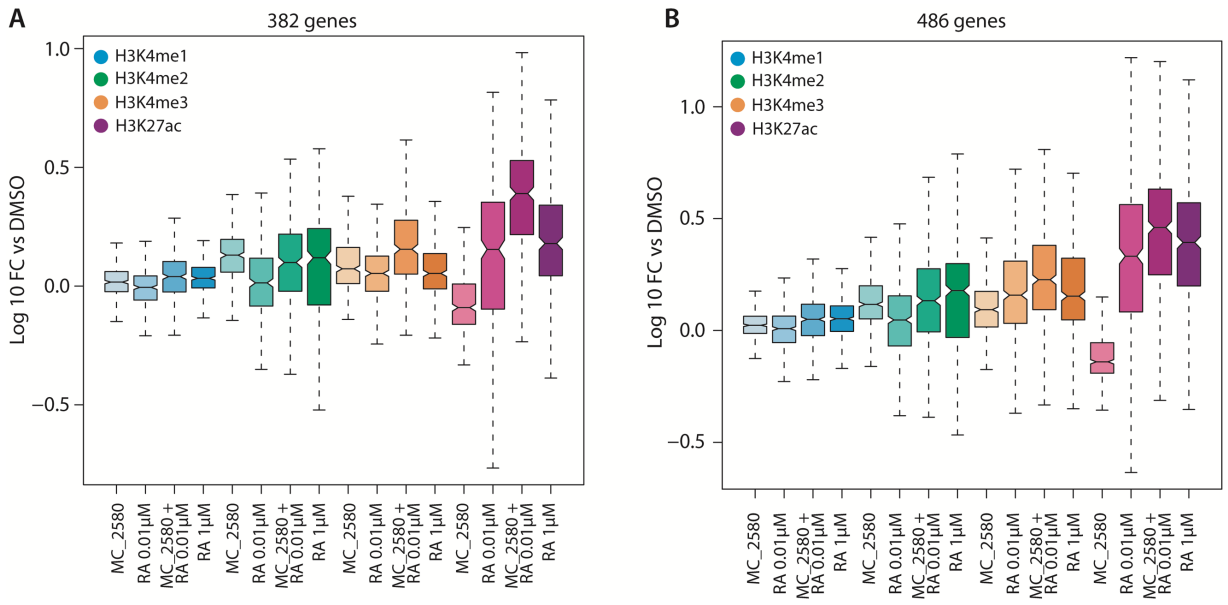

Figure 33. LSD1 inhibition and RA treatment remodel the chromatin landscape of NB4 cells.

A) Boxplot analysis of H3K4me, H3K4me2, H3K4me3 and H3K27ac enrichment upon indicated treatment at genes specifically up- regulated upon MC_2580 plus RA 0.01μM (n = 382, see figure 28). Values are represented as fold change versus DMSO. **B)** Boxplot analysis of H3K4me, H3K4me2, H3K4me3 and H3K27ac enrichment upon indicated treatment at the 486 genes commonly induced by both MC_2580 plus RA low and RA high (see figure 28). Values are represented as fold change versus DMSO.

Although we observed a local (Figure 34) and global (Figure 33) increase of H3K4me2 after LSD1 inhibition, alone or in combination with RA, we observed also an increase of H3K4me2 levels after high doses of RA in genes actively transcribed only after the combination of LSD1i and RA low (n=382, Figure 33 left panel). Interestingly, the increase in H3K4me2 after RA high in those genes is not associated with an increase of their transcriptional activity.

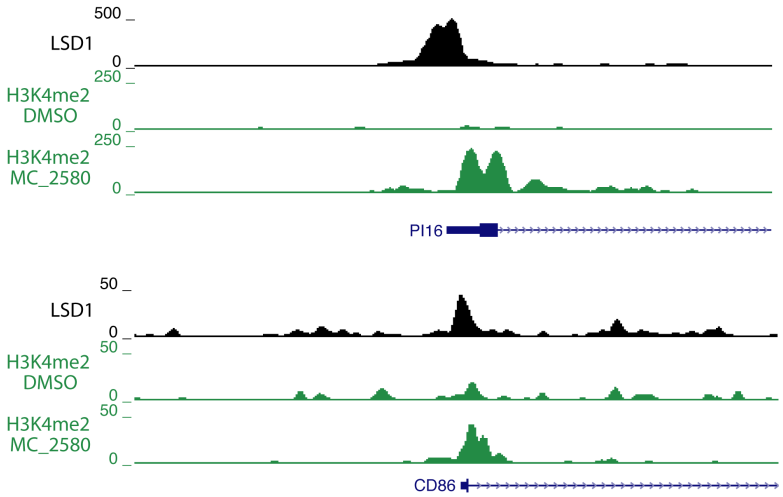

Figure 34. LSD1 inhibition leads to local H3K4me2 increase in LSD1-bound regions.
Representative examples of LSD1-bound regions showing increase in H3K4me2 ChIP-seq signal after LSD1 inhibition. UCSC Genome Browser profile of LSD1 and H3K4me2 (treated with either DMSO or MC_2580) of PI16 and CD86 promoter regions.

To further investigate this phenomenon, we separately analyzed the H3K4me2 levels variations in promoters and enhancers of those genes (n = 382) but we did not find any difference in the methylation pattern between promoters and enhancer (Figure 35). Thus, the RA high-mediated increase of H3K4me2 levels of gene regulatory elements did not translate into active transcription of the same genes, suggesting that H3K4me2 is not sufficient to trigger gene expression changes.

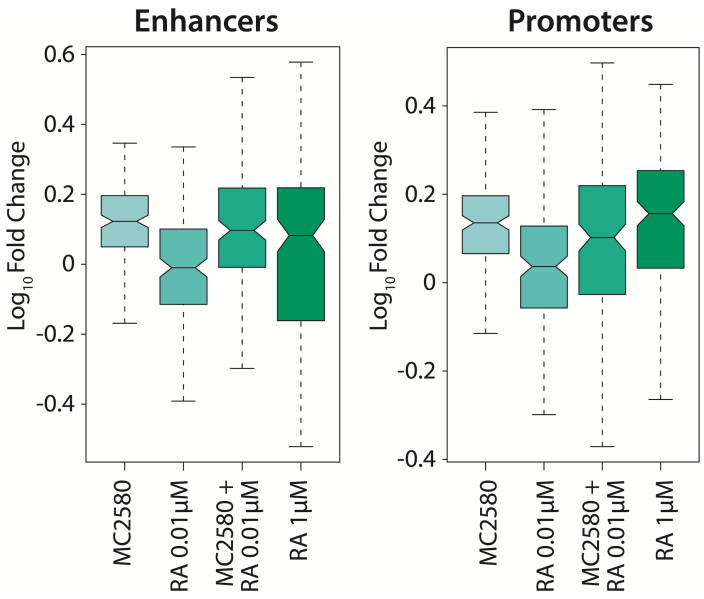

Figure 35. High doses of RA induce H3K4me2 levels of gene regulatory elements without inducing transcription of associated genes.

Boxplot analysis of H3K4me2 enrichment upon indicated treatment at enhancers (left panel) and promoters (right panel) of the 382 genes specifically induced only by LSD1i and RA low (Figure 28). Values are represented as log_{10} fold change versus DMSO.

6. LSD1 catalytic activity is dispensable for sensitization to retinoic acid induced differentiation

The observation that H3K4me2 *per se* is not sufficient to trigger gene expression prompted us to investigate whether LSD1 catalytic activity is required for RA sensitization of leukemic cells. We then reconstituted LSD1 knock-out cells with either wild type or a catalytically inactive mutant (K661A) of LSD1 (Figure 36). While knock-out cells (infected with an empty vector) were very sensitive to low doses of RA, cells reconstituted with either wild type LSD1 or the catalytic mutant LSD1-K661A reacquired resistance to RA, recapitulating the phenotype of wild type NB4 cells.

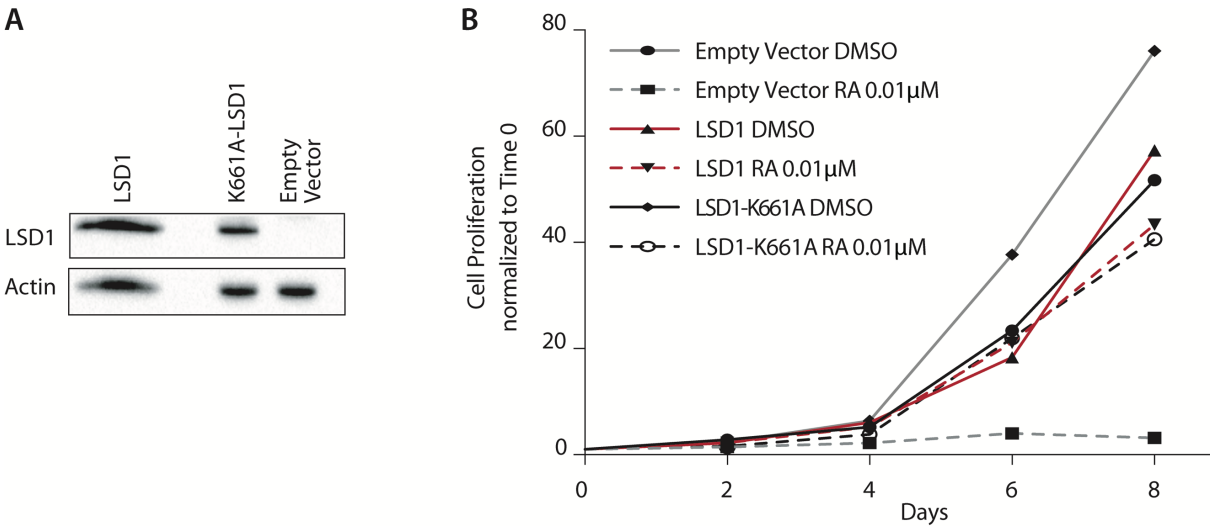

Figure 36. LSD1 catalytic activity is dispensable for RA sensitization of NB4 cells.

A) Western blot analysis of LSD1 levels in NB4 knockout cells transduced with expression vectors encoding for wild-type LSD1 or the catalytically inactive mutant K661A-LSD1. Empty vector was used as control, actin served as loading control. **B)** Growth curve of NB4 knockout cells transduced with Empty vector, LSD1 or K661A-LSD1 and treated with RA 0.01μM (DMSO as control treatment).

In line with the observations in NB4 wild type cells, we observed that inhibition of proliferation of NB4 LSD1 knock-out cells treated with low doses of RA is a consequence of cell differentiation. We indded observed induction of CD11b at the RNA level and an increase of CD11b expressing cells by FACS after 3 days of RA treatment in LSD1 knock-out cells, but not in cells expressing either wild type or the K661A catalytic inactive mutant of LSD1 (Figure 37a, b). Morphological anaylisis of rescued cells confirmed the indirect data of CD11b, with LSD1 knock-out cells treated with RA committed to granulocytic differentiation, while morphology of rescued cells was not affected (Figure 37c).

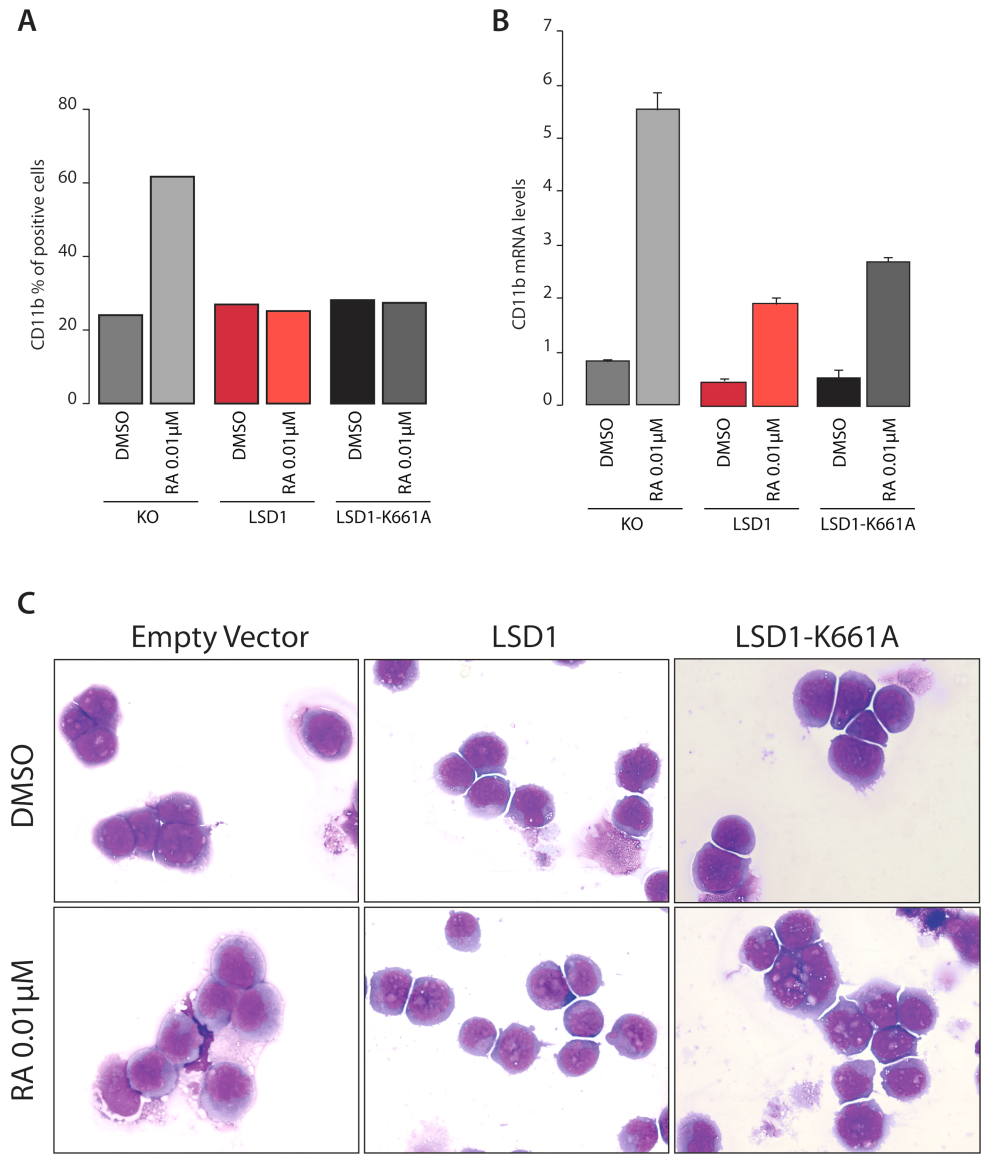

Figure 37. LSD1 catalytic activity is dispensable for RA sensitization of APL cells.

A) Percentage of CD11b expressing cells assessed by fluorescent activated cell sorting (FACS) in NB4 knockout transduced with with expression vectors encoding for LSD1, K661A or Empty vector, treated with RA 0.01µM or DMSO cells for 72 hours. **B)** Analysis of CD11b mRNA levels in NB4 cells treated as described for 72 hours in liquid culture. Values are normalized against GAPDH. Graph represents the mean and standard deviation of three independent experiments. **C)** Morphologic analysis of knockout cells transduced with LSD1 or the catalytically inactive mutant K661A-LSD1 and treated with 0.01µM RA for 8 days. May Grümwald-Giemsa staining.

In order to verify the effective catalytic activity of both wild type and K661A LSD1 mutant, we performed ChIP-qPCR of H3K4me2 at some LSD1 targets in NB4 and NB4 LSD1 knock-out

reconstituted cells (Figure 38). As expected, we observed a local increase of H3K4me2 in LSD1 knock-out cells. Reconstitution of knock-out cells with wild type LSD1 led to a reduction of H3K4me2 to levels similar to normal NB4 cells, while K661A catalytic mutant did not reduced levels of H3K4me2 at the same loci, confirming its catalytical inactivity.

Since both wild type and catalytically inactive LSD1 reconstituted cells are resistant to RA, these data demonstrate that the catalytic activity of LSD1 is dispensable for sensitization to RA induced differentiation of NB4 cells.

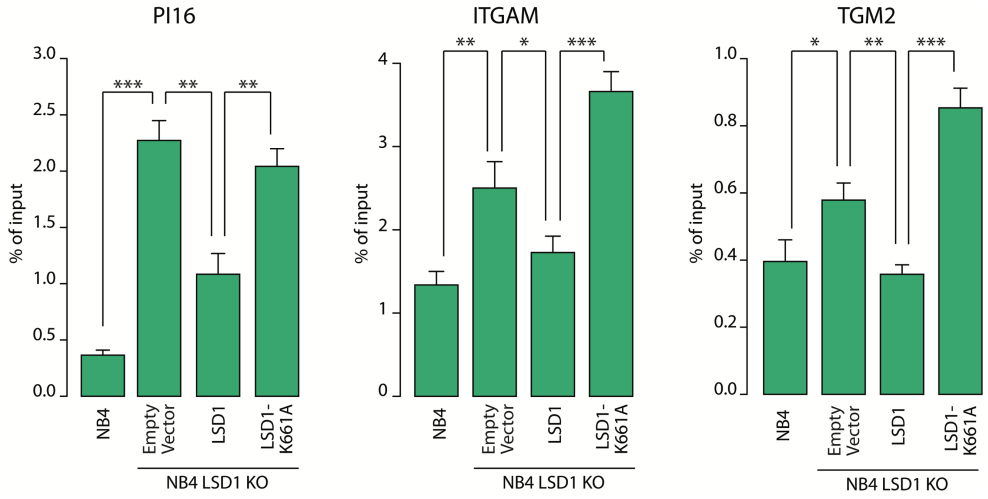

Figure 38. H3K4me2 levels in wild type and LSD1-reconsituted knock-out NB4 cells.

H3K4me2 enrichment at the promoter of PI16 (left), ITGAM (center) and TGM2 (right) in NB4 and NB4 knockout cells transduced with with expression vectors encoding for LSD1, K661A or Empty vector, assessed by ChIP-qPCR. The results represent percentage of input chromatin, error bars indicate s.d. from triplicate experiments and p-values were determined by a two-tailed unpaired Student's t-test (* $p < 0.05$, ** $p < 0.01$, *** $p < 0.001$).

7. LSD1 pharmacological inhibition disrupts its interaction with GFI1

The above results demonstrate that non-enzymatic functions of LSD1 are critical for its activities. We hypothesized that LSD1 may have a main scaffolding role, and that LSD1 inhibitors could somehow interfere with the interaction between LSD1 and other proteins.

To verify this hypothesis, in collaboration with Tiziana Bonaldi's group at IEO, we employed an approach of SILAC-based proteomics in combination with LSD1 immuno-precipitation to study the LSD1 interactome in NB4 cells (Figure 39). Briefly, SILAC (Stable Isotope Labeling by Aminoacid in cell Culture) is a mass spectrometry-based technique that allows detection of protein abundance differences among samples using non-radioactive isotope labeling. Growing cells in light (K0, R0) or heavy (K8, R10) medium leads to metabolic incorporation of amino acids into proteins and results in a mass switch of the corresponding peptide. When samples grown in light and heavy medium are combined, the ratio of peak intensities in the mass spectrum reflects relative protein abundance.

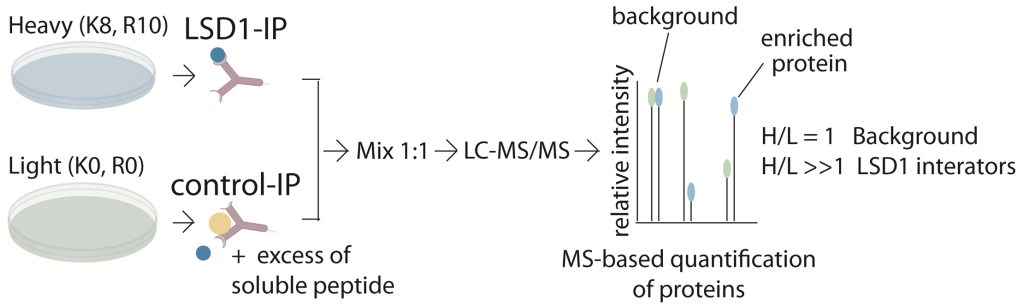

Figure 39. Schematic representation of SILAC mass spectrometry approach to identify LSD1 interactors in NB4 cells.

In the "forward" experiment LSD1 immunoprecipitation was performed on NB4 cells grown in heavy medium, while NB4 cells grown in light medium were used for the control IP (IP with the same LSD1 antibody with the addiction of an excess of soluble LSD1 peptide to block the antibody). In the "reverse" experiment, reactions were inverted (LSD1 IP in light cells, control IP in heavy cells).

By using three different biological replicates, we defined 147 LSD1 putative interactors (Figure 40). Among them, we enriched the CoREST complex, as expected (HDAC1, HDAC2, RCOR1 and RCOR3).

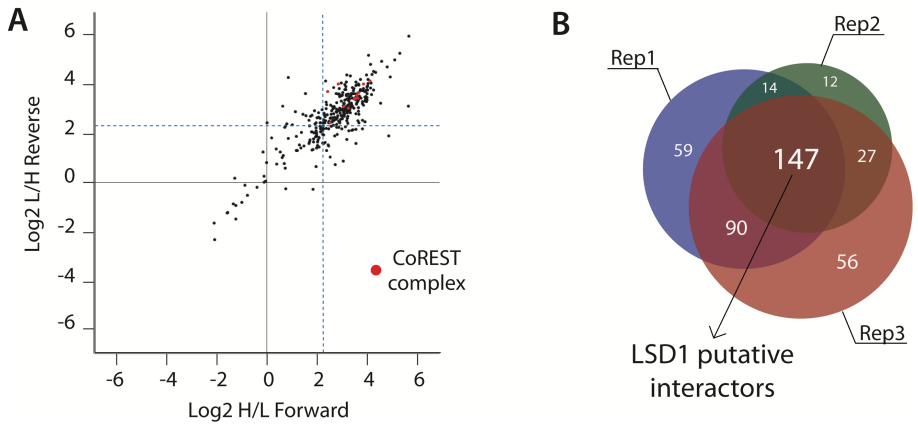

Figure 40. Identification of LSD1 interactors in NB4 cells.

A) Scatterplot showing log_2 (heavy/light) ratio of forward reaction on the *x* axis (Rep1) and the log_2 (light/heavy) ratio of reverse reaction on the *y* axis (Rep3). In the top right quadrant are represented LSD1 interactors. The blue dashed lines define the threshold used to define the LSD1 interactors from the background. Proteins belonging to the CoREST complex are shown in red dots. **B)** Venn diagrams with numbers of individual and overlapping putative LSD1 interactors identified in the three different SILAC replicates.

Western blot analysis of different LSD1 interactors validated the mass-spectrometry data (Figure 41).

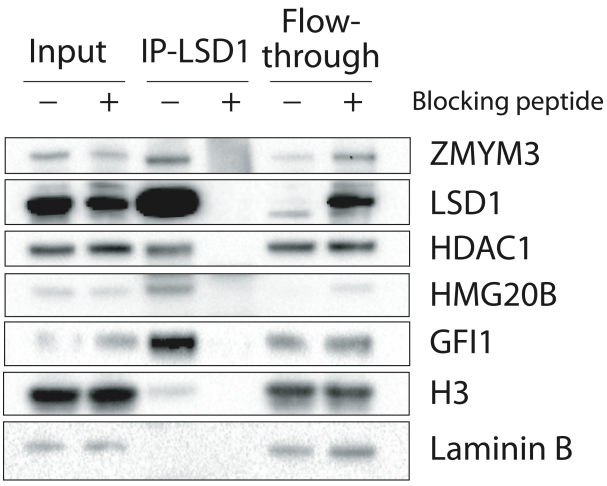

Figure 41. Western blot validation of LSD1 interactors in NB4 cells.

Western blot analysis of LSD1 and some identified interactors in LSD1 immunoprecipitations (IPs), with or without blocking peptide. Lamin B1 is used as loading control.

We then profiled the changes in the LSD1 interactome following treatment with MC_2580 (Figure 42). In this case, we performed LSD1 immunoprecipitation in cells grown in heavy medium and treated with LSD1 inhibitor for 24 hours and in cells grown in light medium and treated with DMSO as control (*vice versa* for "reverse" experiment). Recruited proteins after LSD1 inhibition would result in an increased ratio heavy/light, while evicted proteins in an increased light/heavy ratio.

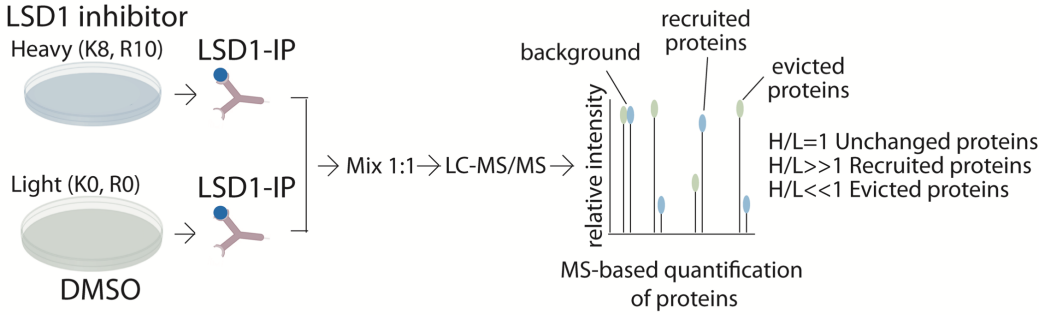

Figure 42. Schematic representation of SILAC mass spectrometry approach to profile changes in LSD1 interactome following treatment with LSD1 inhibitor.

Schematic representation of SILAC mass spectrometry approach to identify recruited and evicted interactors of LSD1, upon LSD1 pharmacological inhibition with MC_2580 2μM for 24 hours.

Most of the interactors remained stably associated with LSD1 upon drug treatment, but in a very few cases (including the interactor GFI1) the binding to LSD1 was strongly affected by the inhibitor (Figure 43).

GFI1 is a transcription factor fondamental in the hematopoietic system. In concert with GFI1b, GFI1 regulates the myeloid lineage differentition, from hematopoietic stem cells to fully differentiated granulocytes, megakayocytes and erythrocytes. Expression of GFI1 and GFI1b varies among the different stages of myeloid differentiation and the two proteins negatively regulate each other's expression. GFI1 and GFI1b have both a DNA-binding domain at the C-terminus and a SNAG domain at the N-terminus. The two proteins are

transcriptional repressors and excert their repressor activity recruting on DNA several chromatin remodellers. In particular, the N-terminal SNAG domain is fundamental for their interaction with LSD1.

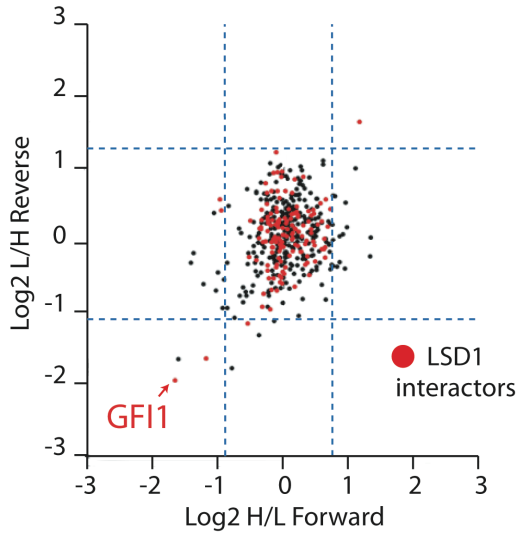

Figure 43. Pharmacological inhibition of LSD1 disrupts its interaction with GFI1.
Scatterplot showing log_2 (heavy/light) ratio of forward reaction on the *x* axis and the log_2 (light/heavy) ratio of reverse reaction on the *y* axis. Proteins recruited by LSD1 after inhibition are present in the top right quadrant , while proteins evicted from the interaction with LSD1 after drug treatment are found in the bottom left quadrant. Proteins previously identified as interactors of LSD1 in NB4 are shown as red dots. The blue dashed lines define the threshold employed to determine recruited and evicted proteins.

Due to the central role of GFI1 in hematopoietic differentiation, we focused our attention on the effects of LSD1i on LSD1-GFI1 interaction. Immunoprecipitation of endogenous GFI1 with anti-LSD1 in untreated and treated cells (using two different LSD1 inhibitors, MC_2580 and DDP_38003) confirmed the results (Figure 44a). Reciprocal IP using the anti-GFI1 in NB4 cells treated with the drugs MC_2580 and DDP_38003 further validated the previous results (Figure 44b).

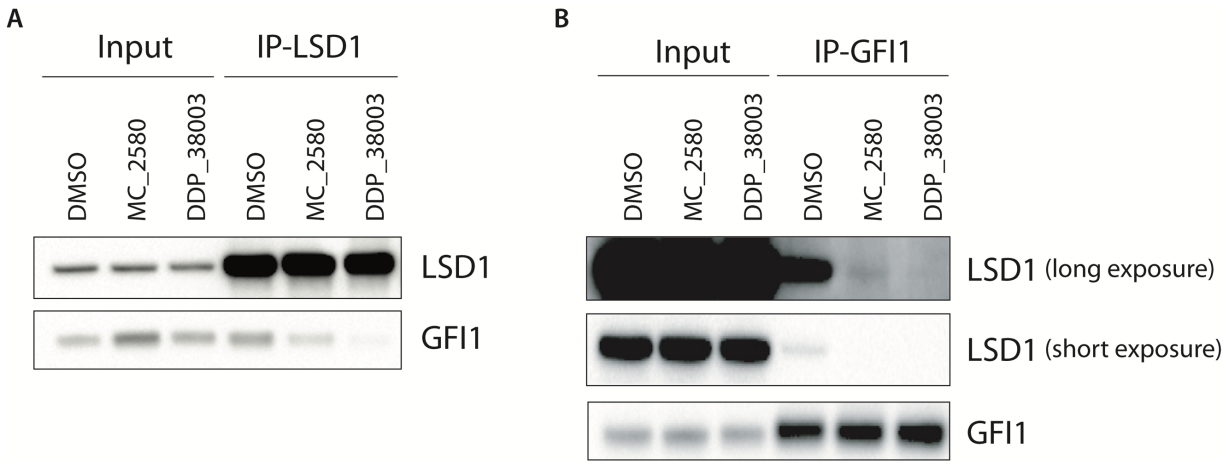

Figure 44. Western blot validation of altered interaction between LSD1 and GFI1 after treatment with LSD1 inhibitors.

A) Western blot analysis of LSD1 and GFI1 in LSD1 immunoprecipitations (IP) in NB4 treated for 24 hours with DMSO, MC_2580 2μM or DDP_38003 2μM. **B)** Western blot analysis of LSD1 and GFI1 in GFI1 immunoprecipitations (IP) in NB4 cells treated for 24 hours with DMSO, MC_2580 2μM or DDP_38003 2μM.

To verify whether the exogenous LSD1 reintroduced in NB4 knock-out cells interacts with GFI1 as the normal endogenous LSD1, we performed GFI1 immunoprecipitation in NB4 knock-out cells reconstituted with either wild type or K661A catalytic mutant LSD1. Importantly, the catalytic inactive LSD1 mutant (K661A-LSD1) bound to GFI1 in a comparable manner to wild-type LSD1, and the LSD1 inhibitor hindered the LSD1 mutant/GFI1 interaction as well (Figure 45). These data show that the LSD1 inhibitors which we used hamper the interaction between LSD1 and GFI1, and that this alteration is not dependent on the inhibition of the catalytic activity of LSD1, implying that LSD1 inhibitors target catalytic as well as non-catalytic functions of LSD1.

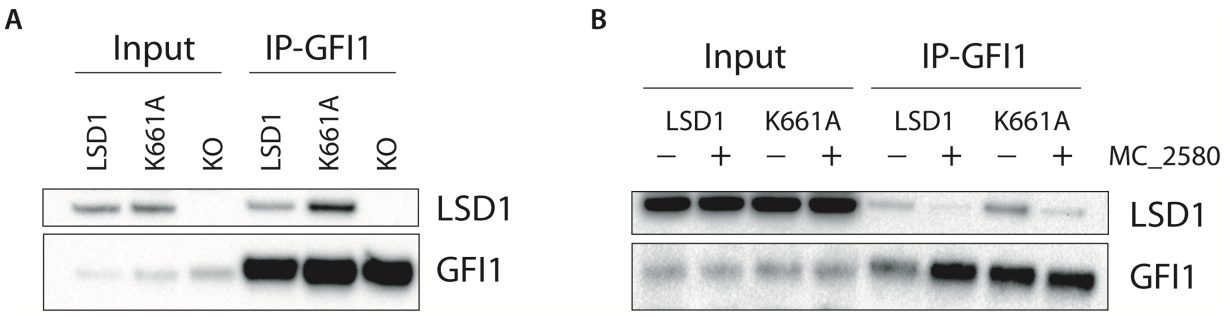

Figure 45. Exogenous LSD1 binds GFI1 and LSD1 inhibition hinders the interaction between GFI1 and both wild type and catalytic mutant LSD1.

A) Western blot analysis of LSD1 and GFI1 in anti-GFI1 immunoprecipitations (IP) in NB4 knockout cells transduced with Empty vector, wild-type or a catalytically inactive (K661A) LSD1 mutant. The arrow indicates a non-specific band. **B)** Western blot analysis of LSD1 and GFI1 in GFI1 immunoprecipitations (IPs) in NB4 KO cells transduced with Empty vector, wild-type or catalytic inactive (K661A) LSD1, treated with MC_2580 2μM or DMSO.

8. LSD1 interaction with GFI1 is fundamental for LSD1 activity in AML cells

Since GFI1 directly binds DNA and excerts its transcriptional repressive functions by recruiting chromatin remodellers, we analyzed the genome-wide distribution of binding sites for GFI1 and LSD1 by ChIP-Seq (Figure 46). We found that 70% of LSD1 peaks overlap with GFI1 peaks, while only 30% of total GFI1 peaks overlap with LSD1 bound regions, hinting to a role for GFI1 which is not totally dependent on its association with LSD1.

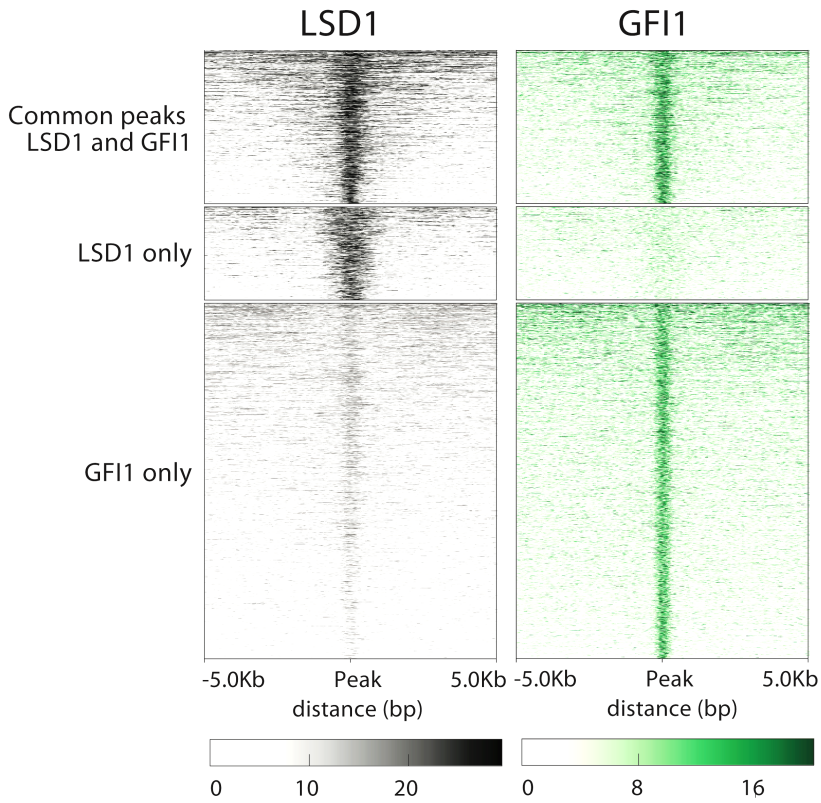

Figure 46. LSD1 bound genomic regions are highly enriched for GFI1 peaks.

Heatmaps showing ChIP-Seq signal of LSD1 and GFI1 ranked according to decrescent LSD1 signal.

Since LSD1 inhibitors hamper GFI1-LSD1 interaction, we interrogated whether LSD1 inhibition also affects LSD1 genomic distribution. Interestingly, we found that, upon 24 hours of treatment with MC_2580, LSD1 was evicted from 732 GFI1-bound regulatory regions of genes involved in hematopoietic differentiation (Figure 47).

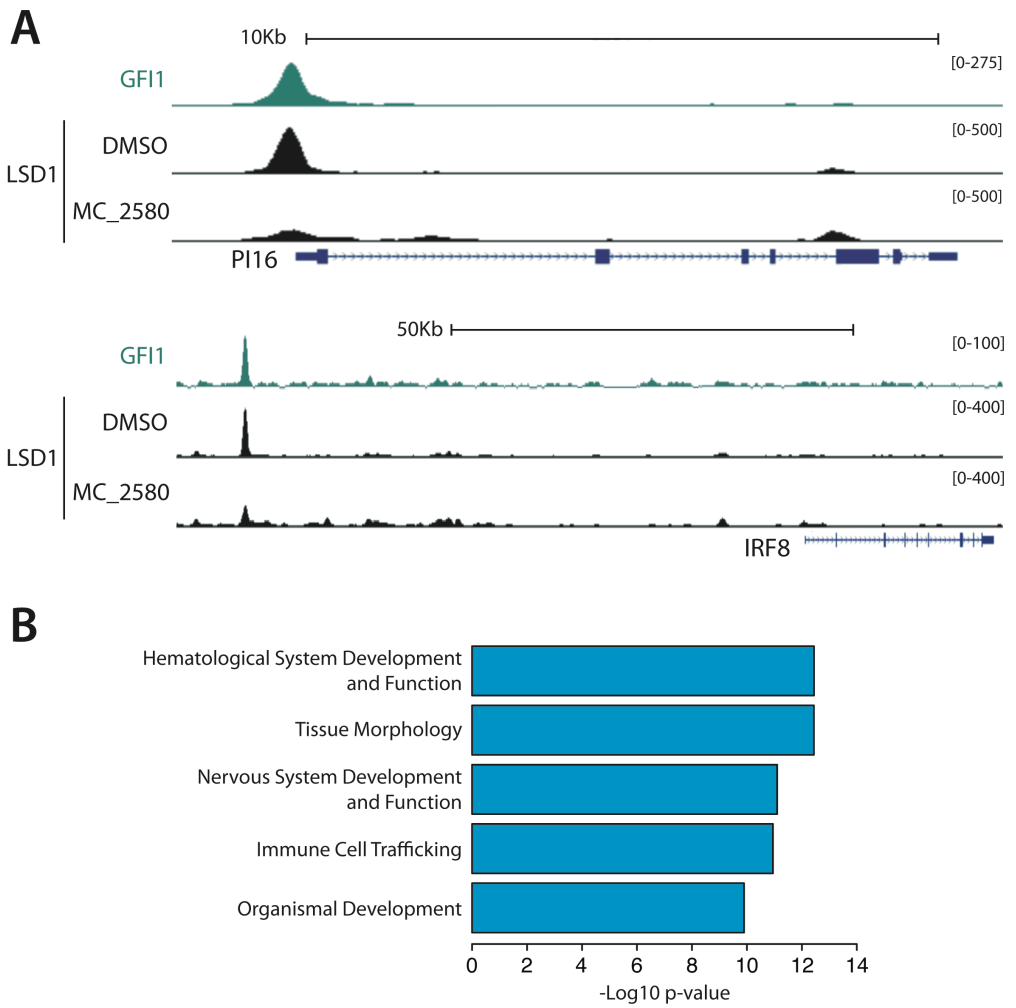

Figure 47. LSD1 inhibition causes LSD1 eviction from GFI1-bound regions.

A) Representative examples of overlapping LSD1 and GFI1 binding regions. UCSC Genome Browser profile of LSD1 and GFI1 ChIP-seq on the PI16 gene promoter and IRF8 putative enhancer. **B)** Ingenuity Pathway Analysis (IPA) of genes associated to the 732 GFI1-bound regions that lose LSD1 ChIP-seq signal after treatment with MC_2580.

Similarly to LSD1, also HDAC1 was displaced from some GFI1 target genes (figure 48), suggesting that non only LSD1, but also its partners are evicted from chromatin when the LSD1-GFI1 interaction is inhibited. This result is in line with what observed with SILAC mass-spectrometry, where LSD1 inhibitor affected the interaction of LSD1 with only few proteins while most of the interactors remain stably associated to LSD1, meaning that after treatment with LSD1 inhibitor all LSD1 complex is displaced from GFI1 target regions.

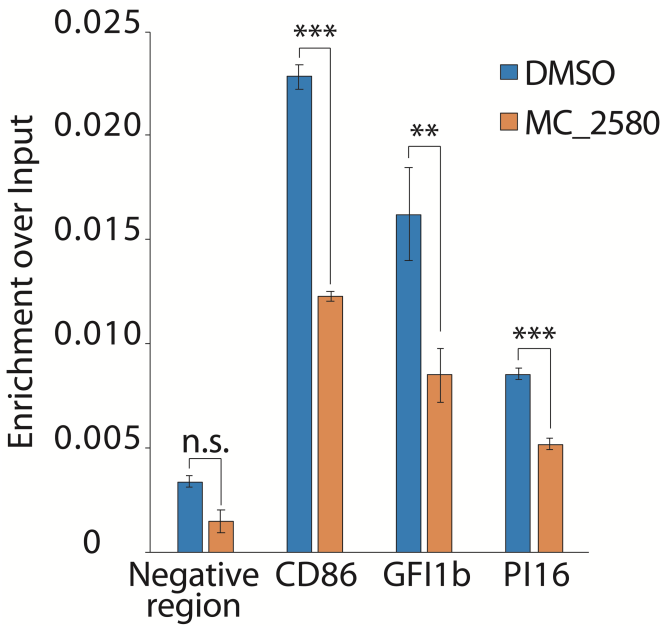

Figure 48. LSD1 inhibition displaces HDAC1 from GFI1-bound regions.

HDAC1 recruitment (ChIP-qPCR) before and after LSD1 inhibition at some GFI1 and LSD1 shared genomic regions.

To verify our hypothesis that the disruption of LSD1-GFI1 interaction is the causative event for the sensitization to RA by LSD1 inhibitors, we took advantage of an LSD1 mutant (D553,555,556A) that is not able to bind the SNAG domain of GFI1, required for their interaction. The three D553, D555 and D556 residues are part of the catalytic cavity as the K661 residue. However, in contrast to the K661 residue that is required for the proper FAD binding and stabilization of the anionic form of the reduced cofactor, the three residues are localized in a pocket of the catalytic cavity that mediates the substrate specificity and binding. It has been already shown that mutation of the three residues impedes the interaction between LSD1 and SNAIL**,** a master regulator of the epithelial to mesenchimal transition (EMT), which occours through the SNAG domain of SNAIL (Lin et al., 2010b). Since also the interaction between LSD1 and GFI1 occours through the SNAG domain of GFI1, we

verified for the first time whether these mutations could impair also GFI1-LSD1 interaction. Consistently, GFI1-LSD1 interaction was strongly hampered by the concomitant mutation of the D553, D555 and D556 residues of LSD1 (Figure 49).

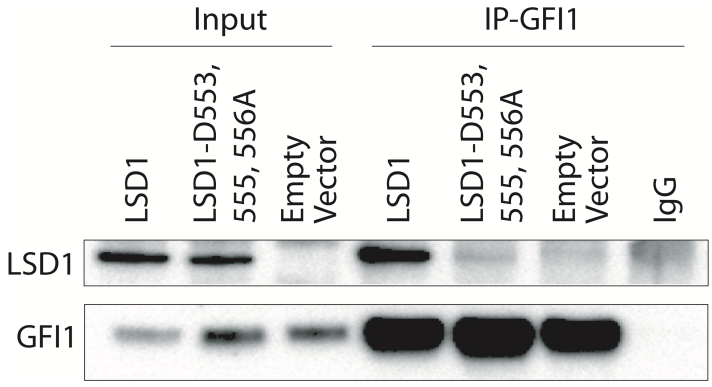

Figure 49. LSD1-D553,555,556A mutant does not bind GFI1.

Western blot analysis of LSD1 and GFI1 in GFI1 immunoprecipitation (IP) in NB4 knockout cells transduced with LSD1, LSD1-D553,555,556A mutant or Empty Vector.

Interestingly, forced expression of D553,555,556A-LSD1 did not rescue NB4 knock-out cells from their sensitivity to low doses of RA (Figure 50), failing to establish a differentiation block. Taken together, these data demonstrate that LSD1-GFI1 interaction is fundamental for the establishment of a differentiation block by LSD1 in APL cells, and that the sensitization to RA triggered by LSD1 inhibitors relies on the disruption of LSD1-GFI1 interaction.

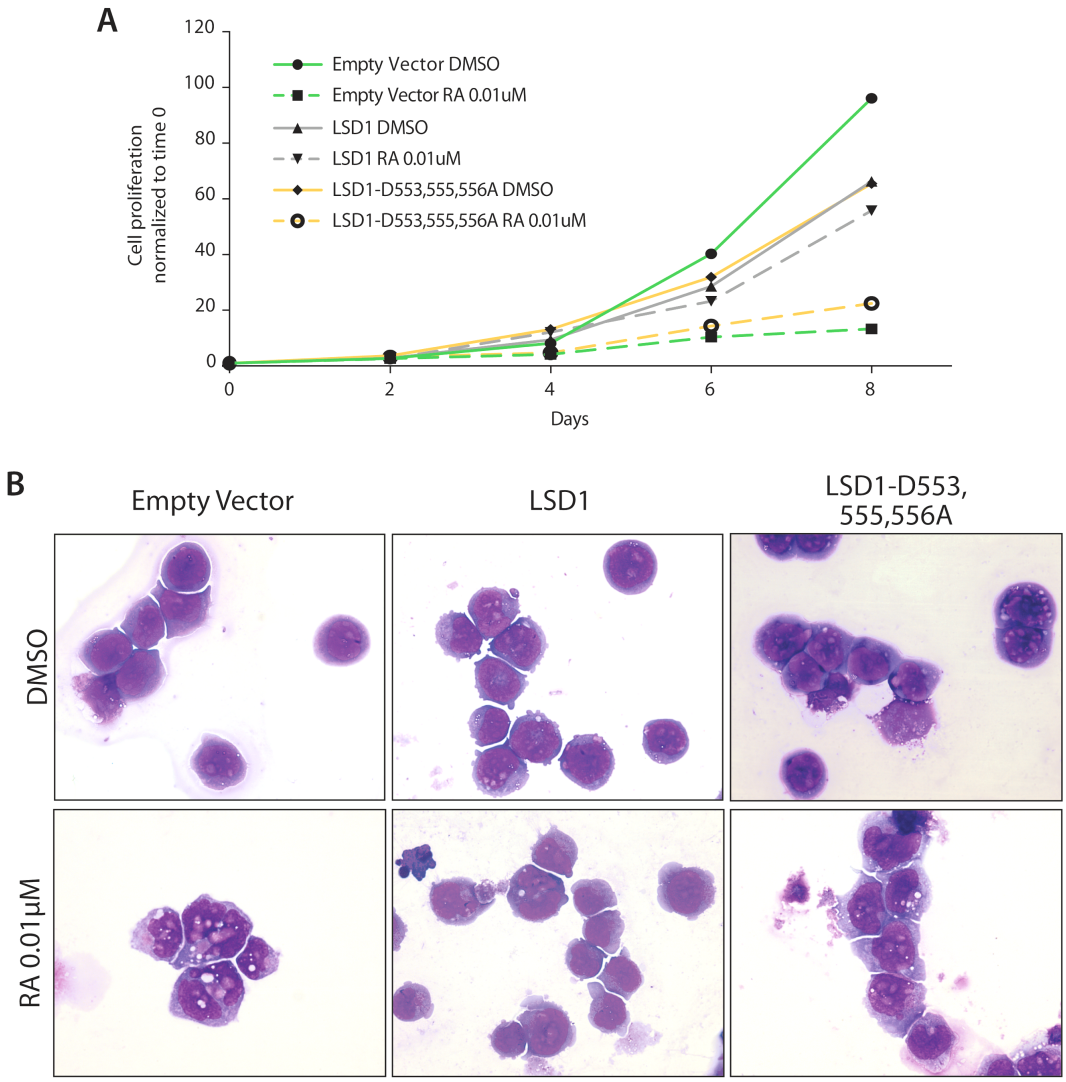

Figure 50. LSD1 interaction with GFI1 is fundamental for RA sensitization of APL cells.

A) Growth curve of NB4 knockout cells transduced with the Empty vector or the LSD1-D553,555,556A (defective for GFI1 binding) mutant treated with RA 0.01µM or DMSO as control. **B)** Morphologic analysis of knockout cells transduced with LSD1 or the LSD1-D553,555,556A mutant and treated with 0.01µM RA for 8 days.. May Grümwald-Giemsa staining.

In order to verify whether the LSD1-GFI1 interaction plays a central role in differentiation of non-APL AMLs and whether the disruption of LSD1-GFI1 axis sensitizes them to RA, we knocked-out LSD1 in MOLM-13 cells. We choose to knock-out LSD1 in MOLM-13 cells because this cell line resulted insensitive to LSD1 inhibition in our previous screening (Figure 16) but, as NB4 cells, it shown cooperation between RA and LSD1 inhibition.

Consistently with our previous results, LSD1 depletion sentitized also MOLM-13 cells to RA , which induced cell differentiation (Figure 51).

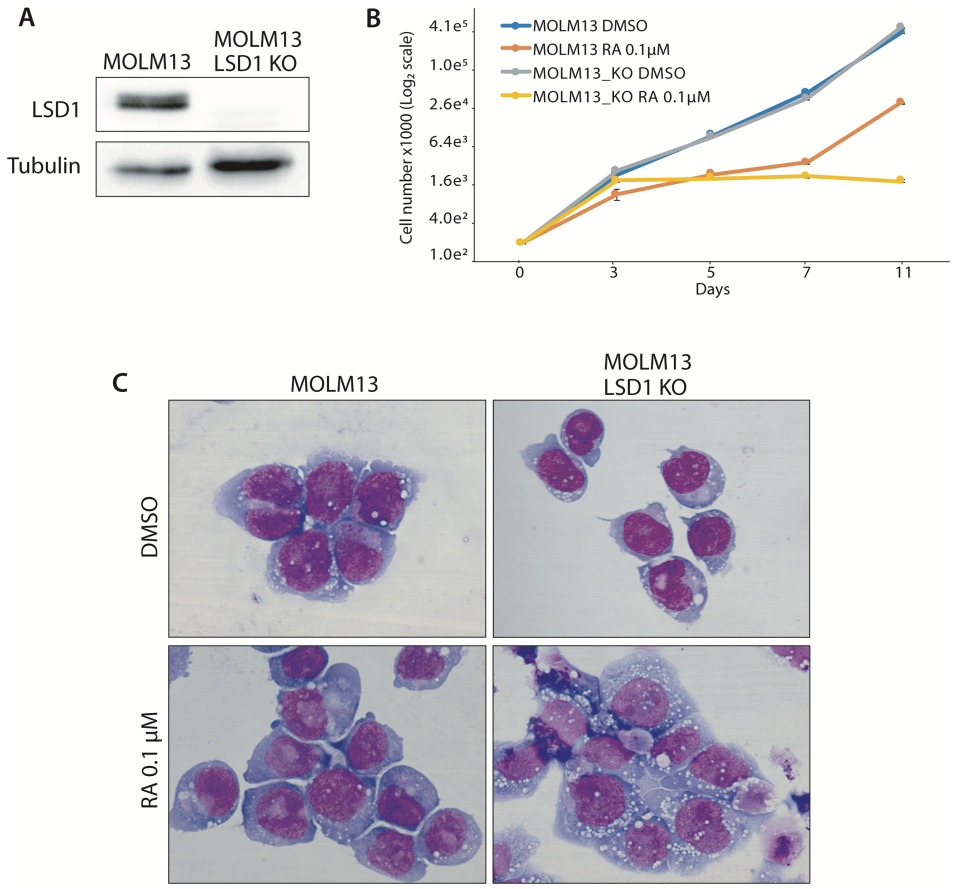

Figure 51. LSD1 depletion sensitizes non-APL AML cells to RA.

A) Western blot analysis of LSD1 in MOLM13 WT and knockout cells. Tubulin served as loading control. **B)** Growth curve of WT and LSD1 knockout MOLM13 cells treated with 0.1µM RA or DMSO as control. **C)** Morpholic analysis of MOLM13 WT and knockout cells treated with 0.1µM RA.

As observed in NB4 cells, reconstitution of MOLM13 knock-out cells with both LSD1 wild type and the catalytic mutant K661A rescued the phenotype, while cells reconsituted with LSD1-D553,555,556A mutant manained the sensitivity to RA (Figure 52).

These results clearly demonstrate that the LSD1-GFI1 axis plays a central role in maintaining a differentiation block also in non-APL AML cells and that the disruption of their interaction,

by either LSD1 inhibitors or LSD1 mutations, leaves leukemic cells in an epigenetic permissive status, prone to differentiation. However, inhibition of LSD1-GFI1 interaction is not sufficient to push leukemic cells toward differentiation, but the combination of LSD1 inhibition with a differentiation stimulus (retinoic acid) results in a dramatic induction of the myeloid differentiation program.

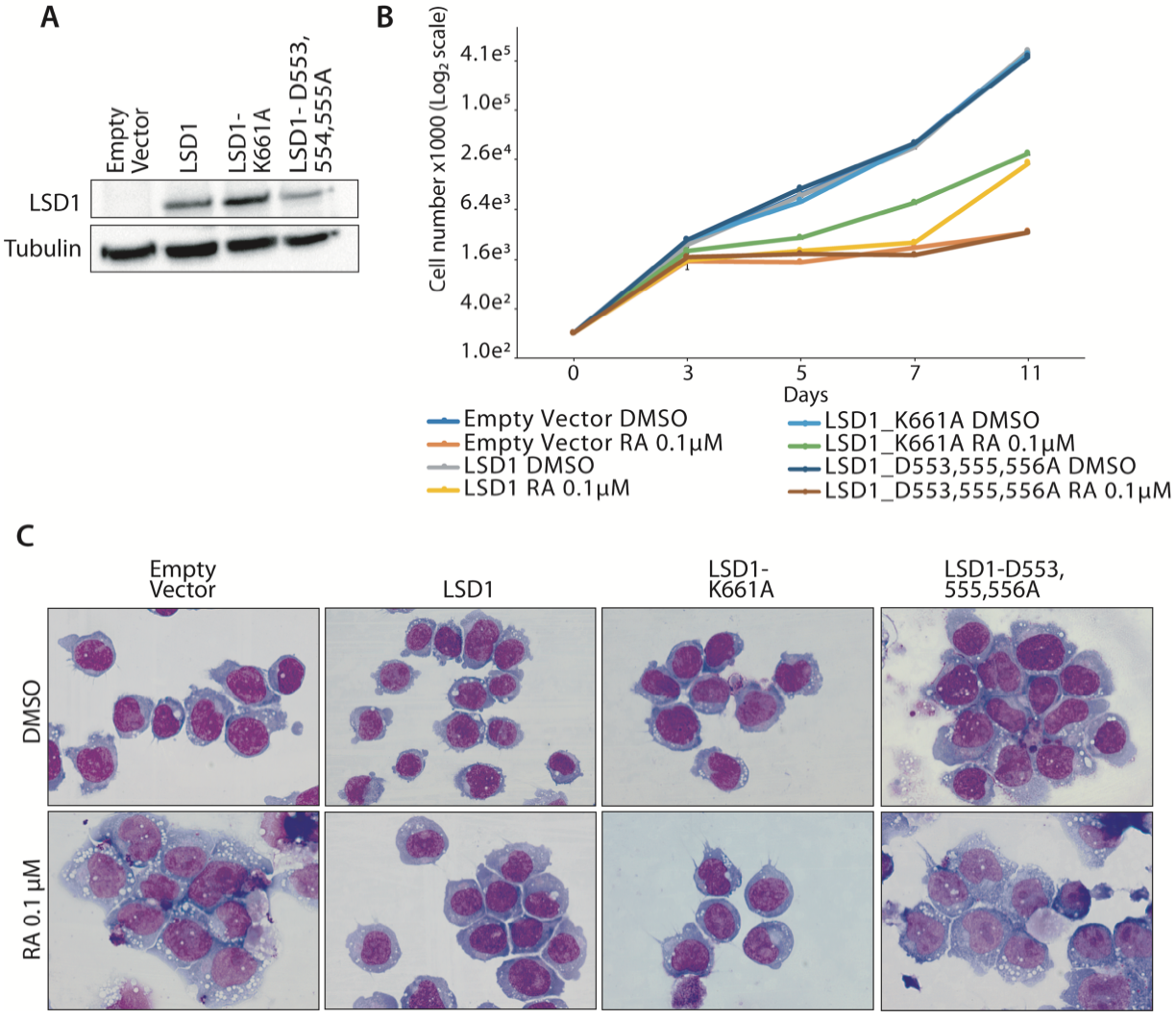

Figure 52. LSD1-GFI1 interaction mediates sensitization to RA of non-APL AML cells.

A) Western blot analysis of LSD1 in MOLM13 knockout cells transduced with indicated vectors. **B)** Growth curve of MOLM13 knockout cells transduced with either LSD1, LSD1-K661A and LSD1-D553,555,556A and treated with 0.1µM RA. **C)** Morpholic analysis of MOLM13 knockout cells transduced as indicated and treated for 11 days with 0.1µM RA. May Grümwald-Giemsa staining.

Discussion

LSD1 catalytic activity was first discovered in the 2004 (Shi et al., 2004) and completely revolutionized the interpretation of histone methylation. From its discovery, the scientific interest on LSD1 has rapidly grown and its involvement in various physiological and pathological processes became evident. Since abnormally high protein levels have been found in several tumors, LSD1 has emerged as an appealing target for cancer therapy. Subsequentely, different LSD1 inhibitors have entered clinical trials for treatment of several cancer types, including acute myeloid leukemia (AML). Nevertheless, AML represents an heterogeneous group of diseases and only a minority of AML cells are sensitive to LSD1 inhibition as single treatment (Mohammad et al., 2015); a strong cooperative action of LSD1i and retinoic acid can be however measured even in those AML subtypes not responsive to either drug alone (Schenk et al., 2012), justifying a clinical investigation of this approach (ClinicalTrials.gov: NCT02261779, NCT02273102, NCT02717884). By testing the combination of RA and LSD1i in several AML cell lines, we observed a cooperation of the two agents in the great majority of tested cells, meaning that the cooperation is a common feature among the different AML subtypes.

Our laboratory, in collaboration with prof. Antonello Mai and prof. Andrea Mattevi, developed the LSD1 inhibitor MC_2580, an analog of TCP that shows increased selectivity for LSD1 compared to TCP. Using this inhibitor, we already reported that LSD1 inihibition sensitizes APL cells to physiological doses of retinoic acid (Binda et al., 2010), but any understanding of the mechanism of action of LSD1i in combination with RA, either in APL or other AML subtypes, has not been reported so far: focusing on this phenomenon in cells resistant to LSD1i provides useful insights to optimize the use of LSD1i in a clinical setting.

Due to the deep knowledge of the system that our group has developed during the years, we took advantage of NB4 cells, an APL cell line, to study the molecular mechanisms of RA sensitization.

Here we show that NB4 cells are resistant to LSD1 inhbition alone, but combination of RA and LSD1i, or LSD1 genetic knock-out, leads to their complete differentiation. Consistently, LSD1 inhibition has almost no impact on global gene expression, but leads to chromatin reorganization and to a global increase in H3K4 methylation, inducing a chromatin landscape more permissive for the response to differentiation stimuli (RA). In this way, the combination of RA and LSD1i leads to the induction of a large set of genes involved in cellular differentiation and to profound changes in chromatin structure, including activation and decommissioning of super-enhancers.

All these changes occur in the continuous presence of PML-RARα. LSD1 inhibition, either in the presence or absence of low doses of RA, does not induce degradation of PML-RARα neither its eviction from chromatin. LSD1 does not directly bind DNA, so it is catched on target genomic loci by different transcription factors that recognize specific binding sites. One hypothesysis is that PML-RARα recruits LSD1 on its targets, but expression of PML-RARα in the PR9 cells (Grignani et al., 1996), an U937-derived cell line that express the fusion protein under a zinc-inducible promoter, shows that PML-RARα does not alter LSD1 genomic distribution (Ravasio et al., 2019). Moreover, LSD1 and PML-RARα share some of their genomic targets, but more than 85% of LSD1 bound regions in NB4 cells do not show any PML-RARα signal, suggesting a role for LSD1 that is independent from the fusion protein. Overall, these results demostrate that the combination of LSD1 inhibition and low doses of RA can induce differentiation of APL cells without affecting PML-RARα functions, making us hypothesize that this mechanistic model applies also to other AML subtypes.

The correlation between transcriptional de-repression and LSD1 catalytic activity is an open debate. LSD1 demethylase activity seems to be essential to maintain the undifferentiated state of human embrionic stem cells (Adamo et al., 2011) and to override oncogene induced senescence (Yu et al., 2018). In contrast, the catalytic activity of LSD1 is not required to block differentiation of AML cells sensitive to LSD1 inhibition (Maiques-Diaz et al., 2018).

Here we analyze for the first time the role of LSD1 catalytic activity in AML cells resistant to LSD1 inhibition. We show that reconstitution of LSD1 knock-out cells with either the wild-type or a catalytically inactive form of the enzyme recovers the differentiation block of leukemic cells in the presence of physiological doses of RA, though the inactive LSD1 (unlike the wild-type form) fails to modify chromatin at its targets. We conclude therefore that LSD1 catalytic activity is dispensable for sensitization to LSD1 inhibition to retinoic acid.

Since the catalytic activity are dispensable, we hypothesized that LSD1 inhibitors could alter somehow also non-enzymatic activity of LSD1. Therefore, we used a proteomic approach to analyze the LSD1 interactome in the absence and in the presence of LSD1 inhibition.

Interestingly, we show that while most interactors remain associated with LSD1 upon treatment with MC_2580, the inhibitor leads to the selective dissociation of GFI1 from LSD1. Based on these results, we hypothesize that the LSD1 complex is therefore not affected by LSD1 inhibition and that the inhibitor acts on the LSD1-GFI1 direct interaction. In particular, LSD1 interacts with GFI1 through the SNAG domain present at the N-terminus of GFI1, that works as a molecular hook to recruit LSD1 (Lin et al., 2010b). Consistently, upon inhibition LSD1 is evicted from chromatin at GFI1 target genes. Reconstitution of LSD1 knock-out cells with a mutant form of LSD1 that is unable to associate with GFI1 does not result in recovery of the differentiation block in the presence of physiological doses of RA. The interaction of GFI1 with LSD1 is therefore critical for the differentiation block maintained by LSD1 in the

absence of RA. Similarly, the association of LSD1 with GFI1 has been reported to be critical for maintaining the differentiation block also of AML cells (Maiques-Diaz et al., 2018), (Barth et al., 2019) and Medulloblastoma cells (Lee et al., 2019) sensitive to LSD1i.

We therefore speculate a primary scaffold role for LSD1. LSD1 interacts with several proteins, some of which are important chromatin modifiers (*e.g.* HDAC1 and 2, HMG20B, SMARCC2). By interacting with GFI1, that has a DNA-binding domain, LSD1 recruits all - or some of – these proteins to GFI1 target genes, modulating their accessibility and transcriptional status. According to our model, the interaction among GFI1 and LSD1 is essential for the ability of the transcription factor to recruit chromatin associated factors and contrast differentiation stimuli. We do not observe a broad effect after LSD1 inhibition, and our observations indeed suggest that LSD1 inhibitors are targeting the activity of a transcriptional regulator (GFI1) fundamental for the maintenance of the oncogenic phenotype. In the absence of a differentiation stimulus, however, our model does not predict a spontaneous push towards differentiation of LSD1i-resistant AML cells. Consistent with this model, LSD1 inhibition alone does not lead to transcriptional changes if not for a handful of genes. Combining LSD1 inhibition with a differentiation stimulus (retinoic acid), however, we observed a dramatic induction of a differentiation-associated transcriptional program responsible for the observed phenotypic changes.

The small-molecule LSD1 inhibitors employed in this study (MC_2580 and DDP_38003) are still able to dissociate GFI1 from a catalytically inactive LSD1. This feature can be explained from the three-dimensional structure of the enzyme-inhibitor and enzyme-GFI1 complexes: the inhibitor- and substrate-binding sites fully overlap. The inhibitor can therefore be expected to create steric hindrance that prevents GFI1 binding (Baron et al., 2011).

All the mechanistic studies were performed in NB4 cells, an APL cell line. However, APL is a particular system due to its intrinsic sensitivity to high doses of retinoic acid. In order to verify whether these observation are valid also in non-APL AML cells, we knocked out LSD1 in MOLM13 cells, an AML cell line harboring the MLL-AF9 fusion. Reconstitution experiments with either LSD1 or the different mutants confirmed the role of LSD1 and of its interaction with GFI1 in strongly enhancing the response of non-APL AML cells to retinoic acid.

Taken together, our results point to a model where in AML cells resistant to LSD1 inhibition, LSD1 acts primarily as a scaffolding module to recruit the Co-REST complex to transcription factors such as GFI1, which functions as a brake to differentiation stimuli (such as RA). The inhibitors of LSD1 that we used are able to trigger dissociation of the complex from GFI1, and favor differentiation by RA. Since most tumor cells tolerate LSD1 inhibition (Mohammad et al., 2015), these results have both mechanistical and translational relevance, and further support the use of LSD1 inhibitors in combination therapy.

Bibliography

Adamo, A., Sesé, B., Boue, S., Castaño, J., Paramonov, I., Barrero, M.J., and Izpisua Belmonte, J.C. (2011). LSD1 regulates the balance between self-renewal and differentiation in human embryonic stem cells. Nat Cell Biol *13*, 652-659.

Alcalay, M., Zangrilli, D., Pandolfi, P.P., Longo, L., Mencarelli, A., Giacomucci, A., Rocchi, M., Biondi, A., Rambaldi, A., and Lo Coco, F. (1991). Translocation breakpoint of acute promyelocytic leukemia lies within the retinoic acid receptor alpha locus. Proc Natl Acad Sci U S A *88*, 1977-1981.

ALLFREY, V.G., FAULKNER, R., and MIRSKY, A.E. (1964). ACETYLATION AND METHYLATION OF HISTONES AND THEIR POSSIBLE ROLE IN THE REGULATION OF RNA SYNTHESIS. Proc Natl Acad Sci U S A *51*, 786-794.

Allis CD, Caparros M, Jenuwein T, and D, R. (2015). Epigenetics. Second edition. (Cold Spring Harbor Laboratory Press).

Allis, C.D., and Jenuwein, T. (2016). The molecular hallmarks of epigenetic control. Nat Rev Genet *17*, 487-500.

Amente, S., Lania, L., and Majello, B. (2013). The histone LSD1 demethylase in stemness and cancer transcription programs. Biochim Biophys Acta *1829*, 981-986.

Annunziato, A. (2008). DNA Packaging: Nucleosomes and Chromatin. (Nature Education).

Arber, D.A., Orazi, A., Hasserjian, R., Thiele, J., Borowitz, M.J., Le Beau, M.M., Bloomfield, C.D., Cazzola, M., and Vardiman, J.W. (2016). The 2016 revision to the World Health Organization classification of myeloid neoplasms and acute leukemia. Blood *127*, 2391-2405.

Atsumi, A., Tomita, A., Kiyoi, H., and Naoe, T. (2006). Histone deacetylase 3 (HDAC3) is recruited to target promoters by PML-RARalpha as a component of the N-CoR co-repressor complex to repress transcription in vivo. Biochem Biophys Res Commun *345*, 1471-1480.

Auclair, G., and Weber, M. (2012). Mechanisms of DNA methylation and demethylation in mammals. Biochimie *94*, 2202-2211.

Ballas, N., Grunseich, C., Lu, D.D., Speh, J.C., and Mandel, G. (2005). REST and its corepressors mediate plasticity of neuronal gene chromatin throughout neurogenesis. Cell *121*, 645-657.

Bannister, A.J., Zegerman, P., Partridge, J.F., Miska, E.A., Thomas, J.O., Allshire, R.C., and Kouzarides, T. (2001). Selective recognition of methylated lysine 9 on histone H3 by the HP1 chromo domain. Nature *410*, 120-124.

Baron, R., Binda, C., Tortorici, M., McCammon, J.A., and Mattevi, A. (2011). Molecular mimicry and ligand recognition in binding and catalysis by the histone demethylase LSD1-CoREST complex. Structure *19*, 212-220.

Barozzi, I., Termanini, A., Minucci, S., and Natoli, G. (2011). Fish the ChIPs: a pipeline for automated genomic annotation of ChIP-Seq data. Biol Direct *6*, 51.

Barth, J., Abou-El-Ardat, K., Dalic, D., Kurrle, N., Maier, A.M., Mohr, S., Schütte, J., Vassen, L., Greve, G., Schulz-Fincke, J.*, et al.* (2019). LSD1 inhibition by tranylcypromine derivatives interferes with GFI1-mediated repression of PU.1 target genes and induces differentiation in AML. Leukemia.

Bedford, M.T., and Clarke, S.G. (2009). Protein arginine methylation in mammals: who, what, and why. Mol Cell *33*, 1-13.

Bennett, J.M., Catovsky, D., Daniel, M.T., Flandrin, G., Galton, D.A., Gralnick, H.R., and Sultan, C. (1976). Proposals for the classification of the acute leukaemias. French-American-British (FAB) co-operative group. Br J Haematol *33*, 451-458.

Berg, T., Cohen, S.B., Desharnais, J., Sonderegger, C., Maslyar, D.J., Goldberg, J., Boger, D.L., and Vogt, P.K. (2002). Small-molecule antagonists of Myc/Max dimerization inhibit Myc-induced transformation of chicken embryo fibroblasts. Proc Natl Acad Sci U S A *99*, 3830-3835.

Bernstein, B.E., Mikkelsen, T.S., Xie, X., Kamal, M., Huebert, D.J., Cuff, J., Fry, B., Meissner, A., Wernig, M., Plath, K.*, et al.* (2006). A bivalent chromatin structure marks key developmental genes in embryonic stem cells. Cell *125*, 315-326.

Binda, C., Valente, S., Romanenghi, M., Pilotto, S., Cirilli, R., Karytinos, A., Ciossani, G., Botrugno, O.A., Forneris, F., Tardugno, M.*, et al.* (2010). Biochemical, structural, and biological evaluation of tranylcypromine derivatives as inhibitors of histone demethylases LSD1 and LSD2. J Am Chem Soc *132*, 6827-6833.

Blanc, R.S., and Richard, S. (2017). Arginine Methylation: The Coming of Age. Mol Cell *65*, 8-24.

Breitman, T.R., Collins, S.J., and Keene, B.R. (1981). Terminal differentiation of human promyelocytic leukemic cells in primary culture in response to retinoic acid. Blood *57*, 1000-1004.

Buschbeck, M., and Hake, S.B. (2017). Variants of core histones and their roles in cell fate decisions, development and cancer. Nat Rev Mol Cell Biol *18*, 299-314.

Carrozza, M.J., Li, B., Florens, L., Suganuma, T., Swanson, S.K., Lee, K.K., Shia, W.J., Anderson, S., Yates, J., Washburn, M.P.*, et al.* (2005). Histone H3 methylation by Set2 directs deacetylation of coding regions by Rpd3S to suppress spurious intragenic transcription. Cell *123*, 581-592.

Castaigne, S., Chomienne, C., Daniel, M.T., Ballerini, P., Berger, R., Fenaux, P., and Degos, L. (1990). All-trans retinoic acid as a differentiation therapy for acute promyelocytic leukemia. I. Clinical results. Blood *76*, 1704-1709.

Cesaroni, M., Cittaro, D., Brozzi, A., Pelicci, P.G., and Luzi, L. (2008). CARPET: a web-based package for the analysis of ChIP-chip and expression tiling data. Bioinformatics *24*, 2918-2920.

Chang, B., Chen, Y., Zhao, Y., and Bruick, R.K. (2007). JMJD6 is a histone arginine demethylase. Science *318*, 444-447.

Chen, Y., Yang, Y., Wang, F., Wan, K., Yamane, K., Zhang, Y., and Lei, M. (2006). Crystal structure of human histone lysine-specific demethylase 1 (LSD1). Proc Natl Acad Sci U S A *103*, 13956-13961.

Cho, H.S., Suzuki, T., Dohmae, N., Hayami, S., Unoki, M., Yoshimatsu, M., Toyokawa, G., Takawa, M., Chen, T., Kurash, J.K.*, et al.* (2011). Demethylation of RB regulator MYPT1 by histone demethylase LSD1 promotes cell cycle progression in cancer cells. Cancer Res *71*, 655-660.

Choi, J., Jang, H., Kim, H., Kim, S.T., Cho, E.J., and Youn, H.D. (2010). Histone demethylase LSD1 is required to induce skeletal muscle differentiation by regulating myogenic factors. Biochem Biophys Res Commun *401*, 327-332.

Clapier, C.R., Iwasa, J., Cairns, B.R., and Peterson, C.L. (2017). Mechanisms of action and regulation of ATP-dependent chromatin-remodelling complexes. Nat Rev Mol Cell Biol *18*, 407-422.

Cloos, P.A., Christensen, J., Agger, K., and Helin, K. (2008). Erasing the methyl mark: histone demethylases at the center of cellular differentiation and disease. Genes Dev *22*, 1115-1140.

Consortium, I.H.G.S. (2004). Finishing the euchromatic sequence of the human genome. Nature *431*, 931-945.

Copeland, R.A., Solomon, M.E., and Richon, V.M. (2009). Protein methyltransferases as a target class for drug discovery. Nat Rev Drug Discov *8*, 724-732.

Cosgrove, M.S., Boeke, J.D., and Wolberger, C. (2004). Regulated nucleosome mobility and the histone code. Nat Struct Mol Biol *11*, 1037-1043.

Cuthbert, G.L., Daujat, S., Snowden, A.W., Erdjument-Bromage, H., Hagiwara, T., Yamada, M., Schneider, R., Gregory, P.D., Tempst, P., Bannister, A.J.*, et al.* (2004). Histone deimination antagonizes arginine methylation. Cell *118*, 545-553.

David, G., Neptune, M.A., and DePinho, R.A. (2002). SUMO-1 modification of histone deacetylase 1 (HDAC1) modulates its biological activities. J Biol Chem *277*, 23658-23663.

Dawson, M.A. (2017). The cancer epigenome: Concepts, challenges, and therapeutic opportunities. Science *355*, 1147-1152.

Dawson, M.A., Prinjha, R.K., Dittmann, A., Giotopoulos, G., Bantscheff, M., Chan, W.I., Robson, S.C., Chung, C.W., Hopf, C., Savitski, M.M.*, et al.* (2011). Inhibition of BET recruitment to chromatin as an effective treatment for MLL-fusion leukaemia. Nature *478*, 529-533.

de Thé, H., and Chen, Z. (2010). Acute promyelocytic leukaemia: novel insights into the mechanisms of cure. Nat Rev Cancer *10*, 775-783.

de Thé, H., Lavau, C., Marchio, A., Chomienne, C., Degos, L., and Dejean, A. (1991). The PML-RAR alpha fusion mRNA generated by the t(15;17) translocation in acute promyelocytic leukemia encodes a functionally altered RAR. Cell *66*, 675-684.

Deschler, B., and Lübbert, M. (2006). Acute myeloid leukemia: epidemiology and etiology. Cancer *107*, 2099-2107.

Di Cerbo, V., Mohn, F., Ryan, D.P., Montellier, E., Kacem, S., Tropberger, P., Kallis, E., Holzner, M., Hoerner, L., Feldmann, A.*, et al.* (2014). Acetylation of histone H3 at lysine 64 regulates nucleosome dynamics and facilitates transcription. Elife *3*, e01632.

Di Lorenzo, A., and Bedford, M.T. (2011). Histone arginine methylation. FEBS Lett *585*, 2024-2031.

Ding, W., Li, Y.P., Nobile, L.M., Grills, G., Carrera, I., Paietta, E., Tallman, M.S., Wiernik, P.H., and Gallagher, R.E. (1998). Leukemic cellular retinoic acid resistance and missense mutations in the PML-RARalpha fusion gene after relapse of acute promyelocytic leukemia from treatment with all-trans retinoic acid and intensive chemotherapy. Blood *92*, 1172-1183.

Dos Santos, G.A., Kats, L., and Pandolfi, P.P. (2013). Synergy against PML-RARa: targeting transcription, proteolysis, differentiation, and self-renewal in acute promyelocytic leukemia. J Exp Med *210*, 2793-2802.

Döhner, H., Estey, E., Grimwade, D., Amadori, S., Appelbaum, F.R., Büchner, T., Dombret, H., Ebert, B.L., Fenaux, P., Larson, R.A.*, et al.* (2017). Diagnosis and management of AML in adults: 2017 ELN recommendations from an international expert panel. Blood *129*, 424-447.

Edmondson, D.E., Binda, C., and Mattevi, A. (2007). Structural insights into the mechanism of amine oxidation by monoamine oxidases A and B. Arch Biochem Biophys *464*, 269-276.

Falkenberg, K.J., and Johnstone, R.W. (2014). Histone deacetylases and their inhibitors in cancer, neurological diseases and immune disorders. Nat Rev Drug Discov *13*, 673-691.

Feinberg, A.P., and Vogelstein, B. (1983). Hypomethylation distinguishes genes of some human cancers from their normal counterparts. Nature *301*, 89-92.

Felsenfeld, G. (2014). A brief history of epigenetics. Cold Spring Harb Perspect Biol *6*.

Fenaux, P., Wang, Z.Z., and Degos, L. (2007). Treatment of acute promyelocytic leukemia by retinoids. Curr Top Microbiol Immunol *313*, 101-128.

Ferrari-Amorotti, G., Fragliasso, V., Esteki, R., Prudente, Z., Soliera, A.R., Cattelani, S., Manzotti, G., Grisendi, G., Dominici, M., Pieraccioli, M.*, et al.* (2013). Inhibiting interactions of lysine demethylase LSD1 with snail/slug blocks cancer cell invasion. Cancer Res *73*, 235-245.

Filippakopoulos, P., Qi, J., Picaud, S., Shen, Y., Smith, W.B., Fedorov, O., Morse, E.M., Keates, T., Hickman, T.T., Felletar, I.*, et al.* (2010). Selective inhibition of BET bromodomains. Nature *468*, 1067-1073.

Flavahan, W.A., Gaskell, E., and Bernstein, B.E. (2017). Epigenetic plasticity and the hallmarks of cancer. Science *357*.

Flenghi, L., Fagioli, M., Tomassoni, L., Pileri, S., Gambacorta, M., Pacini, R., Grignani, F., Casini, T., Ferrucci, P.F., and Martelli, M.F. (1995). Characterization of a new monoclonal antibody (PG-M3) directed against the aminoterminal portion of the PML gene product: immunocytochemical evidence for high expression of PML proteins on activated macrophages, endothelial cells, and epithelia. Blood *85*, 1871-1880.

Forneris, F., Binda, C., Adamo, A., Battaglioli, E., and Mattevi, A. (2007). Structural basis of LSD1-CoREST selectivity in histone H3 recognition. J Biol Chem *282*, 20070-20074.

Forneris, F., Binda, C., Vanoni, M.A., Mattevi, A., and Battaglioli, E. (2005). Histone demethylation catalysed by LSD1 is a flavin-dependent oxidative process. FEBS Lett *579*, 2203-2207.

Fung, S.M., Ramsay, G., and Katzen, A.L. (2003). MYB and CBP: physiological relevance of a biochemical interaction. Mech Dev *120*, 711-720.

Garcia-Bassets, I., Kwon, Y.S., Telese, F., Prefontaine, G.G., Hutt, K.R., Cheng, C.S., Ju, B.G., Ohgi, K.A., Wang, J., Escoubet-Lozach, L.*, et al.* (2007). Histone methylation-dependent mechanisms impose ligand dependency for gene activation by nuclear receptors. Cell *128*, 505-518.

Goldberg, A.D., Allis, C.D., and Bernstein, E. (2007). Epigenetics: a landscape takes shape. Cell *128*, 635-638.

Greenblatt, S.M., and Nimer, S.D. (2014). Chromatin modifiers and the promise of epigenetic therapy in acute leukemia. Leukemia *28*, 1396-1406.

Greer, E.L., and Shi, Y. (2012). Histone methylation: a dynamic mark in health, disease and inheritance. Nat Rev Genet *13*, 343-357.

Grignani, F., Testa, U., Rogaia, D., Ferrucci, P.F., Samoggia, P., Pinto, A., Aldinucci, D., Gelmetti, V., Fagioli, M., Alcalay, M.*, et al.* (1996). Effects on differentiation by the promyelocytic leukemia PML/RARalpha protein depend on the fusion of the PML protein dimerization and RARalpha DNA binding domains. EMBO J *15*, 4949-4958.

Guccione, E., Bassi, C., Casadio, F., Martinato, F., Cesaroni, M., Schuchlautz, H., Lüscher, B., and Amati, B. (2007). Methylation of histone H3R2 by PRMT6 and H3K4 by an MLL complex are mutually exclusive. Nature *449*, 933-937.

Guo, Y., Fu, X., Huo, B., Wang, Y., Sun, J., Meng, L., Hao, T., Zhao, Z.J., and Hu, X. (2016). GATA2 regulates GATA1 expression through LSD1-mediated histone modification. Am J Transl Res *8*, 2265-2274.

Hakimi, M.A., Bochar, D.A., Chenoweth, J., Lane, W.S., Mandel, G., and Shiekhattar, R. (2002). A core-BRAF35 complex containing histone deacetylase mediates repression of neuronal-specific genes. Proc Natl Acad Sci U S A *99*, 7420-7425.

Hakimi, M.A., Dong, Y., Lane, W.S., Speicher, D.W., and Shiekhattar, R. (2003). A candidate X-linked mental retardation gene is a component of a new family of histone deacetylase-containing complexes. J Biol Chem *278*, 7234-7239.

Harris, W.J., Huang, X., Lynch, J.T., Spencer, G.J., Hitchin, J.R., Li, Y., Ciceri, F., Blaser, J.G., Greystoke, B.F., Jordan, A.M.*, et al.* (2012). The histone demethylase KDM1A sustains the oncogenic potential of MLL-AF9 leukemia stem cells. Cancer Cell *21*, 473-487.

Harvey, S.R., Porrini, M., Stachl, C., MacMillan, D., Zinzalla, G., and Barran, P.E. (2012). Small-molecule inhibition of c-MYC:MAX leucine zipper formation is revealed by ion mobility mass spectrometry. J Am Chem Soc *134*, 19384-19392.

Hausinger, R.P. (2004). FeII/alpha-ketoglutarate-dependent hydroxylases and related enzymes. Crit Rev Biochem Mol Biol *39*, 21-68.

Heintzman, N.D., Stuart, R.K., Hon, G., Fu, Y., Ching, C.W., Hawkins, R.D., Barrera, L.O., Van Calcar, S., Qu, C., Ching, K.A.*, et al.* (2007). Distinct and predictive chromatin signatures of transcriptional promoters and enhancers in the human genome. Nat Genet *39*, 311-318.

HILLESTAD, L.K. (1957). Acute promyelocytic leukemia. Acta Med Scand *159*, 189-194.

Hnisz, D., Abraham, B.J., Lee, T.I., Lau, A., Saint-André, V., Sigova, A.A., Hoke, H.A., and Young, R.A. (2013). Super-enhancers in the control of cell identity and disease. Cell *155*, 934-947.

Holliday, R., and Pugh, J.E. (1975). DNA modification mechanisms and gene activity during development. Science *187*, 226-232.

Hosseini, A., and Minucci, S. (2017). A comprehensive review of lysine-specific demethylase 1 and its roles in cancer. Epigenomics *9*, 1123-1142.

HOTCHKISS, R.D. (1948). The quantitative separation of purines, pyrimidines, and nucleosides by paper chromatography. J Biol Chem *175*, 315-332.

Hou, H., and Yu, H. (2010). Structural insights into histone lysine demethylation. Curr Opin Struct Biol *20*, 739-748.

Hu, X., Li, X., Valverde, K., Fu, X., Noguchi, C., Qiu, Y., and Huang, S. (2009). LSD1-mediated epigenetic modification is required for TAL1 function and hematopoiesis. Proc Natl Acad Sci U S A *106*, 10141-10146.

Huang, J., Sengupta, R., Espejo, A.B., Lee, M.G., Dorsey, J.A., Richter, M., Opravil, S., Shiekhattar, R., Bedford, M.T., Jenuwein, T.*, et al.* (2007). p53 is regulated by the lysine demethylase LSD1. Nature *449*, 105-108.

Huang, M.E., Ye, Y.C., Chen, S.R., Chai, J.R., Lu, J.X., Zhoa, L., Gu, L.J., and Wang, Z.Y. (1988). Use of all-trans retinoic acid in the treatment of acute promyelocytic leukemia. Blood *72*, 567-572.

Huang, Z., Li, S., Song, W., Li, X., Li, Q., Zhang, Z., Han, Y., Zhang, X., Miao, S., Du, R.*, et al.* (2013). Lysine-specific demethylase 1 (LSD1/KDM1A) contributes to colorectal tumorigenesis via activation of the Wnt/β-catenin pathway by down-regulating Dickkopf-1 (DKK1) [corrected]. PLoS One *8*, e70077.

Hyun, K., Jeon, J., Park, K., and Kim, J. (2017). Writing, erasing and reading histone lysine methylations. Exp Mol Med *49*, e324.

Illingworth, R.S., and Bird, A.P. (2009). CpG islands--'a rough guide'. FEBS Lett *583*, 1713-1720.

Ishikawa, Y., Gamo, K., Yabuki, M., Takagi, S., Toyoshima, K., Nakayama, K., Nakayama, A., Morimoto, M., Miyashita, H., Dairiki, R.*, et al.* (2017). A Novel LSD1 Inhibitor T-3775440 Disrupts GFI1B-Containing Complex Leading to Transdifferentiation and Impaired Growth of AML Cells. Mol Cancer Ther *16*, 273-284.

Itoh, Y., Aihara, K., Mellini, P., Tojo, T., Ota, Y., Tsumoto, H., Solomon, V.R., Zhan, P., Suzuki, M., Ogasawara, D.*, et al.* (2016). Identification of SNAIL1 Peptide-Based Irreversible Lysine-Specific Demethylase 1-Selective Inactivators. J Med Chem *59*, 1531-1544.

Jablonka, E., and Lamb, M.J. (2002). The changing concept of epigenetics. Ann N Y Acad Sci *981*, 82-96.

Jacobs, S.A., Taverna, S.D., Zhang, Y., Briggs, S.D., Li, J., Eissenberg, J.C., Allis, C.D., and Khorasanizadeh, S. (2001). Specificity of the HP1 chromo domain for the methylated N-terminus of histone H3. EMBO J *20*, 5232-5241.

Jin, L., Hanigan, C.L., Wu, Y., Wang, W., Park, B.H., Woster, P.M., and Casero, R.A. (2013). Loss of LSD1 (lysine-specific demethylase 1) suppresses growth and alters gene expression of human colon cancer cells in a p53- and DNMT1(DNA methyltransferase 1)-independent manner. Biochem J *449*, 459-468.

Jing, Y., Wang, L., Xia, L., Chen, G.Q., Chen, Z., Miller, W.H., and Waxman, S. (2001). Combined effect of all-trans retinoic acid and arsenic trioxide in acute promyelocytic leukemia cells in vitro and in vivo. Blood *97*, 264-269.

Kamashev, D., Vitoux, D., and De Thé, H. (2004). PML-RARA-RXR oligomers mediate retinoid and rexinoid/cAMP cross-talk in acute promyelocytic leukemia cell differentiation. J Exp Med *199*, 1163-1174.

Kerenyi, M.A., Shao, Z., Hsu, Y.J., Guo, G., Luc, S., O'Brien, K., Fujiwara, Y., Peng, C., Nguyen, M., and Orkin, S.H. (2013). Histone demethylase Lsd1 represses hematopoietic stem and progenitor cell signatures during blood cell maturation. Elife *2*, e00633.

Kim, J., Singh, A.K., Takata, Y., Lin, K., Shen, J., Lu, Y., Kerenyi, M.A., Orkin, S.H., and Chen, T. (2015). LSD1 is essential for oocyte meiotic progression by regulating CDC25B expression in mice. Nat Commun *6*, 10116.

Klose, R.J., and Bird, A.P. (2006). Genomic DNA methylation: the mark and its mediators. Trends Biochem Sci *31*, 89-97.

Klose, R.J., and Zhang, Y. (2007). Regulation of histone methylation by demethylimination and demethylation. Nat Rev Mol Cell Biol *8*, 307-318.

Kontaki, H., and Talianidis, I. (2010). Lysine methylation regulates E2F1-induced cell death. Mol Cell *39*, 152-160.

Kornberg, R.D. (1974). Chromatin structure: a repeating unit of histones and DNA. Science *184*, 868-871.

Kornberg, R.D., and Lorch, Y. (1999). Twenty-five years of the nucleosome, fundamental particle of the eukaryote chromosome. Cell *98*, 285-294.

Kouzarides, T. (2007). Chromatin modifications and their function. Cell *128*, 693-705.

Kulis, M., and Esteller, M. (2010). DNA methylation and cancer. Adv Genet *70*, 27-56.

Kumarasinghe, I.R., and Woster, P.M. (2014). Synthesis and evaluation of novel cyclic Peptide inhibitors of lysine-specific demethylase 1. ACS Med Chem Lett *5*, 29-33.

Lachner, M., O'Carroll, D., Rea, S., Mechtler, K., and Jenuwein, T. (2001). Methylation of histone H3 lysine 9 creates a binding site for HP1 proteins. Nature *410*, 116-120.

Lachner, M., O'Sullivan, R.J., and Jenuwein, T. (2003). An epigenetic road map for histone lysine methylation. J Cell Sci *116*, 2117-2124.

Lallemand-Breitenbach, V., Guillemin, M.C., Janin, A., Daniel, M.T., Degos, L., Kogan, S.C., Bishop, J.M., and de Thé, H. (1999). Retinoic acid and arsenic synergize to eradicate leukemic cells in a mouse model of acute promyelocytic leukemia. J Exp Med *189*, 1043-1052.

Lamouille, S., Xu, J., and Derynck, R. (2014). Molecular mechanisms of epithelial-mesenchymal transition. Nat Rev Mol Cell Biol *15*, 178-196.

Lan, W., Zhang, D., and Jiang, J. (2013). The roles of LSD1-mediated epigenetic modifications in maintaining the pluripotency of bladder cancer stem cells. Med Hypotheses *81*, 823-825.

Langmead, B., Trapnell, C., Pop, M., and Salzberg, S.L. (2009). Ultrafast and memory-efficient alignment of short DNA sequences to the human genome. Genome Biol *10*, R25.

Lanotte, M., Martin-Thouvenin, V., Najman, S., Balerini, P., Valensi, F., and Berger, R. (1991). NB4, a maturation inducible cell line with t(15;17) marker isolated from a human acute promyelocytic leukemia (M3). Blood *77*, 1080-1086.

Laurent, B., Ruitu, L., Murn, J., Hempel, K., Ferrao, R., Xiang, Y., Liu, S., Garcia, B.A., Wu, H., Wu, F*., et al*. (2015). A specific LSD1/KDM1A isoform regulates neuronal differentiation through H3K9 demethylation. Mol Cell *57*, 957-970.

Lee, C., Rudneva, V.A., Erkek, S., Zapatka, M., Chau, L.Q., Tacheva-Grigorova, S.K., Garancher, A., Rusert, J.M., Aksoy, O., Lea, R., *et al.* (2019). Lsd1 as a therapeutic target in Gfi1-activated medulloblastoma. Nat Commun *10*, 332.

Lee, M.G., Wynder, C., Cooch, N., and Shiekhattar, R. (2005). An essential role for CoREST in nucleosomal histone 3 lysine 4 demethylation. Nature *437*, 432-435.

Li, Y., Deng, C., Hu, X., Patel, B., Fu, X., Qiu, Y., Brand, M., Zhao, K., and Huang, S. (2012). Dynamic interaction between TAL1 oncoprotein and LSD1 regulates TAL1 function in hematopoiesis and leukemogenesis. Oncogene *31*, 5007-5018.

Li, Y., and Seto, E. (2016). HDACs and HDAC Inhibitors in Cancer Development and Therapy. Cold Spring Harb Perspect Med *6*.

Li, Y., Trojer, P., Xu, C.F., Cheung, P., Kuo, A., Drury, W.J., Qiao, Q., Neubert, T.A., Xu, R.M., Gozani, O., *et al.* (2009). The target of the NSD family of histone lysine methyltransferases depends on the nature of the substrate. J Biol Chem *284*, 34283-34295.

Liang, G., Lin, J.C., Wei, V., Yoo, C., Cheng, J.C., Nguyen, C.T., Weisenberger, D.J., Egger, G., Takai, D., Gonzales, F.A., *et al.* (2004). Distinct localization of histone H3 acetylation and H3-K4 methylation to the transcription start sites in the human genome. Proc Natl Acad Sci U S A *101*, 7357-7362.

Lim, S., Janzer, A., Becker, A., Zimmer, A., Schüle, R., Buettner, R., and Kirfel, J. (2010). Lysine-specific demethylase 1 (LSD1) is highly expressed in ER-negative breast cancers and a biomarker predicting aggressive biology. Carcinogenesis *31*, 512-520.

Lin, R.J., Nagy, L., Inoue, S., Shao, W., Miller, W.H., and Evans, R.M. (1998). Role of the histone deacetylase complex in acute promyelocytic leukaemia. Nature *391*, 811-814.

Lin, T., Ponn, A., Hu, X., Law, B.K., and Lu, J. (2010a). Requirement of the histone demethylase LSD1 in Snai1-mediated transcriptional repression during epithelial-mesenchymal transition. Oncogene *29*, 4896-4904.

Lin, Y., Wu, Y., Li, J., Dong, C., Ye, X., Chi, Y.I., Evers, B.M., and Zhou, B.P. (2010b). The SNAG domain of Snail1 functions as a molecular hook for recruiting lysine-specific demethylase 1. EMBO J *29*, 1803-1816.

Liu, L., Souto, J., Liao, W., Jiang, Y., Li, Y., Nishinakamura, R., Huang, S., Rosengart, T., Yang, V.W., Schuster, M., *et al.* (2013). Histone lysine-specific demethylase 1 (LSD1) protein is involved in Sal-like protein 4 (SALL4)-mediated transcriptional repression in hematopoietic stem cells. J Biol Chem *288*, 34719-34728.

Liyanage, V.R., Jarmasz, J.S., Murugeshan, N., Del Bigio, M.R., Rastegar, M., and Davie, J.R. (2014). DNA modifications: function and applications in normal and disease States. Biology (Basel) *3*, 670-723.

Lo-Coco, F., and Ammatuna, E. (2006). The biology of acute promyelocytic leukemia and its impact on diagnosis and treatment. Hematology Am Soc Hematol Educ Program, 156-161, 514.

Luger, K., Mäder, A.W., Richmond, R.K., Sargent, D.F., and Richmond, T.J. (1997). Crystal structure of the nucleosome core particle at 2.8 A resolution. Nature *389*, 251-260.

Maes, T., Mascaró, C., Tirapu, I., Estiarte, A., Ciceri, F., Lunardi, S., Guibourt, N., Perdones, A., Lufino, M.M.P., Somervaille, T.C.P.*, et al.* (2018). ORY-1001, a Potent and Selective Covalent KDM1A Inhibitor, for the Treatment of Acute Leukemia. Cancer Cell *33*, 495-511.e412.

Maile, T.M., Izrael-Tomasevic, A., Cheung, T., Guler, G.D., Tindell, C., Masselot, A., Liang, J., Zhao, F., Trojer, P., Classon, M.*, et al.* (2015). Mass spectrometric quantification of histone post-translational modifications by a hybrid chemical labeling method. Mol Cell Proteomics *14*, 1148-1158.

Maiques-Diaz, A., Spencer, G.J., Lynch, J.T., Ciceri, F., Williams, E.L., Amaral, F.M.R., Wiseman, D.H., Harris, W.J., Li, Y., Sahoo, S.*, et al.* (2018). Enhancer Activation by Pharmacologic Displacement of LSD1 from GFI1 Induces Differentiation in Acute Myeloid Leukemia. Cell Rep *22*, 3641-3659.

Margueron, R., Li, G., Sarma, K., Blais, A., Zavadil, J., Woodcock, C.L., Dynlacht, B.D., and Reinberg, D. (2008). Ezh1 and Ezh2 maintain repressive chromatin through different mechanisms. Mol Cell *32*, 503-518.

Margueron, R., and Reinberg, D. (2010). Chromatin structure and the inheritance of epigenetic information. Nat Rev Genet *11*, 285-296.

Martens, J.H., Brinkman, A.B., Simmer, F., Francoijs, K.J., Nebbioso, A., Ferrara, F., Altucci, L., and Stunnenberg, H.G. (2010). PML-RARalpha/RXR Alters the Epigenetic Landscape in Acute Promyelocytic Leukemia. Cancer Cell *17*, 173-185.

Martens, J.H., and Stunnenberg, H.G. (2010). The molecular signature of oncofusion proteins in acute myeloid leukemia. FEBS Lett *584*, 2662-2669.

Martinez-Zamudio, R., and Ha, H.C. (2012). Histone ADP-ribosylation facilitates gene transcription by directly remodeling nucleosomes. Mol Cell Biol *32*, 2490-2502.

Matsuo, Y., MacLeod, R.A., Uphoff, C.C., Drexler, H.G., Nishizaki, C., Katayama, Y., Kimura, G., Fujii, N., Omoto, E., Harada, M.*, et al.* (1997). Two acute monocytic leukemia (AML-M5a) cell lines (MOLM-13 and MOLM-14) with interclonal phenotypic heterogeneity showing MLL-AF9 fusion resulting from an occult chromosome insertion, ins(11;9)(q23;p22p23). Leukemia *11*, 1469-1477.

McGrath, J.P., Williamson, K.E., Balasubramanian, S., Odate, S., Arora, S., Hatton, C., Edwards, T.M., O'Brien, T., Magnuson, S., Stokoe, D.*, et al.* (2016). Pharmacological Inhibition of the Histone Lysine Demethylase KDM1A Suppresses the Growth of Multiple Acute Myeloid Leukemia Subtypes. Cancer Res *76*, 1975-1988.

Melnick, A., and Licht, J.D. (1999). Deconstructing a disease: RARalpha, its fusion partners, and their roles in the pathogenesis of acute promyelocytic leukemia. Blood *93*, 3167-3215.

Messner, S., and Hottiger, M.O. (2011). Histone ADP-ribosylation in DNA repair, replication and transcription. Trends Cell Biol *21*, 534-542.

Metzger, E., Wissmann, M., Yin, N., Müller, J.M., Schneider, R., Peters, A.H., Günther, T., Buettner, R., and Schüle, R. (2005). LSD1 demethylates repressive histone marks to promote androgen-receptor-dependent transcription. Nature *437*, 436-439.

Meyer, C., Burmeister, T., Gröger, D., Tsaur, G., Fechina, L., Renneville, A., Sutton, R., Venn, N.C., Emerenciano, M., Pombo-de-Oliveira, M.S.*, et al.* (2018). The MLL recombinome of acute leukemias in 2017. Leukemia *32*, 273-284.

Minucci, S., Maccarana, M., Cioce, M., De Luca, P., Gelmetti, V., Segalla, S., Di Croce, L., Giavara, S., Matteucci, C., Gobbi, A.*, et al.* (2000). Oligomerization of RAR and AML1 transcription factors as a novel mechanism of oncogenic activation. Mol Cell *5*, 811-820.

Minucci, S., Monestiroli, S., Giavara, S., Ronzoni, S., Marchesi, F., Insinga, A., Diverio, D., Gasparini, P., Capillo, M., Colombo, E.*, et al.* (2002). PML-RAR induces promyelocytic leukemias with high efficiency following retroviral gene transfer into purified murine hematopoietic progenitors. Blood *100*, 2989-2995.

Minucci, S., and Pelicci, P.G. (2006). Histone deacetylase inhibitors and the promise of epigenetic (and more) treatments for cancer. Nat Rev Cancer *6*, 38-51.

Mohammad, H.P., Smitheman, K.N., Kamat, C.D., Soong, D., Federowicz, K.E., Van Aller, G.S., Schneck, J.L., Carson, J.D., Liu, Y., Butticello, M.*, et al.* (2015). A DNA Hypomethylation Signature Predicts Antitumor Activity of LSD1 Inhibitors in SCLC. Cancer Cell *28*, 57-69.

Mosammaparast, N., and Shi, Y. (2010). Reversal of histone methylation: biochemical and molecular mechanisms of histone demethylases. Annu Rev Biochem *79*, 155-179.

Murr, R. (2010). Interplay between different epigenetic modifications and mechanisms. Adv Genet *70*, 101-141.

Musri, M.M., Carmona, M.C., Hanzu, F.A., Kaliman, P., Gomis, R., and Párrizas, M. (2010). Histone demethylase LSD1 regulates adipogenesis. J Biol Chem *285*, 30034-30041.

Müller, I., Larsson, K., Frenzel, A., Oliynyk, G., Zirath, H., Prochownik, E.V., Westwood, N.J., and Henriksson, M.A. (2014). Targeting of the MYCN protein with small molecule c-MYC inhibitors. PLoS One *9*, e97285.

Narlikar, G.J., Fan, H.Y., and Kingston, R.E. (2002). Cooperation between complexes that regulate chromatin structure and transcription. Cell *108*, 475-487.

Nasr, R., and de Thé, H. (2010). Eradication of acute promyelocytic leukemia-initiating cells by PML/RARA-targeting. Int J Hematol *91*, 742-747.

Nasr, R., Guillemin, M.C., Ferhi, O., Soilihi, H., Peres, L., Berthier, C., Rousselot, P., Robledo-Sarmiento, M., Lallemand-Breitenbach, V., Gourmel, B.*, et al.* (2008). Eradication of acute promyelocytic leukemia-initiating cells through PML-RARA degradation. Nat Med *14*, 1333-1342.

Nathan, D., Ingvarsdottir, K., Sterner, D.E., Bylebyl, G.R., Dokmanovic, M., Dorsey, J.A., Whelan, K.A., Krsmanovic, M., Lane, W.S., Meluh, P.B*., et al.* (2006). Histone sumoylation is a negative regulator in Saccharomyces cerevisiae and shows dynamic interplay with positive-acting histone modifications. Genes Dev *20*, 966-976.

Ndlovu, M.N., Denis, H., and Fuks, F. (2011). Exposing the DNA methylome iceberg. Trends Biochem Sci *36*, 381-387.

Nervi, C., Ferrara, F.F., Fanelli, M., Rippo, M.R., Tomassini, B., Ferrucci, P.F., Ruthardt, M., Gelmetti, V., Gambacorti-Passerini, C., Diverio, D*., et al.* (1998). Caspases mediate retinoic acid-induced degradation of the acute promyelocytic leukemia PML/RARalpha fusion protein. Blood *92*, 2244-2251.

Nguyen, A.T., and Zhang, Y. (2011). The diverse functions of Dot1 and H3K79 methylation. Genes Dev *25*, 1345-1358.

Oelgeschläger, M., Janknecht, R., Krieg, J., Schreek, S., and Lüscher, B. (1996). Interaction of the co-activator CBP with Myb proteins: effects on Myb-specific transactivation and on the cooperativity with NF-M. EMBO J *15*, 2771-2780.

Olins, A.L., and Olins, D.E. (1974). Spheroid chromatin units (v bodies). Science *183*, 330-332.

Ong, S.E., Blagoev, B., Kratchmarova, I., Kristensen, D.B., Steen, H., Pandey, A., and Mann, M. (2002). Stable isotope labeling by amino acids in cell culture, SILAC, as a simple and accurate approach to expression proteomics. Mol Cell Proteomics *1*, 376-386.

Oudet, P., Gross-Bellard, M., and Chambon, P. (1975). Electron microscopic and biochemical evidence that chromatin structure is a repeating unit. Cell *4*, 281-300.

Pandolfi, P.P., Alcalay, M., Fagioli, M., Zangrilli, D., Mencarelli, A., Diverio, D., Biondi, A., Lo Coco, F., Rambaldi, A., and Grignani, F. (1992). Genomic variability and alternative splicing generate multiple PML/RAR alpha transcripts that encode aberrant PML proteins and PML/RAR alpha isoforms in acute promyelocytic leukaemia. EMBO J *11*, 1397-1407.

Pedersen, M.T., and Helin, K. (2010). Histone demethylases in development and disease. Trends Cell Biol *20*, 662-671.

Pellegrino, S., Ronda, L., Annoni, C., Contini, A., Erba, E., Gelmi, M.L., Piano, R., Paredi, G., Mozzarelli, A., and Bettati, S. (2014). Molecular insights into dimerization inhibition of c-Maf transcription factor. Biochim Biophys Acta *1844*, 2108-2115.

Quinlan, A.R., and Hall, I.M. (2010). BEDTools: a flexible suite of utilities for comparing genomic features. Bioinformatics *26*, 841-842.

Racanicchi, S., Maccherani, C., Liberatore, C., Billi, M., Gelmetti, V., Panigada, M., Rizzo, G., Nervi, C., and Grignani, F. (2005). Targeting fusion protein/corepressor contact restores differentiation response in leukemia cells. EMBO J *24*, 1232-1242.

Ramírez, F., Ryan, D.P., Grüning, B., Bhardwaj, V., Kilpert, F., Richter, A.S., Heyne, S., Dündar, F., and Manke, T. (2016). deepTools2: a next generation web server for deep-sequencing data analysis. Nucleic Acids Res *44*, W160-165.

Rappsilber, J., Mann, M., and Ishihama, Y. (2007). Protocol for micro-purification, enrichment, pre-fractionation and storage of peptides for proteomics using StageTips. Nat Protoc *2*, 1896-1906.

Ravasio, R., Ceccacci, E., Nicosia, L., Hosseini, A., Rossi, P.L., Barozzi, I., Fornasari, L., Dal Zuffo, R., Valente, S., Fioravanti, R.*, et al.* (2019). Targeting the scaffolding role of LSD1 (KDM1A) poises acute myeloid leukemia cells for Retinoic Acid induced differentiation. (Under Revision).

Rea, S., Eisenhaber, F., O'Carroll, D., Strahl, B.D., Sun, Z.W., Schmid, M., Opravil, S., Mechtler, K., Ponting, C.P., Allis, C.D.*, et al.* (2000). Regulation of chromatin structure by site-specific histone H3 methyltransferases. Nature *406*, 593-599.

Rego, E.M., He, L.Z., Warrell, R.P., Wang, Z.G., and Pandolfi, P.P. (2000). Retinoic acid (RA) and As2O3 treatment in transgenic models of acute promyelocytic leukemia (APL) unravel the distinct nature of the leukemogenic process induced by the PML-RARalpha and PLZF-RARalpha oncoproteins. Proc Natl Acad Sci U S A *97*, 10173-10178.

Riggs AD, Martienssen RA, and VEA, R. (1996). Introduction . In Epigenetic mechanisms of gene regulation (ed. Russo VEA, et al.). (Cold Spring Harbor, NY, Cold Spring Harbor Laboratory Press), pp. 1–4.

Riggs AD, and TN, P. (1996). Overview of epigenetic mechanisms . In Epigenetic mechanisms of gene regulation (ed. Russo VEA, Martienssen R, Riggs AD). (Cold Spring Harbor, NY, Cold Spring Harbor Laboratory Press), pp. 29–45.

Rossetto, D., Avvakumov, N., and Côté, J. (2012). Histone phosphorylation: a chromatin modification involved in diverse nuclear events. Epigenetics *7*, 1098-1108.

Roth, S.Y., Denu, J.M., and Allis, C.D. (2001). Histone acetyltransferases. Annu Rev Biochem *70*, 81-120.

Rotili, D., and Mai, A. (2011). Targeting Histone Demethylases: A New Avenue for the Fight against Cancer. Genes Cancer *2*, 663-679.

Ruthenburg, A.J., Allis, C.D., and Wysocka, J. (2007). Methylation of lysine 4 on histone H3: intricacy of writing and reading a single epigenetic mark. Mol Cell *25*, 15-30.

Saleque, S., Kim, J., Rooke, H.M., and Orkin, S.H. (2007). Epigenetic regulation of hematopoietic differentiation by Gfi-1 and Gfi-1b is mediated by the cofactors CoREST and LSD1. Mol Cell *27*, 562-572.

Sampurno, S., Bijenhof, A., Cheasley, D., Xu, H., Robine, S., Hilton, D., Alexander, W.S., Pereira, L., Mantamadiotis, T., Malaterre, J.*, et al.* (2013). The Myb-p300-CREB axis modulates intestine homeostasis, radiosensitivity and tumorigenesis. Cell Death Dis *4*, e605.

Sanz, M.A., Fenaux, P., Tallman, M.S., Estey, E.H., Löwenberg, B., Naoe, T., Lengfelder, E., Döhner, H., Burnett, A.K., Chen, S.J., *et al.* (2019). Management of acute promyelocytic leukemia: updated recommendations from an expert panel of the European LeukemiaNet. Blood *133*, 1630-1643.

Schenk, T., Chen, W.C., Göllner, S., Howell, L., Jin, L., Hebestreit, K., Klein, H.U., Popescu, A.C., Burnett, A., Mills, K., *et al.* (2012). Inhibition of the LSD1 (KDM1A) demethylase reactivates the all-trans-retinoic acid differentiation pathway in acute myeloid leukemia. Nat Med *18*, 605-611.

Seto, E., and Yoshida, M. (2014). Erasers of histone acetylation: the histone deacetylase enzymes. Cold Spring Harb Perspect Biol *6*, a018713.

Shalem, O., Sanjana, N.E., Hartenian, E., Shi, X., Scott, D.A., Mikkelson, T., Heckl, D., Ebert, B.L., Root, D.E., Doench, J.G., *et al.* (2014). Genome-scale CRISPR-Cas9 knockout screening in human cells. Science *343*, 84-87.

Shen, Z.X., Chen, G.Q., Ni, J.H., Li, X.S., Xiong, S.M., Qiu, Q.Y., Zhu, J., Tang, W., Sun, G.L., Yang, K.Q., *et al.* (1997). Use of arsenic trioxide (As2O3) in the treatment of acute promyelocytic leukemia (APL): II. Clinical efficacy and pharmacokinetics in relapsed patients. Blood *89*, 3354-3360.

Shevchenko, A., Tomas, H., Havlis, J., Olsen, J.V., and Mann, M. (2006). In-gel digestion for mass spectrometric characterization of proteins and proteomes. Nat Protoc *1*, 2856-2860.

Shi, Y., Lan, F., Matson, C., Mulligan, P., Whetstine, J.R., Cole, P.A., and Casero, R.A. (2004). Histone demethylation mediated by the nuclear amine oxidase homolog LSD1. Cell *119*, 941-953.

Shi, Y.J., Matson, C., Lan, F., Iwase, S., Baba, T., and Shi, Y. (2005). Regulation of LSD1 histone demethylase activity by its associated factors. Mol Cell *19*, 857-864.

Soldi, M., and Bonaldi, T. (2013). The proteomic investigation of chromatin functional domains reveals novel synergisms among distinct heterochromatin components. Mol Cell Proteomics *12*, 764-780.

Somervaille, T.C., and Cleary, M.L. (2006). Identification and characterization of leukemia stem cells in murine MLL-AF9 acute myeloid leukemia. Cancer Cell *10*, 257-268.

Soprano, D.R., Qin, P., and Soprano, K.J. (2004). Retinoic acid receptors and cancers. Annu Rev Nutr *24*, 201-221.

Stavropoulos, P., Blobel, G., and Hoelz, A. (2006). Crystal structure and mechanism of human lysine-specific demethylase-1. Nat Struct Mol Biol *13*, 626-632.

Sugino, N., Kawahara, M., Tatsumi, G., Kanai, A., Matsui, H., Yamamoto, R., Nagai, Y., Fujii, S., Shimazu, Y., Hishizawa, M., *et al.* (2017). A novel LSD1 inhibitor NCD38 ameliorates MDS-related leukemia with complex karyotype by attenuating leukemia programs via activating super-enhancers. Leukemia *31*, 2303-2314.

Tachiwana, H., Kagawa, W., Shiga, T., Osakabe, A., Miya, Y., Saito, K., Hayashi-Takanaka, Y., Oda, T., Sato, M., Park, S.Y., *et al.* (2011). Crystal structure of the human centromeric nucleosome containing CENP-A. Nature *476*, 232-235.

Takeuchi, M., Fuse, Y., Watanabe, M., Andrea, C.S., Nakajima, H., Ohashi, K., Kaneko, H., Kobayashi-Osaki, M., Yamamoto, M., and Kobayashi, M. (2015). LSD1/KDM1A promotes hematopoietic commitment of hemangioblasts through downregulation of Etv2. Proc Natl Acad Sci U S A *112*, 13922-13927.

Tallman, M.S., Andersen, J.W., Schiffer, C.A., Appelbaum, F.R., Feusner, J.H., Ogden, A., Shepherd, L., Willman, C., Bloomfield, C.D., Rowe, J.M., *et al.* (1997). All-trans-retinoic acid in acute promyelocytic leukemia. N Engl J Med *337*, 1021-1028.

Thambyrajah, R., Mazan, M., Patel, R., Moignard, V., Stefanska, M., Marinopoulou, E., Li, Y., Lancrin, C., Clapes, T., Möröy, T., *et al.* (2016). GFI1 proteins orchestrate the emergence of haematopoietic stem cells through recruitment of LSD1. Nat Cell Biol *18*, 21-32.

Thiagalingam, S., Cheng, K.H., Lee, H.J., Mineva, N., Thiagalingam, A., and Ponte, J.F. (2003). Histone deacetylases: unique players in shaping the epigenetic histone code. Ann N Y Acad Sci *983*, 84-100.

Thinnes, C.C., England, K.S., Kawamura, A., Chowdhury, R., Schofield, C.J., and Hopkinson, R.J. (2014). Targeting histone lysine demethylases - progress, challenges, and the future. Biochim Biophys Acta *1839*, 1416-1432.

Toffolo, E., Rusconi, F., Paganini, L., Tortorici, M., Pilotto, S., Heise, C., Verpelli, C., Tedeschi, G., Maffioli, E., Sala, C., *et al.* (2014). Phosphorylation of neuronal Lysine-Specific Demethylase 1LSD1/KDM1A impairs transcriptional repression by regulating interaction with CoREST and histone deacetylases HDAC1/2. J Neurochem *128*, 603-616.

Trapnell, C., Williams, B.A., Pertea, G., Mortazavi, A., Kwan, G., van Baren, M.J., Salzberg, S.L., Wold, B.J., and Pachter, L. (2010). Transcript assembly and quantification by RNA-Seq reveals unannotated transcripts and isoform switching during cell differentiation. Nat Biotechnol *28*, 511-515.

Tropberger, P., Pott, S., Keller, C., Kamieniarz-Gdula, K., Caron, M., Richter, F., Li, G., Mittler, G., Liu, E.T., Bühler, M., *et al.* (2013). Regulation of transcription through acetylation of H3K122 on the lateral surface of the histone octamer. Cell *152*, 859-872.

Tsukiyama, T., Daniel, C., Tamkun, J., and Wu, C. (1995). ISWI, a member of the SWI2/SNF2 ATPase family, encodes the 140 kDa subunit of the nucleosome remodeling factor. Cell *83*, 1021-1026.

Upadhyay, G., Chowdhury, A.H., Vaidyanathan, B., Kim, D., and Saleque, S. (2014). Antagonistic actions of Rcor proteins regulate LSD1 activity and cellular differentiation. Proc Natl Acad Sci U S A *111*, 8071-8076.

Valk-Lingbeek, M.E., Bruggeman, S.W., and van Lohuizen, M. (2004). Stem cells and cancer; the polycomb connection. Cell *118*, 409-418.

Vardiman, J.W., Harris, N.L., and Brunning, R.D. (2002). The World Health Organization (WHO) classification of the myeloid neoplasms. Blood *100*, 2292-2302.

Varga-Weisz, P.D., Wilm, M., Bonte, E., Dumas, K., Mann, M., and Becker, P.B. (1997). Chromatin-remodelling factor CHRAC contains the ATPases ISWI and topoisomerase II. Nature *388*, 598-602.

Vianello, P., Botrugno, O.A., Cappa, A., Dal Zuffo, R., Dessanti, P., Mai, A., Marrocco, B., Mattevi, A., Meroni, G., Minucci, S.*, et al.* (2016). Discovery of a Novel Inhibitor of Histone Lysine-Specific Demethylase 1A (KDM1A/LSD1) as Orally Active Antitumor Agent. J Med Chem *59*, 1501-1517.

Villa, R., Pasini, D., Gutierrez, A., Morey, L., Occhionorelli, M., Viré, E., Nomdedeu, J.F., Jenuwein, T., Pelicci, P.G., Minucci, S.*, et al.* (2007). Role of the polycomb repressive complex 2 in acute promyelocytic leukemia. Cancer Cell *11*, 513-525.

Wang, F., Travins, J., DeLaBarre, B., Penard-Lacronique, V., Schalm, S., Hansen, E., Straley, K., Kernytsky, A., Liu, W., Gliser, C.*, et al.* (2013). Targeted inhibition of mutant IDH2 in leukemia cells induces cellular differentiation. Science *340*, 622-626.

Wang, H., Wang, L., Erdjument-Bromage, H., Vidal, M., Tempst, P., Jones, R.S., and Zhang, Y. (2004a). Role of histone H2A ubiquitination in Polycomb silencing. Nature *431*, 873-878.

Wang, J., Hevi, S., Kurash, J.K., Lei, H., Gay, F., Bajko, J., Su, H., Sun, W., Chang, H., Xu, G.*, et al.* (2009a). The lysine demethylase LSD1 (KDM1) is required for maintenance of global DNA methylation. Nat Genet *41*, 125-129.

Wang, J., Scully, K., Zhu, X., Cai, L., Zhang, J., Prefontaine, G.G., Krones, A., Ohgi, K.A., Zhu, P., Garcia-Bassets, I.*, et al.* (2007). Opposing LSD1 complexes function in developmental gene activation and repression programmes. Nature *446*, 882-887.

Wang, J., Telese, F., Tan, Y., Li, W., Jin, C., He, X., Basnet, H., Ma, Q., Merkurjev, D., Zhu, X.*, et al.* (2015). LSD1n is an H4K20 demethylase regulating memory formation via transcriptional elongation control. Nat Neurosci *18*, 1256-1264.

Wang, Y., Wysocka, J., Sayegh, J., Lee, Y.H., Perlin, J.R., Leonelli, L., Sonbuchner, L.S., McDonald, C.H., Cook, R.G., Dou, Y.*, et al.* (2004b). Human PAD4 regulates histone arginine methylation levels via demethylimination. Science *306*, 279-283.

Wang, Y., Zhang, H., Chen, Y., Sun, Y., Yang, F., Yu, W., Liang, J., Sun, L., Yang, X., Shi, L.*, et al.* (2009b). LSD1 is a subunit of the NuRD complex and targets the metastasis programs in breast cancer. Cell *138*, 660-672.

Warrell, R.P., Frankel, S.R., Miller, W.H., Scheinberg, D.A., Itri, L.M., Hittelman, W.N., Vyas, R., Andreeff, M., Tafuri, A., and Jakubowski, A. (1991). Differentiation therapy of acute promyelocytic leukemia with tretinoin (all-trans-retinoic acid). N Engl J Med *324*, 1385-1393.

Webby, C.J., Wolf, A., Gromak, N., Dreger, M., Kramer, H., Kessler, B., Nielsen, M.L., Schmitz, C., Butler, D.S., Yates, J.R.*, et al.* (2009). Jmjd6 catalyses lysyl-hydroxylation of U2AF65, a protein associated with RNA splicing. Science *325*, 90-93.

Wissmann, M., Yin, N., Müller, J.M., Greschik, H., Fodor, B.D., Jenuwein, T., Vogler, C., Schneider, R., Günther, T., Buettner, R.*, et al.* (2007). Cooperative demethylation by JMJD2C and LSD1 promotes androgen receptor-dependent gene expression. Nat Cell Biol *9*, 347-353.

Xu, F., Zhang, K., and Grunstein, M. (2005). Acetylation in histone H3 globular domain regulates gene expression in yeast. Cell *121*, 375-385.

Yang, G.J., Lei, P.M., Wong, S.Y., Ma, D.L., and Leung, C.H. (2018). Pharmacological Inhibition of LSD1 for Cancer Treatment. Molecules *23*.

Yang, J., Huang, J., Dasgupta, M., Sears, N., Miyagi, M., Wang, B., Chance, M.R., Chen, X., Du, Y., Wang, Y.*, et al.* (2010). Reversible methylation of promoter-bound STAT3 by histone-modifying enzymes. Proc Natl Acad Sci U S A *107*, 21499-21504.

Yang, M., Culhane, J.C., Szewczuk, L.M., Jalili, P., Ball, H.L., Machius, M., Cole, P.A., and Yu, H. (2007). Structural basis for the inhibition of the LSD1 histone demethylase by the antidepressant trans-2-phenylcyclopropylamine. Biochemistry *46*, 8058-8065.

Yokoyama, A., Takezawa, S., Schüle, R., Kitagawa, H., and Kato, S. (2008). Transrepressive function of TLX requires the histone demethylase LSD1. Mol Cell Biol *28*, 3995-4003.

Yu, Y., Schleich, K., Yue, B., Ji, S., Lohneis, P., Kemper, K., Silvis, M.R., Qutob, N., van Rooijen, E., Werner-Klein, M.*, et al.* (2018). Targeting the Senescence-Overriding Cooperative Activity of Structurally Unrelated H3K9 Demethylases in Melanoma. Cancer Cell *33*, 322-336.e328.

Zambelli, F., Pesole, G., and Pavesi, G. (2013). PscanChIP: Finding over-represented transcription factor-binding site motifs and their correlations in sequences from ChIP-Seq experiments. Nucleic Acids Res *41*, W535-543.

Zheng, Y.C., Yu, B., Chen, Z.S., Liu, Y., and Liu, H.M. (2016). TCPs: privileged scaffolds for identifying potent LSD1 inhibitors for cancer therapy. Epigenomics *8*, 651-666.

Zhou, D.C., Kim, S.H., Ding, W., Schultz, C., Warrell, R.P., and Gallagher, R.E. (2002). Frequent mutations in the ligand-binding domain of PML-RARalpha after multiple relapses of acute promyelocytic leukemia: analysis for functional relationship to response to all-trans retinoic acid and histone deacetylase inhibitors in vitro and in vivo. Blood *99*, 1356-1363.

Zhu, B., Zheng, Y., Pham, A.D., Mandal, S.S., Erdjument-Bromage, H., Tempst, P., and Reinberg, D. (2005). Monoubiquitination of human histone H2B: the factors involved and their roles in HOX gene regulation. Mol Cell *20*, 601-611.

Zibetti, C., Adamo, A., Binda, C., Forneris, F., Toffolo, E., Verpelli, C., Ginelli, E., Mattevi, A., Sala, C., and Battaglioli, E. (2010). Alternative splicing of the histone demethylase LSD1/KDM1 contributes to the modulation of neurite morphogenesis in the mammalian nervous system. J Neurosci *30*, 2521-2532.

Zuber, J., Shi, J., Wang, E., Rappaport, A.R., Herrmann, H., Sison, E.A., Magoon, D., Qi, J., Blatt, K., Wunderlich, M.*, et al.* (2011). RNAi screen identifies Brd4 as a therapeutic target in acute myeloid leukaemia. Nature *478*, 524-528.